5-3-2019

Identifying the molecular mechanisms responsible for persistent effects of developmental exposure to chlorpyrifos on behavior

Navatha Alugubelly

Identifying the molecular mechanisms responsible for persistent effects of developmental exposure to chlorpyrifos on behavior

By

Navatha Alugubelly

A Dissertation
Submitted to the Faculty of
Mississippi State University
in Partial Fulfillment of the Requirements
for the Degree of Doctor of Philosophy
in Environmental Toxicology
in the College of Veterinary Medicine

Mississippi State, Mississippi

May 2019

Identifying the molecular mechanisms responsible for persistent effects of developmental exposure to chlorpyrifos on behavior

By

Navatha Alugubelly

Approved:

_____

Russell Carr
(Major Professor/ Graduate Coordinator)

_____

Matthew K. Ross
(Committee Member)

_____

Jeffrey B. Eells
(Committee Member)

_____

Bindu Nanduri
(Committee Member)

_____

Mariola J. Edelmann
(Committee Member)

_____

Stephen B. Pruett
Associate Dean
College of Veterinary Medicine

Name: Navatha Alugubelly

Date of Degree: May 3, 2019

Institution: Mississippi State University

Major Field: Environmental Toxicology

Major Professor: Russell L. Carr

Title of Study: Identifying the molecular mechanisms responsible for persistent effects of developmental exposure to chlorpyrifos on behavior

Pages in Study: 201

Candidate for Degree of Doctor of Philosophy

Chlorpyrifos (CPF) is one of the most widely used organophosphorus insecticides (OPs). The developmental exposure to low levels of CPF results in the inhibition of the endocannabinoid metabolizing enzyme fatty acid amide hydrolase (FAAH) and in altered emotional behavior (increased social play) without affecting the acetylcholinesterase, the canonical target of OPs. However, the molecular mechanisms responsible for this increased social play are not known. In this study, male rat pups were exposed orally to either corn oil, 0.75 mg/kg CPF, or 0.02 mg/kg PF-04457845 (PF; a specific inhibitor of FAAH) daily from postnatal day 10 (PND10) - PND16. This dosage of CPF does not alter brain cholinergic activity but inhibits FAAH. Once these rats reached adolescence (PND38), they were divided into two cohorts and each cohort contained all treatments. One cohort underwent social behavior testing and the other cohort remained naïve to behavioral testing. Following testing, the amygdala was collected from each cohort and protein expression was determined using a label-free shotgun proteomic approach. The obtained differentially expressed proteins from the different cohorts were analyzed by DAVID and Ingenuity Pathway Analysis software.

Comparison of control non-behavior and control behavior rats suggests that social play altered the systems involved in the regulation of reward such as the opioid, dopaminergic, and serotonergic systems. These data also suggest that synaptic levels of GABA and glutamate increased during play. Comparison of non-behavior control and treated rats suggests that FAAH inhibition resulting from developmental exposure to CPF and PF persistently affects glutamatergic and GABAergic signaling. These data also suggest that there is a similar pattern of protein expression between CPF and PF. Comparison of the data from the behavioral groups of rats suggests that alterations in glutamatergic and GABAergic signaling and improper activation of opioid signaling could be responsible for the increased social play behavior. These alterations in the neurotransmitter signaling were observed in both CPF and PF treated rats. Overall, the results suggest that FAAH inhibition by either CPF or PF leads to alterations in opioid, glutamatergic, and GABAergic signaling that could be responsible for increased levels of social play.

DEDICATION

I would like to dedicate this dissertation to my family especially to my husband Dr. Karthikeshwar Vangala and to my parents Narsi Reddy and Nagamani Alugubelly for their constant support, encouragement and love. To my brother, Naveen Reddy Alugubelly, for his support. Finally, to my little princess who indirectly motivated me to finish my dissertation faster.

ACKNOWLEDGEMENTS

First, I would like to thank my major advisor Dr. Russell Carr for allowing me to join his laboratory in the middle of my Ph.D. program and for helping me to successfully defend my doctoral dissertation. You are not just an advisor but a good friend to me. With your guidance, I have learned to be a good research scientist. I would like to thank my dissertation committee for their critical feedback, encouragement, and support. I would also like to thank all the Center for Environmental and Health Sciences faculty, staff, and students for their support through the years. I would also like to thank my fellow graduate students for their friendship and encouragement which was much needed during graduate school. Most importantly, I thank my husband, mom, dad, and my brother for their encouragement in times when I felt I cannot do it but was able to do it with the help of my beautiful family.

TABLE OF CONTENTS

LIST OF TABLES

LIST OF FIGURES

CHAPTER I

INTRODUCTION

1.1 Organophosphate insecticides (OP insecticides)

OP insecticides are either esters, amides, or thiol derivatives of phosphoric, phosphonic, or phosphinic acids. The French chemists, Jean Louis Lassaigne and Philip De Clermont, developed the first OPs in the nineteenth century. However, the development of OPs as insecticides and chemical warfare agents occurred in the early twentieth century by German chemist Gerhard Schrader (Tucker 2006, Terry 2012). OP insecticides are the most common class of chemicals used to eradicate pests on agricultural farms and to kill disease-carrying vectors (Iyer et al. 2015, King and Aaron 2015). Since their introduction in the 1800s, OPs have been used as insecticides (e.g., malathion, parathion, dichlorvos, diazinon, chlorpyrifos), chemical warfare agents or nerve gases (e.g., soman, sarin, tabun), ophthalmic agents (e.g., echothiophate, isoflurophate), herbicides (tribufos, merphos), solvents, and lubricants (Terry 2012). However, most of the OPs were developed as insecticides. There are over 100 different OP insecticides on the world market (Kwong 2002, Suratman et al. 2015). The lower environmental stability, effectiveness against a variety of insect species, and the ban of most of the organochlorine compounds like DDT led to the increased use of OP insecticides. However, the higher mammalian toxicity of these compounds due to widespread use and easy availability have been led to 3 million OP intoxications

worldwide (Kwong 2002, Balali-Mood and Balali-Mood 2008). In addition, OP insecticides poisoning either through deliberate consumption or accidental exposure has accounted for a 30% mortality rate worldwide especially in developing countries because of ease of access to OPs and low level of regulations governing their use (Gunnell et al. 2007).

1.2 Mechanism of toxicity of OP insecticides

Exposure to OP insecticides activates the cholinergic system through the inhibition of acetylcholinesterase (AChE). Most of the OP insecticides, such as chlorpyrifos (CPF), malathion, parathion, and diazinon, cannot bind efficiently to AChE but must be converted to their respective oxon metabolite inside the body. These metabolites bind to AChE and inhibit its function by phosphorylating the serine residue in its active site (Buratti et al. 2002, Buratti et al. 2003, Hodgson and Rose 2007). The inhibition of AChE results in the accumulation of acetylcholine at nerve terminals, autonomic ganglia, neuromuscular junctions, and in the peripheral nervous system leading to excess stimulation of neurons through activation of nicotinic and muscarinic receptors (Forsyth and Chambers 1989, Buratti et al. 2002). At high exposure levels, this induces the characteristic toxicological signs of OP poisoning including salivation, lacrimation, urination, defecation, gastrointestinal distress, emesis, miosis, tremors, fasciculations, and respiratory failure, the latter of which eventually leads to death (Zheng et al. 2000, Gupta 2004).

1.3 Neurotoxicity of OP insecticides

The adverse health outcome resulting from exposure of humans of all ages to high levels of OP insecticides has been well described. Epidemiological studies have suggested that acute exposure to OP insecticides demonstrated additional adverse effects on adult neurobehavior rather than just acetylcholinesterase inhibition. The acute exposure to OP insecticides has been associated with deficits in several neurobehavioral functions including sustained attention, memory, problem-solving, hand-eye coordination, simple reaction time, finger tapping, and mood (tension, depression, anxiety, fatigue, and confusion) (Steenland et al. 1994, Terry 2012). The chronic exposure to OP insecticides also demonstrated similar deficits in neurobehavioral symptoms including drowsiness, confusion, anxiety, lethargy, visual memory, problem-solving, and speed of information processing. These neurobehavioral changes have been termed together as chronic OP-induced neuropsychiatric disorders (COPIND) (Stephens et al. 1995, Singh and Sharma 2000). Animal studies also demonstrated that repeated exposure to OPs that are not associated with any cholinergic symptoms (no overt signs of acute toxicity) resulted in abnormal neurobehavioral symptoms. The exposure of adult rats to diisopropylfluorophosphate (DFP) produced deficits in working memory, reference memory, and motor function (Bushnell et al. 1991). Repeated exposure to CPF resulted in impairments in sustained attention and increased impulsivity in adult rats as measured by 5 Choice Serial Reaction Time Task which measures different parameters including sustained attention, impulsive behavior, and motivation (Middlemore-Risher et al. 2010, Cardona et al. 2011, Montes de Oca et al. 2013).

1.4 Chlorpyrifos

One of the most widely used OP insecticides is CPF. CPF is a component of 800 registered products on the market across the world (Giesy et al. 1999, Wang et al. 2016). Since its introduction into the world market in 1965, CPF has been used to kill insects in households, in work places, and in agricultural settings. CPF was first introduced into the USA market as a termiticide in 1980. However, since 2000, the use of CPF has been decreased by 50% due to voluntary restriction of its household uses in the USA (Iyer et al. 2015). The usage of OP insecticides in the USA has declined gradually from 70 million pounds in 2000 to 20 million pounds in 2012 because of the elimination of household use of some of the OP insecticides such as CPF, diazinon, and methyl parathion (Atwood and Paisley-Jones 2017). However, these pesticides are still heavily used in the agriculture and people living in agricultural communities are still at great risk of exposure to these pesticides. In fact, the biological markers of OP exposure, including non-specific OP metabolites, specific metabolites for CPF and malathion, and the actual parent compounds, have been detected in blood and urine samples collected from agricultural families (Eskenazi et al. 2004, Huen et al. 2012). A significant amount of research related to the neurotoxicity of OP insecticides has been focused on chlorpyrifos.

Studies investigating chronic exposure to levels of CPF that did not produce overt signs of the cholinergic toxicity reported deficits in spatial learning, information processing, and cognitive function and also reported neurochemical changes such as decreased levels of nerve growth factor receptors and other cholinergic proteins including the vesicular acetylcholine transporter and the high-affinity choline transporter. These deficits were accompanied by decreases in fast and slow axonal transport in adult rats

(Terry et al. 2003, Terry et al. 2007). Exposure to either CPF or CPF-oxon resulted in an increase in mitochondrial length, a decrease in mitochondrial number, and a decrease in the mitochondrial movement in the axons (Middlemore-Risher et al. 2011). Similarly, repeated exposure of adult rats to the OP diisopropylfluorophosphate resulted in deficits in specific domains of cognition in the water maze test and the novel object recognition test and these deficits were associated with neurochemical changes in cholinergic markers and nerve growth factor related proteins (Terry et al. 2011). Moreover, these deficits in the cognitive domains such as spatial learning and memory persisted for long periods of time after exposure to OP insecticides (Terry et al. 2012). Speed et al. (2012) also demonstrated the long-term effects of OP exposure on synaptic transmission. The exposure of adult mice to levels of CPF that produce no signs of cholinergic toxicity produced increased hippocampal synaptic transmission immediately after exposure but three months after exposure produced decreased synaptic transmission associated with decreased synaptic spine density. All of these studies suggest that repeated exposure to OP insecticides, at levels not associated with any cholinergic symptoms, causes delayed persistent damage in the adult brain.

1.5 Role of pesticides in pathogenesis of neurodegenerative diseases

Although genetic susceptibility is one of the main predisposing factors for most of the neurodegenerative disorders, it only accounts for 40% and growing evidence suggests that environmental exposures in combination with individual genetic factors play a major role in the pathogenesis of these disorders. There are concerns that gene × environment interactions have detrimental effects on cognitive dysfunction and other neurological abnormalities. The general consensus is that pesticides are involved in the etiology of

neurodegenerative diseases such as Alzheimer's disease (AD) and Parkinson's disease (PD). Long-term changes in behavior including increased motor activity in the open field and worsened retention in the water maze were observed in adult mice (a mouse model of AD) that were repeatedly exposed to CPF (Peris-Sampedro et al. 2014). Long-term changes in amyloid β levels in cortical and hippocampal regions of the brain and persistent behavioral changes including decreased retention in water maze task were observed in a mouse model of AD after acute exposure to CPF (Salazar et al. 2011). These findings raise concerns about the risk of vulnerable subjects developing neurodegenerative diseases following repeated exposure to OP insecticides. It has also been demonstrated that developmental exposure to OPs triggers transcriptional changes in genes associated with PD both *in vitro* and *in vivo* (Slotkin and Seidler 2011). Epidemiological studies have also reported that there is a potential link between OP exposure and neurodegenerative diseases such as AD (Hayden et al. 2010) and PD (Moretto and Colosio 2013). Most of the studies hypothesized that exposure to pesticides causes oxidative stress and mitochondrial dysfunction which may be involved in the pathogenesis of PD. A case-control study conducted in Central Valley of California used a geographic information system-based exposure assessment tool to estimate ambient exposure to 30 OPs from 1974-1999. This study provided a strong evidence that OPs are involved in the etiology of PD at high exposure levels (Wang et al. 2014).

1.6 Developmental neurotoxicity

Most of the studies discussed so far reported the effects of high-level exposure to OPs on neurological processes and behavior in adults. According to the American Association of Poison Control Centers' National Poison Data System, about 32% of OP

insecticide exposures reported in 2013 involved children (Mowry et al. 2014). Therefore, it is important to study the effects of exposure to OP insecticides on brain development in children. Increased vulnerability to pesticides among infants and children can be attributed to several factors. For example, the developing nervous system in children is more susceptible to the effects of exposure in comparison to adults; along with this, children have less ability to metabolize and detoxify most of the toxicants. Also, much lower levels of exposure are required to induce toxicity in children than in adults. However, one advantage for children is that they possess faster recovery of cholinergic parameters, such as AChE activity (Lassiter et al. 1998) and can recover faster from exposure. Epidemiological studies demonstrate that *in utero* or childhood exposure to OP insecticides adversely affect fetal growth, neurodevelopment, and behavior. The Columbia Center for Children's Environmental Health evaluated the effects of prenatal insecticide exposures among urban minorities in New York City. This prenatal exposure resulted in lower mean birth weight, smaller head circumference, and shorter birth length in infants. CPF, diazinon, and propoxur were detected in blood samples of both mothers and infants. However, the levels of insecticides in blood samples decreased significantly after 2000 due to the ban of these insecticides from residential use (Whyatt et al. 2005). A longitudinal birth cohort study involving Latina women living in an agricultural community of California reported the association between higher prenatal urinary OP metabolite concentrations and an increase in abnormal infant reflexes in 3-day old infants (Young et al. 2005). Another longitudinal study involving agricultural families in California investigated the relationship between prenatal and child urinary OP metabolite levels and children's neurodevelopment. This study reported the adverse associations of

prenatal and child nonspecific dialkyl phosphate (DAP) metabolite levels with pervasive developmental problems. However, only prenatal DAP metabolite levels were associated with adverse mental development (Eskenazi et al. 2007).

An illegal application of methyl parathion for pest control in Mississippi and Ohio residencies resulted in an abnormal neurobehavioral development in children that were 6 years old or younger. Exposed children had a greater difficulty with tasks involving short-term memory and attention. Based on parental reporting, these exposed children exhibited more behavioral and motor skill problems than did unexposed children (Ruckart et al. 2004). In addition, children highly exposed to CPF (CPF levels of >6.17 pg/g plasma in umbilical cord blood) scored significantly lower on the Psychomotor and Mental indices of Bayley Scales of Infant development at 3 years of age. These children also displayed attentional problems, such as impaired cognition and motor function and attentional deficit hyperactivity disorder problems (Rauh et al. 2006). The prenatal exposure to CPF was associated with deficits in working memory and full scale-intelligence quotient in children at 7 years of age (Rauh et al. 2011) and childhood tremors at 11 years of age (Rauh et al. 2015). Along with this, brain anomalies including enlargement of temporal and frontal gyrus, and frontal and cortical thinning were observed in children exposed prenatally to CPF (Rauh et al. 2012). Even though many scientists question these associations (Davies 2016), These studies still suggest that CPF can exert neurodevelopmental effects.

The literature suggests that children are more susceptible to high level OP insecticide exposure as compared to adults. However, it is important to study the effects of low-level exposures on children since the real-world scenarios involve low levels of

OPs. Also, dietary intake of pesticides is the most important source of exposure to humans. These exposure levels are 2-3 orders of magnitude below levels that have been demonstrated to cause overt signs of cholinergic toxicity. In many of the developmental OP studies, a low-level exposure is considered to be an exposure to concentrations that are devoid of any overt toxicity and cause only minimal acetylcholinesterase inhibition. This level of inhibition would be insufficient to produce any signs of systemic toxicity. The detrimental effects of low-level OP exposure in children have been discussed in some published reviews (Jamal et al. 2002, Ross et al. 2013). A meta-analysis study was performed to attempt to quantitatively evaluate the study findings concerning the neurotoxicity of low-level exposure to OPs. This study concluded that majority of studies found a significant association between low-level exposure to OPs and impaired neurobehavioral function, such as visuospatial ability, executive function, psychomotor speed, working and visual memory (Ross et al. 2013). All of these studies suggest that low-level exposure to pesticides results in neurobehavioral impairments in children.

1.6.1 Non-cholinergic targets of OPs

Although most of the studies attribute OP toxicity to the inhibition of acetylcholinesterase, new additional targets of OPs specific to the developing brain have been explored and those targets are discussed below. OPs disrupt the different neuronal processes including neuronal maturation and the formation of new synapses. OPs also disrupt the proliferation and differentiation of neurons and the formation of axons (Casida and Quistad 2004, Slotkin 2004b). The widely used OP insecticide CPF inhibited DNA and protein synthesis in neonatal rats (Whitney et al. 1995a). In addition, prolonged administration of CPF in neonatal rats elicited a loss of cell numbers, or DNA content,

throughout the brain, which was accompanied by delayed deterioration of synaptic signaling. This suggested that the programming of synaptic development had been altered by OP exposure during an early developmental period. CPF elicited damage by affecting neural cell replication in early stages and axonogenesis and terminal differentiation in later stages. At higher concentrations, CPF also inhibited neuritic outgrowth (Slotkin 1999). These defects persisted through adolescence and into adulthood and were accompanied by behavioral abnormalities (Levin et al. 2001, Levin et al. 2002). These data indicate that disturbances in early neurodevelopmental events may have a plethora of effects on events in later life.

Developmental exposure to levels of OP insecticides that do not induce cholinergic signs of toxicity has been implicated in producing long-lasting negative impacts, including decreased cognitive abilities and motor skills (Engel et al. 2011), reduced anxiety-like behavior (Chen et al. 2011a, Carr et al. 2015), increased manifestation of attention-deficit/hyperactivity disorder (Rauh et al. 2006), anhedonia (Aldridge et al. 2005a), and depressive-like behavior (Chen et al. 2014). Epidemiological literature has documented the adverse health outcomes associated with exposure to pesticides at young ages. This age-related susceptibility is due to the critical window of nervous system development that includes formation of new neurons, differentiation, migration, synaptogenesis, myelination, and axonogenesis. Thus, any disturbances that occur during nervous system development could disrupt the critical processes that are required for normal maturation and behavior (Pope 1999, Barone et al. 2000, Slotkin 2004a). Several studies have reported altered neurochemical parameters and disrupted behavior following developmental exposure to OP insecticides. Moreover, negative

impacts have been observed with multiple OP insecticides at levels that cause only minimal inhibition of AChE (Levin et al. 2002, Aldridge et al. 2004, Slotkin et al. 2006). These studies suggest that OP insecticides exhibit their toxicity through a different mechanism, which does not involve AChE inhibition. However, none of these studies have explained the mechanisms of toxicity although some of the studies have reported the neurotransmitter systems as potential non-cholinergic targets of OPs.

The adverse effects of developmental exposure to OP insecticides have been observed on different neurotransmitter systems including the serotonergic (Aldridge et al. 2003, Aldridge et al. 2004, Aldridge et al. 2005a, Aldridge et al. 2005c), dopaminergic (Aldridge et al. 2005a, Chen et al. 2011b, Zhang et al. 2015), norepinephrine ((Slotkin et al. 2002, Slotkin et al. 2015b), and endocannabinoid system (Carr et al. 2011, Carr et al. 2013, Carr et al. 2014, Carr et al. 2015). The reason behind neurotransmitter systems being the target of developmental exposure to OPs is due to the role of neurotransmitters in cellular and architectural development of the brain. The neurotransmitters when activated play a role in promoting neural cell replication, initiating the switch from replication to differentiation, enhancing or retarding axonogenesis or synaptogenesis, and enabling the specific cell population to migrate to their target regions in the brain (Lauder 1985). Thus, any exposure during brain development might negatively affect the neurotransmitter systems and disrupt neurotransmitter activity resulting in detrimental effects on the developing brain. In addition, various organophosphates target specific neurotransmitter systems differently from each other at doses spanning the threshold for cholinesterase inhibition (Slotkin et al. 2006).

1.6.1.1 Norepinephrine system

The long-term effects of developmental OP exposure have been observed on the norepinephrine system. Early postnatal day (PND) 1-4) or late (PND 11-14) neonatal exposure to CPF persistently suppressed norepinephrine turnover, which is a measure of presynaptic neuronal activity, across multiple brain regions such as the striatum, cerebellum, and cerebral cortex when tested during adolescence and adulthood (Slotkin et al. 2002). Early neonatal exposure (PND 1-4) of offspring rats to CPF, whose mothers were exposed to nicotine or dexamethasone during gestation, caused deficits in presynaptic norepinephrine levels and β-adrenergic receptor binding in both cerebellum and cerebral cortex during adolescence and adulthood. This suggests that prenatal drug exposure sensitizes noradrenergic circuits to subsequent disruption by CPF (Slotkin et al. 2015b). Developmental exposure to diazinon also caused a deficit in norepinephrine levels, whereas exposure to parathion elicited a net increase. Both of these chemicals had no effect on β-adrenergic receptor levels when measured during adolescence or adulthood (Slotkin et al. 2017). The effects are likely to contribute to persistent alterations in behavioral performance.

1.6.1.2 Serotonergic system

The serotonergic system is particularly sensitive to disruption by OPs in the developing brain. Aldridge et al. (2005a) reported that postnatal exposure to CPF results in lasting disruption of serotonin (5-HT) synaptic activity, specifically changes in 5-HT turnover levels. Changes in 5-HT activity were also confirmed by another study where neonatal exposure to CPF increased the expression of serotonin receptors (5HT1A and 5HT2) and increased serotonin turnover (5HIAA/5HT ratio) levels (Slotkin et al. 2015a).

Based on these data, authors proposed that inappropriate 5-HT turnover leads to miswiring of 5-HT innervations, which may lead to behavioral deficits (Aldridge et al. 2005a). Fetal and neonatal exposure to CPF alters the development of serotonin synaptic function, specifically inducing long-lasting changes in 5-HT receptors, presynaptic 5-HT transporter, and 5-HT mediated signal transduction. Those changes persisted into adulthood (Aldridge et al. 2004). The effects of other OPs, such as diazinon and parathion, on serotonergic activity was also studied. The early developmental exposure to diazinon demonstrated deficits in 5HT1A receptors and upregulation of the 5HT transporter during adolescence and adulthood (Slotkin et al. 2008). In contrast, postnatal exposure to parathion demonstrated upregulation of 5HT1A receptors in frontal cortex but downregulation in temporal cortex, brain stem, and striatum on PND60; but, these effects were diminished by PND100 (Slotkin et al. 2009). In addition, the exposure to methamidophos reported upregulation of 5HT1A and 5HT2 receptors in the brain stem with upregulation of only 5HT2 receptors in the cortex (Lima et al. 2013). These results suggest that different OPs have different effects on the serotonergic system that depended on brain region, sex, and age of the animal tested.

The alteration in serotonergic synaptic function results in behavioral abnormalities that are usually associated with 5-HT deficiencies (Aldridge et al. 2005a). Neonatal exposure to CPF increased the time spent in open arms of an elevated plus maze and demonstrated lasting effects on cognitive function in adult rats. These CPF treated rats also demonstrated decreased preference to chocolate milk as compared to water, indicating anhedonia (Aldridge et al. 2005a). Repeated exposure of adolescent rats to CPF increased the number of shocks in Vogel's conflict test, time spent in open arms in

elevated plus maze, and significantly decreased the latency to feed in the novelty-suppressed feeding test. As a result, it suggests that exposure to CPF reported alterations in emotional behaviors related to the serotonergic system (Chen et al. 2011a). Neonatal methamidophos exposure elicited different effects on 5HT1A and 5HT2 receptor levels and increased depressive-like behavior and impaired decision-making ability in mice (Lima et al. 2013). Neonatal exposure to parathion demonstrated deficits in spatial learning and memory by showing working memory errors when tested in the radial arm maze. In association with the effects on cognitive function, neonatal parathion exposure also demonstrated deficits in serotonergic synaptic function, characterized by the upregulation of 5HT2 receptors and 5HT transporter (Levin et al. 2010). Although no effects of CPF were observed in forced swimming test, the CPF treated mice failed to show the typical behaviors of altered serotonergic activity caused by the administration of 5HT transporter inhibitor fluvoxamine which demonstrates the disrupting effects of prenatal CPF exposure on serotonergic neurotransmission and associated alterations in socio-emotional behavior (Venerosi et al. 2010). All these behavioral abnormalities suggest that developmental exposure to an OP insecticide may have caused architectural miswiring of 5-HT circuits resulting in deficits in serotonin-related functions that further lead to abnormal behavior.

1.6.1.3 Dopaminergic system

Neonatal exposure of rats to CPF exerts lasting effects on the dopaminergic system. Specifically, there is a progressive and significant loss of dopaminergic neurons in substantia nigra, which is mediated by the inflammatory response that occurs through activation of NF-κB and MAPK signaling pathways (Zhang et al. 2015). Developmental

exposure to CPF has been reported to induce adverse effects on noradrenergic and dopaminergic pathways that persist into adulthood. These effects are likely to contribute to the reported alterations in behavioral performance (Slotkin et al. 2002). Exposure to CPF at different developmental periods has demonstrated changes in dopamine levels in different brain regions with the greatest level of change occurring in the hippocampus than in cerebral cortex on gestational day (GD) 17 and PND 14 and 60 following exposure from GD 7.5 to 11.5. In contrast, CPF exposure from GD 13-17 elicited changes in dopamine levels on PND 14 and 60 with more changes in cerebral cortex than in hippocampus (Chen et al. 2011b). Another study also supports these data where gestational exposure to CPF caused deficits in hippocampal dopamine levels and dopamine turnover; whereas, early postnatal exposure to CPF increased dopamine turnover in midbrain and striatum but decreased turnover in the cerebral cortex (Aldridge et al. 2005a). These data suggest that exposure to OPs during different critical periods have divergent effects on the dopaminergic system.

Miswiring of the architecture of the dopamine, norepinephrine and serotonin projections could result in circuitry defects and may likely contribute to the plethora of neurochemical and behavioral deficits that have been reported following CPF developmental exposure. Although developmental exposure to OPs elicited defects in the neurotransmitter systems, these functional components of these systems may not be the direct targets of OPs, because none of these previous studies identified the binding of an OP to one of these components. However, the possibility is that the effects of OPs on these neurotransmitter systems may be the downstream effect of action of OPs on another target.

1.6.1.4 Endocannabinoid system

Our studies have implicated the endocannabinoid system as a potential target during developmental exposure to OPs (Carr et al. 2013, Carr et al. 2014, Carr et al. 2015). The endocannabinoid system is a unique neuromodulatory system that plays a role in several physiological processes including appetite, memory, mood, and pain sensation. This system consists of CB1 and CB2 receptors, highly expressed in the brain and periphery, respectively. The endogenous ligands for these receptors are 2-arachidonoyl glycerol (2-AG) and arachidonoylethanolamide (anandamide or AEA) (Devane et al. 1992, Di Marzo et al. 1994, Stella et al. 1997). 2-AG and AEA are not stored in vesicles due to their lipophilic nature, are synthesized and released on demand after neuronal depolarization, and are degraded mainly by monoacylglycerol lipase (MAGL) and fatty acid amide hydrolase (FAAH), respectively (Di Marzo et al. 1994). Delta^9-tetrahydrocannabinol (THC), a plant derived cannabinoid, also binds to the same receptors as endocannabinoids and alters endocannabinoid signaling. This alteration of signaling induced during developmental exposure to THC alters the function of multiple neurotransmitter systems including the serotonergic (Molina-Holgado et al. 1996, Molina-Holgado et al. 1997), GABAergic (Garcia-Gil et al. 1999), and opioid systems (Kumar et al. 1990, Fernandez-Ruiz et al. 2004). This indicates that the endocannabinoid system plays an important role in normal brain development. Thus, exposure to any agent, such as an OP, that alters endocannabinoid signaling during development may lead to disruption in the function of multiple neurotransmitter systems including possibly the endocannabinoid system itself.

Our own work has demonstrated that the developmental exposure to low-levels of CPF affects the endocannabinoid metabolizing enzymes (Carr et al. 2011, Carr et al. 2013, Carr et al. 2014). The developmental exposure to a low level of CPF (1.0 mg/kg) from PND 10-16 resulted in inhibition of rat forebrain AChE, FAAH, and MAGL when measured at 4h following the last administration on PND16. The inhibition of all enzymes occurred in a dose dependent manner with the extent of inhibition from highest to lowest level being FAAH>AChE>MAGL (Carr et al. 2011). In a time-course inhibition study, the highest inhibition of AChE and FAAH was observed at 12 h; whereas, the highest inhibition of MAGL was observed at 4 h post treatment analysis. In addition, the highest accumulation of endocannabinoids such as 2-AG and AEA was observed at 12 h after the last dose (Carr et al. 2013). In the follow-up study, the dosage was reduced to 0.5 mg/kg and the effects of repeated exposure to this low dosage of CPF on activities of AChE, FAAH, and MAGL was determined. This low dosage exposure resulted in no measurable inhibition of AChE and MAGL but significant FAAH inhibition and a significant increase in AEA levels but not 2-AG levels (Carr et al. 2014). The lack of cholinesterase inhibition indicates that the observed effect on FAAH inhibition and subsequent accumulation of its substrate could be a measurable non-cholinergic effect of CPF at low dosages.

1.7 Social/ emotional behavior

The endocannabinoid system plays an important role in regulating emotionality and anxiety (Zanettini et al. 2011). It has been demonstrated that developmental exposure to exogenous cannabinoids induces long-term alterations in emotionality and social behavior (O'Shea et al. 2004, O'Shea et al. 2006). In addition, emotional and social

behaviors are also altered by developmental exposure to OP insecticides (Aldridge et al. 2005a, Ricceri et al. 2006). The consequences of CPF-induced disruption of endocannabinoid signaling on emotional behavior of rats were investigated. To understand these consequences of FAAH inhibition and AEA accumulation on emotionality, the rat pups were exposed orally to either corn oil, 0.5 mg/kg, 0.75 mg/kg, or 1.0 mg/kg CPF from PND10-16. As expected, exposure to the highest dosage (1.0 mg/kg) resulted in the inhibition of FAAH, AChE, and MAGL but exposure to the medium (0.75 mg/kg) and low (0.5 mg/kg) dosages resulted in inhibition of FAAH only. On PND25, the latency to emerge from a dark container into a highly illuminated open field was measured as an indicator of anxiety. All CPF treated groups spent significantly less time in the dark container prior to emerging than did controls suggesting a decreased level of anxiety (Carr et al. 2017). However, a single behavioral test is not enough to assess the effects of CPF on emotional behavior. Therefore, in a follow-up study, the effect of developmental CPF exposure on the social behavior of adolescent rats was investigated using the same exposure paradigm and treatment groups as in the previous study. The different behavioral parameters including social grooming, body and genital sniffing, crawling over/under, chasing, nape attacks, time spent playing, and pinning were measured. Significant alterations in social play behaviors, such as frequency of chasing, frequency of crawling over/under, frequency of play fighting, and time spent play fighting were observed with all treatment groups (Figure 1.1).

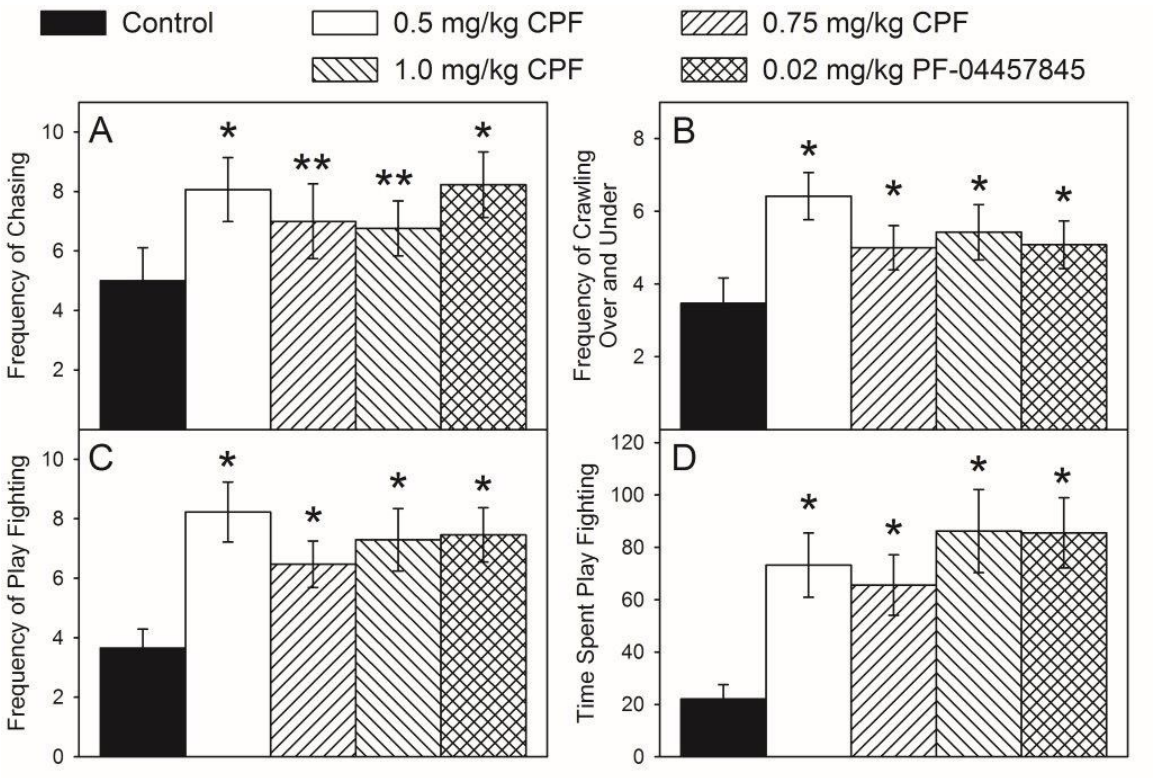

Figure 1.1 The effect of chlorpyrifos on social play

Frequency of chasing (A), frequency of crawling over and under (B), frequency of play fighting (C), and time spent play fighting (D) during social interactions on postnatal day 35 following daily exposure from postnatal day 10 through 16 to either corn oil (control) or 0.5, 0.75, or 1.0 mg/kg chlorpyrifos (CPF) or 0.02 mg/kg PF-04457845, a specific inhibitor of FAAH. Values are expressed as mean ± SE. Bars indicated with a double asterisk (**) are statistically significant ($p \leq 0.1$) and bars indicated with an asterisk (*) are statistically significant ($p \leq 0.05$) from control.

With respect to social behaviors in rodents, social play is a frequently studied behavior. Social play is a non-mother directed behavior and refers to specific behaviors, such as social, sexual, or aggressive behaviors, that are directed towards conspecifics. This behavior involves both the initiation of soliciting the partner to play and the interactions between play partners. This behavior has a high reward value (Pellis and Pellis 1991). Analysis of social play is characterized by measuring different behavioral

patterns including social grooming, body and genital sniffing, crawling over/under, chasing, pouncing, nape attacks, wrestling, boxing, and pinning (Panksepp and Beatty 1980, Meaney and Stewart 1981, Plonsky and Freeman 1982). The latter four of these are measures of play fighting. Participation in play fighting is necessary for juveniles in order to develop proper cognitive, emotional, and social competency (Pellis and Pellis 2007). It has been suggested that play fighting in juvenile rats induces secretion of growth factors in different regions of the brain, including the brain stem, mid brain, lower fore brain, and parts of cortex. These growth factors are necessary for the development of those specific brain regions (Gordon et al. 2003). The effects of developmental exposure to OP insecticides on social behavior have been investigated to some extent. Outside of a study on the gestational exposure of rats to sumithion that increased social interactions in the adult offspring (Lehotzky et al. 1989), the majority of the work has focused on CPF in mice. Gestational exposure to CPF increased social interactions including ultrasound vocalizations and social investigation behavior in adolescent mice (Venerosi et al. 2006). Early postnatal CPF exposure increased aggressive behavior in male adult mice toward a male intruder (Ricceri et al. 2003, Ricceri et al. 2006). However, gestational CPF exposure decreased the aggressive attacks of nesting female mice towards a male intruder (Venerosi et al. 2010). Postnatal exposure of mice to CPF had no effect on social novelty preference but increased social investigatory behaviors such as social sniffing, following the partner, and mutual circling in female mice at adulthood (Venerosi et al. 2008). Gestational exposure to CPF also increased the social investigatory behavior (De Felice et al. 2014). All of these studies suggest that developmental exposure to OPs alter social behavior in adult rodents.

The disruption of several neurotransmitter systems can alter behavior during social play. Studies have been performed to attempt to understand the role of the endocannabinoid, opioid, and dopaminergic system in modulating social play behavior (Trezza and Vanderschuren 2008a, Trezza and Vanderschuren 2008b, Trezza and Vanderschuren 2009, Trezza et al. 2012). Trezza and Vanderschuren (2008a) demonstrated that the WIN55-215-22, a CB1 receptor agonist, reduced social play; whereas URB597, which indirectly stimulates the endocannabinoid system by the inhibition of FAAH and accumulation of AEA, increased social play. This indicates that stimulating the endocannabinoid system can have both negative (via global activation) and positive (via activation induced by AEA) effects on play. In another study, treatment with morphine, an opioid receptor agonist, enhanced social play, but this effect was reduced by CB1 receptor antagonist, SR141716A. Similarly, the effect of URB597 on the social play was completely blocked by naloxone, an opioid receptor antagonist (Trezza and Vanderschuren 2008b). The effects of URB597 but not morphine on social play were blocked by alpha-flupenthixol, a dopamine receptor antagonist (Trezza and Vanderschuren 2008b) suggesting that the activation of the endocannabinoid system by URB597 required increased activity of dopaminergic neurons (Lupica and Riegel 2005). These findings suggest a role for the endocannabinoid, opioid, and dopaminergic systems in the modulation of social play. In addition, all three work together in regulation of the reward process (Fattore et al. 2005, Berridge 2007). To date, our data suggest that developmental exposure to CPF alters the function of neurotransmitter systems that are required for normal social play. However, the neurotransmitter system that is impacted by CPF which is responsible for the altered social play is unknown and this is a critical gap

in the knowledge base. Thus, it is important to identify the molecular components that are the basis through which CPF exposure alters behavior.

1.8 Importance of proteomics in toxicology

Mass spectrometry-based proteomics is an experimental approach that focuses on protein characterization and quantification, and posttranslational modifications at a genome scale. The proteomic approach has been used in research to identify the key proteins and pathways that are altered in response to a toxicant. The main objective of using proteomics is to identify the new drug targets, new biomarkers, or toxicity signatures during preclinical studies, vulnerability evaluations, or diagnosis. It is also used to identify and understand the molecular mechanisms responsible for toxicity shown by different chemicals (George et al. 2010, George and Shukla 2011). Proteomics can be applied in different disciplines including toxicology to: 1) identify the subcellular location of different proteins; 2) identify and develop biomarkers from biological fluids such as serum and plasma; 3) identify the post-translational modifications (ubiquitination, phosphorylation, glycosylation, etc.) which will help elucidate the active forms of proteins during homeostasis and disease; and 4) identify the xenobiotic-protein adducts which will provide insights into cellular injury and necrosis and toxicological responses to an environmental chemical (Wetmore and Merrick 2004, Merrick 2008). Different proteomic techniques are available to analyze the proteome and these techniques were well described in the literature (Miller et al. 2014). In the beginning, the analysis involved the separation of proteins by 2-dimensional (2D) or 1 dimensional (1D) electrophoresis and subsequent identification by MS based techniques. However, in recent times, the gel-free separation by chromatographic techniques such as affinity

chromatography, ion exchange chromatography, and isoelectric focusing have been widely used to separate the proteins (Maurer 2012). For the quantitative analysis, labeling techniques have been introduced such as stable isotope labeling by amino acids in cell culture (SILAC), isobaric tag for relative and absolute quantitation (iTRAQ), and isotope-coded affinity tag (ICAT) (Chen et al. 2015, Moulder et al. 2017). However, label-free approaches, including spectral counting, ion intensity measurement, and multiple reaction monitoring are also used for quantitative analysis (Wolf-Yadlin et al. 2007). With regards to toxicology, there is no recommendation or restriction on the use of specific techniques. The selection of techniques is purely based on the research questions that need to be answered.

Proteomic approaches have been applied to identify the biomarkers of OP toxicity. A hybrid liquid chromatography (LC)/mass spectrometry (MS)/MS proteomics method was developed for the analysis of tryptic peptides resulting from butyrylcholinesterase inhibition following exposure to different pesticides including OPs (Sun and Lynn 2009). In the follow-up study, the authors utilized this method and identified acylpeptide hydrolase, a red blood cell cytosolic serine proteinase that removes N-acetylated amino acids from peptides and cleaves oxidized proteins, as a candidate biomarker of organophosphorus tricresyl phosphate exposure (Kim et al. 2010). Protein expression profiles in the liver of rats exposed to diazinon were analyzed by 2D-PAGE and mass spectrometry. Several proteins were significantly altered due to diazinon exposure and these proteins were involved in apoptosis, cell metabolism, and transport. Exposure to diazinon decreased the levels of catalase and thiolase, whereas increased the levels of isomerase suggesting that diazinon induces hepatotoxicity through oxidative

stress and apoptosis (Lari et al. 2014). Proteomic analysis was also used for detailed characterization of glycoprotein human butyrylcholinesterase, which is a potential bioscavenger of toxic OPs. This study demonstrated that only N-glycosylation sites, specifically mono and disialylated glycans, were present on butyrylcholinesterase; yet, no O-glycosylation or any other posttranslational modifications were present (Kolarich et al. 2008).

Proteomics techniques are also used to understand the mechanisms and neural circuits involved in pesticide induced neurodegenerative diseases. Alterations in the post-translational modifications of several proteins, including Parkin, tau, and superoxide dismutase 1 (SOD 1), have been linked to PD, AD, and Amyotrophic Lateral Sclerosis respectively. PD is a neurological disorder characterized by progressive degeneration of dopaminergic neurons in substantia nigra. Age, exposure to pesticides, and genetic factors are known risk factors for PD (Brown et al. 2006). Three differentially expressed proteins, complexin-1, alpha-enolase, and glia maturation factor-beta, were identified in striatum of maneb and paraquat treated mice by utilizing 2D-PAGE and mass spectrometry. These chemicals are known to play a role in etiology of PD and these results suggest the involvement of these three proteins in the chemical induced PD phenotype in mice (Patel et al. 2007). 2D-PAGE followed by LC-MS approach was used to identify the differentially expressed nigrostriatal proteins in cypermethrin induced dopaminergic neurodegeneration. Several proteins were differentially expressed in striatum and substantia nigra of cypermethrin treated rats. The pattern of expression of some of the proteins was related to microglial activation; whereas, the expression of other proteins was related to mitochondrial dysfunction. This suggests that cypermethrin

produces microglial activation dependent and independent changes in the expression pattern of proteins (Singh et al. 2011).

Proteomic approach has been applied to study the proteome of different brain regions. Proteomic analysis was utilized to identify the differentially expressed proteins in the amygdala of rats that were exposed to valproic acid (VPA) prenatally. Prenatal exposure to VPA leads to autism spectrum disorder phenotype in humans and rats. VPA altered a number of pathways, as determined by proteomic analysis, including signaling by Rho family GTPases, PKA signaling, and pathways involved in nervous system and cellular development (Barrett et al. 2017). In another study, 2D gel electrophoresis combined with mass spectrometry was utilized to establish synaptic proteome changes associated with motherhood. In the hypothalamus of mother rats, 29 differentially expressed proteins were identified that play a major role in energy homeostasis, protein folding, and metabolic processes suggesting the involvement of these processes in maternal adaptation (Udvari et al. 2017). The proteins and cellular signaling pathways involved in the molecular mechanisms of opioid addiction in the amygdala were analyzed by identifying the proteins involved in the process of morphine induced conditioned place preference by using 2D gel electrophoresis. Eighty proteins were differentially expressed, and these proteins were involved in metabolism, structure, cell signaling pathway, and the ubiquitin proteasome pathway (Lin et al. 2011). A quantitative label-free shotgun proteomics approach was utilized to identify differentially expressed proteins in the dorsal and ventral hippocampus of rats maintained on a high saturated fat and refined sugar (HFS) diet. For the dorsal hippocampus, 59 proteins were upregulated and 36 downregulated in HFS treated rats and pathway analysis indicated that these proteins

were involved in molecular transport and cellular and molecular signaling. For the ventral hippocampus, 27 proteins were upregulated while 25 proteins downregulated due to the HFS diet and these proteins were involved in cellular signaling and molecular functions (Francis et al. 2013). The protein expression in the orbitofrontal cortex of male Sprague-Dawley rats exposed to caffeine was analyzed using label-free shotgun proteomics. The protein expression was measured after behavioral testing and identified 157 differentially expressed proteins that play a role in cell to cell communication, mitochondrial function, and cytoskeletal regulation (Franklin et al. 2016). All of these data suggest that the proteomics technique can be successfully applied to analyze the changes in the proteome of different brain regions and this technique can be applied in our research to study the proteome of the amygdala and the effects of chemical exposure on the proteome.

1.9 Research objectives and significance

We have previously demonstrated that low-level CPF exposure inhibits the endocannabinoid metabolizing enzyme FAAH but does not inhibit AChE. This suggests that exposure to low levels of CPF can alter the endocannabinoid signaling without affecting the cholinergic system. We have also reported that early life exposure to low dosages of CPF reduces anxiety-like behavior in preadolescent rats. Our preliminary data demonstrates that this early life exposure to CPF also alters social behavior specifically enhancing social play. These data suggest that disruption of endocannabinoid system function may be responsible for the altered behavior of rats. Unfortunately, little progress has been made in understanding the molecular mechanisms of CPF at the low levels. Therefore, the *critical gap* in the knowledge base is the lack of understanding of the molecular mechanisms responsible for the persistent effects of

CPF on altered behavior. It is important to identify the mechanism of toxicity induced by exposure to low levels of CPF because this knowledge will help us to identify the most effective therapeutic strategies for OP-induced neurodegenerative disorders.

The *overall objective* of this research is to identify the neurotransmitter systems and their downstream pathways that are perturbed during CPF toxicity that are responsible for altered social behavior. The *central hypothesis* of the proposed research is that "*Developmental exposure to CPF inhibits FAAH, resulting in altered endocannabinoid signaling, which further leads to alterations in the functions of other neurotransmitter systems that are required for normal social behavior*". Our central hypothesis is based on several factors: 1) inhibition of FAAH by developmental exposure to CPF at levels that do not cause AChE inhibition; 2) developmental exposure to CPF alters the functions of the serotonergic, noradrenergic, and dopaminergic systems; 3) the endocannabinoid system plays an important role in normal brain development; 4) developmental exposure to CPF alters social behavior 5) the opioid and dopaminergic systems are important in regulating social behavior.

Finally, it is clear that there is a critical need to determine the basis for the developmental toxicity induced by exposure to CPF at low levels. Our preliminary studies have made the initial steps towards filling this critical gap in the knowledge base and provide support for this research. The next step is to fully understand the molecular mechanisms responsible for the altered behavior induced by CPF exposure. As an outcome of the research, we expect to have a positive impact on understanding those mechanisms because the identified changes in protein expression will identify the neurotransmitter systems that are the actual toxicological targets, which result in the

altered behavioral function induced by low level CPF exposure. This research is significant because the application of resulting new knowledge is expected to unveil the mechanistic target of CPF and how this mechanism leads to long-term effects on behavior. This new knowledge will allow us to develop better protective strategies and give insights into the detailed mechanisms of CPF.

This research was designed to identify the molecular mechanisms responsible for increased social play behavior in adolescent rats developmentally exposed to CPF. Chapter II will determine the changes in protein and gene expression in adolescent rats that are involved in social play, and also identify the neurotransmitter systems and downstream pathways that are altered by the social play. Chapter III will investigate the long-term changes in protein expression and associated neurotransmitter systems in adolescent rats following developmental exposure to CPF. Chapter IV will investigate the expression of proteins and associated neurotransmitter systems altered by early developmental exposure to CPF that are responsible for the increased levels of social play in CPF exposed rats. Chapter V will state the overall conclusions on the mechanisms responsible for altered behavior of rats developmentally exposed to CPF.

CHAPTER II

PROTEOMIC AND TRANSCRIPTIONAL PROFILING OF RAT AMYGDALA FOLLOWING SOCIAL PLAY

2.1 Abstract

Social play is a frequently studied behavior and it is the most characteristic form of social interaction observed in adolescent rats**.** Social play is necessary for adolescents to develop proper cognitive, emotional, and social competency. Deficits in social play have been observed in several neurodegenerative disorders such as autism, schizophrenia, and attention deficit hyperactivity disorder. However, the information available on neural substrates and the mechanism involved in social play is still limited. This study characterized social play by proteomic and transcriptional profiling studies. Social play was performed on male Sprague Dawley rats on postnatal day 38 and protein and gene expression in the amygdala was determined following behavioral testing. The proteomic analysis led to the identification of 170 differentially expressed proteins ($p \leq 0.05$) with 67 upregulated and 103 downregulated proteins. The transcriptomic analysis led to the identification of 188 genes (FDR$\leq$0.05) with 55 upregulated and 133 downregulated genes. Based on both protein and gene expression data, DAVID analysis revealed that social play altered neurotransmitter signaling including GABAergic and glutamatergic signaling and G-protein coupled receptor (GPCR) signaling. These data suggest that the synaptic levels of GABA and glutamate increased during play. Ingenuity Pathway

Analysis (IPA) confirmed these alterations. IPA also revealed that differentially expressed genes/proteins in our data had significant over representation of additional neurotransmitter signaling systems, including the opioid, serotonin, and dopamine systems, suggesting that play alters the systems involved in the regulation of reward. In addition, corticotropin-releasing hormone signaling was altered indicating that an increased level of stress occurs during play. Our data suggest that increased inhibitory GPCR signaling in these neurotransmitter pathways occurs following social play as a physiological response to regulate the induced level of reward and stress and to maintain the excitatory-inhibitory balance in the neurotransmitter systems.

2.2 Introduction

Social play is a non-mother directed behavior and refers to specific social, sexual, or aggressive behaviors that are directed at conspecifics. This behavior involves both the solicitation of the potential play partner and the actual interactions that occur between the play partners with the latter having a high reward value (Pellis and Pellis 1991). Social play behavior is observed in the majority of mammalian species including humans. When compared to other species including mice, rats are the ideal species to study social behavior because they show abundant levels of social play during adolescence and it is easy to characterize and quantify the different aspects of social play in rats (Vanderschuren and Trezza 2014). The analysis of social play is characterized by measuring different behavioral events such as social grooming, body and genital sniffing, crawling over/under, chasing, pouncing, nape attacks, wrestling, boxing, and pinning (Panksepp and Beatty 1980, Meaney and Stewart 1981, Plonsky and Freeman 1982). Monitoring social play serves as a guide to measure different aspects of social

development. For example, rats who play more show stronger bonds with the group later in life. Social play can also assess cognitive abilities which are necessary to express and communicate in society (Meaney and Stewart 1981, Meaney et al. 1985, Takahashi 1986). Social play is accompanied by the sensation of pleasure and excitement and has a function in emotional development. Finally, social play is important in the development of social skills that are necessary to function normally in society.

Social play is also referred to as play fighting or rough-and-tumble play (Panksepp et al. 1984, Vanderschuren and Trezza 2014) and is a form of play where one rat attacks and the other defends. The frequency of the attacks and the defense tactics utilized vary between groups and have been linked to different neural mechanisms (Pellis and Pellis 1998). The play usually starts before weaning but occurs most frequently during adolescence (PND 30-40) and then declines with the onset of sexual maturity (Vanderschuren et al. 1997b, Vanderschuren et al. 2016). This covers from the juvenile period to mid-adolescence in rodents and from childhood to early/mid-adolescence in humans. Participation in social play during adolescence is necessary in order to develop proper cognitive, emotional, and social competency (Pellis and Pellis 2007). It has been suggested that adolescent social play induces the secretion of growth factors in different regions of the brain such as the brain stem, midbrain, lower forebrain, and parts of the cortex and that these growth factors are necessary for the development of those specific regions (Gordon et al. 2003). Generally, social play only occurs when the primary needs are met and the environmental conditions are considered safe. Food deprivation, unfamiliar environments, and high-intensity light usually suppress social play (Siviy and Panksepp 1985, Vanderschuren et al. 1995b).

Most of the knowledge concerning the role of different neurotransmitter systems involved in social play has been derived from studies involving the effects of pharmacological manipulations on play activity(Trezza and Vanderschuren 2008a, Trezza and Vanderschuren 2008b, Trezza and Vanderschuren 2009). From these studies, it has been demonstrated that the opioid, dopaminergic, serotonergic, and endocannabinoid systems play prominent roles in the modulation of social play. These studies have described the role of each neurotransmitter systems in the development of social play rather than how these systems are modulated during social play in a normal animal. Thus, the complete understanding of the neural substrates and the mechanisms that are involved in social play is still quite limited. There is a need to determine the changes in these systems and other neural pathways that occur as a result of participation in social play without the introduction of any pharmacological manipulations.

The positive emotions that are processed by the brain during social play are important for emotional well-being and human health. Any social play impairments, including social isolation during adolescence, can induce a variety of behavioral impairments such as autism, attention deficit hyperactivity disorder, and early onset schizophrenia in later life (Alessandri 1992, Moller and Husby 2000, Jordan 2003). Therefore, understanding the neurobiology involved in social play is important for the potential development of therapeutic strategies to treat certain social impairments that are present in many psychiatric disorders (Vanderschuren et al. 2016).

The objective of this study is to investigate the changes in protein and gene expression that occur in adolescent rats involved in social play in order to identify the neurotransmitter systems and downstream pathways that are altered by that involvement.

For this purpose, label-free shotgun proteomics was utilized to measure the differential protein expression and RNA-sequencing (RNA-seq) was performed to measure the gene expression in the amygdala of adolescent rats involved in play and adolescent rats not involved in play. Social play stimulates the reward pathway but most of the literature focus has been on the role of the ventral tegmental area (VTA) and nucleus accumbens (NAc) in that pathway. Much less attention has been given to the involvement of the reward pathway in social play in other regions. The amygdala plays a prominent role in reward processing mainly through critical interconnections with the VTA, NAc, and frontal cortex regions (Haber and Knutson 2010, Vanderschuren and Trezza 2014). However, the information available about the reward pathway in the amygdala during social play is limited. Therefore, the changes in the proteome and transcriptome of the amygdala that occur as a result of participation in social play were determined. Analysis of the differentially expressed genes and proteins in the context of canonical pathways and molecular functions involved in social play was also performed.

2.3 Methods

2.3.1 Animal maintenance

Adult male and female Sprague Dawley rats (CD IGS; Envigo, Indianapolis, IN) were used for breeding. These rats were housed in an Association for Assessment and Accreditation of Laboratory Animal Care--accredited facility under constant temperature (22˚C), on a 12 h light and 12 h dark cycle with lights on between 0700 and 1900. Rats were provided with food and water freely available during experimentation. The procedures used in this project were approved by the Mississippi State University Institutional Animal Care and Use Committee. Females were separated from males once

they appeared to be pregnant. The date of birth was designated as PND0. Male rat pups within each litter were used for behavioral testing. Rats were weaned on PND21 and marking was continued until behavioral testing to allow identification.

2.3.2 Behavioral testing

The behavioral arena was a clear empty plastic cage with bright light (~700 lux). Each test session was recorded using a remotely operated Canon EOS Rebel digital camera. Testing was performed on PND38. Following a 24-hour isolation period, two rats of the same treatment, age, and size but from different litters were placed into different corners of the behavioral arena. The rats remained in the arena together for 600s. After each test, the cage was emptied, cleaned with 70% ethanol, dried, and refilled with fresh litter.

For each behavioral pair, one rat was sacrificed for transcriptomic analysis at 15 min following social play and the other rat was sacrificed for proteomic analysis at 3 hours following social play. The non-behavioral rats were also sacrificed on PND 38 following a 24-hour isolation period. At sacrifice, whole brains were collected and stored at -80˚C. An RNAase free environment was maintained throughout the tissue collection process. A total of three rat brains from each group were used for each analysis. Frozen brains were sliced using a manual tissue slicer to obtain 500-micron sections which were stored on microscopic slides until the amygdala was collected using punches (1mm size). The Paxinos and Watson (1998) atlas was used as a reference. The obtained amygdala tissue was processed for proteomic and transcriptomic analysis.

2.3.3 Proteomic analyses

2.3.3.1 Protein extraction, fractionation and digestion

Collected amygdala tissue was lysed in NP-40 lysis buffer (150 mM NaCl, 20 mM $MgCl_2$, 50 mM Tris-HCl pH 7.4, 0.5% NP-40) supplemented with 1mM of the serine protease inhibitor, phenylmethylsulfonyl fluoride (PMSF) using a Microson™ ultrasonic cell disruptor. The debris was removed by centrifugation at 21,000g at 4˚C for 30 min. The protein concentration was measured using a Pierce™ BCA protein assay kit (Thermo Scientific). From each sample, 100 µg of protein was precipitated by chloroform/methanol extraction. Briefly, the sample volume was adjusted to 200 µl using NP-40 lysis buffer. To each sample, 600 µl of methanol, 150 µl of chloroform, and 450 µl of milliQ-H_20 were added, vortexed, and centrifuged at room temp for 1 min, at 21,000g. The upper aqueous phase was discarded and 450 µl of methanol was added to the lower phase, vortexed, and centrifuged under the same conditions for 2 min. The supernatant was discarded and protein digestion was performed by suspending the pellet in 33 µl of 100 mM Tris-HCl (pH 7.8) containing 6 M urea. The samples were reduced with 1.6 µl of 200 mM dithiothreitol (DTT) for 45min at room temperature and alkylated with 6.6 µl of 200 mM iodoacetamide (IAA) for 45 min at room temperature. The alkylation reaction was then quenched by adding 20 µl of 200 mM DTT for 45 min at room temperature. The urea concentration was reduced by adding 258 µl of milliQ-H_20. Finally, the proteins were digested with trypsin (sequencing grade modified trypsin, Promega) at 1:50 ratio for 18 hr at 37˚C. Protein digestion was terminated by lowering the pH of each sample to <6 by adding concentrated acetic acid. The samples were desalted using C18 SepPak columns (Waters, USA). The sample was then dried down in

speed vac. All samples were submitted to the University of Arizona Proteomic Consortium for analysis by tandem mass spectrometry coupled to liquid chromatography (LC-MS/MS).

2.3.3.2 Mass spectrometry

The LC-MS/MS analysis of trypsin digested protein samples was carried out using a LTQ Orbitrap Velos mass spectrometer (Thermo Fisher Scientific, San Jose, CA) equipped with an Advion nanomate ESI source (Advion, Ithaca, NY. Peptides were eluted from a C18 precolumn (100-µm id × 2 cm, Thermo Fisher Scientific) onto an analytical column (75-µm ID × 10 cm, C18, Thermo Fisher Scientific) using a beginning concentration of 2% solvent B (acetonitrile, 0.1% formic acid) for 5 minutes, then a 2–7% gradient of solvent B over 5 minutes, followed by a 7-15 % gradient of solvent B over 50 minutes, a 15-35% gradient of solvent B over 60 minutes, a 35-40% gradient of solvent B over 28 minutes, a 40-85% gradient of solvent B over 5 minutes, held at solvent 85% B for 10 minutes, 85-2% gradient of solvent B for 1 minute then held at 2% solvent B for 16 min. All flow rates were at 400 nl/min. Solvent A consisted of water and 0.1% formic acid. Data dependent scanning was performed by the Xcalibur v 2.1.0 software using a survey mass scan at 60,000 resolutions in the Orbitrap analyzer scanning m/z 400–1600, followed by collision-induced dissociation (CID) tandem mass spectrometry (MS/MS) of the fourteen most intense ions in the linear ion trap analyzer. Precursor ions were selected by the monoisotopic precursor selection (MIPS) setting with selection or rejection of ions held to a +/− 10 ppm window. Dynamic exclusion was set to place any selected m/z on an exclusion list for 45 seconds after a single MS/MS.

2.3.3.3 Data processing and quantitation

The tandem mass spectra were extracted by Thermo Proteome Discoverer 1.3 (Thermo Scientific, USA) using the Sequest algorithm (Thermo Fisher Scientific, San Jose, CA, USA; version 1.3.0.339). Sequest was set up to search RattusNovergicus_UniprotKB assuming the digestion enzyme as trypsin. Fully tryptic peptides with up to 2 missed cleavage sites were selected. While searching with Sequest, fragment ion mass tolerance of 0.8 Da and a parent ion tolerance of 10.0 PPM were used. Oxidation of methionine and carbamidomethyl of cysteine were specified in Sequest as variable modifications. The results were also validated using X!Tandem, another search engine and displayed with Scaffold v 4.5.1 (Proteome Software Inc., Portland OR), a program that relies on various search engine results (i.e.: Sequest, X!Tandem, MASCOT) and uses Bayesian statistics to reliably identify more spectra (Keller et al. 2002). Peptide identifications were accepted if they could be established at greater than 95.0% probability by the Scaffold Local FDR algorithm. Protein identifications were accepted if they could be established at greater than 95.0% probability and contained at least 2 identified peptides. Protein probabilities were assigned by the Protein Prophet algorithm (Nesvizhskii et al. 2003). Proteins that contain similar peptides and cannot be differentiated based on MS/MS analysis alone were grouped to satisfy the principles of parsimony. Proteins sharing significant peptide evidence were grouped into clusters. Label-free protein quantitation using the sum of weighted spectra associated with a protein was performed in Scaffold. The proteins that passed the Fisher's exact test with a p-value of ≤ 0.05 were used for biological interpretation. Differentially expressed proteins (DEP) were identified based on a fold change value, which was calculated by

applying normalization in Scaffold. A minimum value of 0.2 was used for the samples in which a protein was not identified.

2.3.4 RNA-seq and Transcriptomic Analysis

Total RNA was isolated from amygdala using a Qiagen miRNA easy micro kit (Germantown, MD) which is specialized for isolation of RNA from lipid rich tissue. The RNA quality was verified by NanoDrop. Each RNA sample containing 1 µg of RNA was used for poly A selected RNA-seq library preparation using the NEB Ultra-Directional RNA Library Prep Kit for Illumina, E7420. Stranded paired-end sequencing data with read lengths of 100 bp (2x100 bp) were generated by Institute for Genomics, Biocomputing & Biotechnology core using the Illumina HiSeq 4000 system. An average of 52.8 million read pairs per replicate were generated. RNA-seq reads were mapped to the rat reference genome (rn6) and transcriptome (Ensembl, release 84) by STAR aligner (v.2.5.2b) (Dobin et al. 2013) allowing up to 3 mismatches per read. Cuffdiff (v2.2.1) (Trapnell et al. 2013) program was used to calculate RNA-seq based gene expression levels using the FPKM (fragments per kilobase of exon per million fragments mapped) and then differentially expressed genes (DEG) were identified between two conditions at FDR<=5%, and greater than two-fold difference in average FPKM.

2.3.5 Gene ontology analysis

The database for Annotation, Visualization and Integrated Discovery (DAVID) was used for obtaining functional annotation of differentially expressed genes and proteins and to perform GO enrichment analysis. GO terms with a p-value < 0.05 and FDR <0.05 were considered to be enriched in our gene/protein lists. Statistical

significance of these enriched GO terms was determined by EASE Score Threshold, which is a modified Fisher exact p-value along with FDR correction. The cellular location and biological processes enriched among DEP and DEG were identified (Dennis et al. 2003). The number of molecules for each GO term was calculated and plotted in Excel.

2.3.6 Pathway analysis

Functional annotations, canonical pathways, and networks of DEP and DEG were analyzed using Ingenuity Pathway Analysis (IPA, QIAGEN Inc., https://www.qiagenbioinformatics.com/products/ingenuity-pathway-analysis). Fisher's exact test was utilized in all those analyses to identify the overrepresented proteins or genes with a p-value of less than 0.05. Functional annotation tool in IPA was used to classify the DEP and DEG based on their physiological and molecular functions. Network analysis is a visual representation of the interactions among identified proteins or genes. In addition to identifying the canonical pathways associated with different neurotransmitter systems including the opioid, serotonergic, and dopaminergic systems, other functions associated with DEP and DEG including behavior, nervous system development and function, cell-cell signaling, and cellular assembly and organization were also identified.

2.3.7 Western blotting

Three hours following behavioral testing, brains were extracted and frozen on dry ice. Brains were also collected from a matching cohort of non-behavioral animals. Frozen brains were sliced at 500-micron increments, and the amygdala was collected by

punching. The collected tissue was lysed in NP-40 lysis buffer (150 mM NaCl, 20 mM $MgCl_2$, 50 mM Tris-HCl pH 7.4, 0.5% NP-40) supplemented with 1mM of the serine protease inhibitor, phenylmethylsulfonyl fluoride (PMSF) using a Microson™ ultrasonic cell disruptor. The debris was removed by centrifugation at 21,000g at 4˚C for 30 min. The protein concentration was measured using a Pierce™ BCA protein assay kit (Thermo Scientific). The protein extracts containing the same amount of protein were resolved by 10% polyacrylamide gel electrophoresis and then transferred to a polyvinylidene difluoride (PVDF) membrane. The proteins of interest were detected using primary antibodies against regulatory G-protein signaling 7 (1:1000 dilution, Santa Cruz Biotechnology, USA), G protein alpha o (1:750 dilution, Santa Cruz Biotechnology, USA), monoamine oxidase A (1:500 dilution, Santa Cruz Biotechnology, USA), and GABA type A receptor (1:500 dilution, Santa Cruz Biotechnology, USA) followed by a mouse IgGk light chain binding protein conjugate to horseradish peroxidase (1:5000 dilution, Santa Cruz Biotechnology, USA) and visualized using SuperSignal West Pico PLUS Chemiluminescent substrate. The bands were then quantified using ImageJ software (National Institute of Health). Anti-beta actin antibody was used as a loading control (1:20,000 dilution, Sigma Aldrich, USA) (n=3).

2.3.8 Statistical analysis

Statistical analysis was performed on western blot data using GraphPad Prism version 7.00 for Windows, GraphPad Software, California, USA. The t-test was used to identify the statistically significant differences between behavioral control and non-behavioral control samples at $p<0.05$. Prior to analysis, the data were normalized by log transformation.

2.4 Results

In this study, we investigated the changes in the proteome and transcriptome of the amygdala of adolescent rats following participation in social play. In the proteome, the total number of proteins identified were 1387, of those 102 proteins were unique to the non-behavioral group and 196 proteins were unique to the behavioral group. The fold change values and p-values were calculated for all proteins and only those proteins with a p-value of less than 0.05 were selected for further analysis. A total of 170 DEP were selected with 67 upregulated and 103 downregulated proteins (Table A.1). In the transcriptome, the total number of genes expressed was 19,107. The number of differentially expressed genes identified at FDR<0.05 and p-value <0.05 were 188. Of those, 133 genes were downregulated, and 55 genes were upregulated due to social play (Table A.2).

2.4.1 Gene ontology analysis

The 170 DEP and 188 DEG were further analyzed by DAVID functional annotation tool. Annotations in DAVID are based on Gene Ontology tool that describes cellular location, molecular function, and biological processes, and this bioinformatics resource enables the identification of enriched GO terms among DEP and DEG (Dennis et al. 2003). In our analysis, with respect to protein expression, 169 of 170 DEP mapped to the database and were subjected to GO analysis to interpret their cellular location and biological processes. An analysis of the 169 proteins using DAVID functional annotation tool, GOTERM_CC_DIRECT, resulted in the identification of 58 terms and using GOTERM_BP_DIRECT resulted in the identification of 44 terms as significantly changed ($p \leq 0.05$). Most of the proteins were located in the myelin sheath, dendrite,

axon, synaptic vesicle, proteasome complex, and synapse. Some of the significantly ($p \leq 0.05$) changed GO terms related to the cellular location are listed in Figure 2.1A and Table 2.1. The important biological processes enriched among DEP were neurotransmitter secretion and transport, axonogenesis, regulation of GTPase activity, locomotory behavior, and axon guidance. The significantly changed terms related to biological processes are listed in Figure 2.1B and Table 2.2.

With respect to gene expression, DAVID mapped 170 of 188 genes and GOTERM_CC_DIRECT analysis resulted in 20 terms and GOTERM_BP_DIRECT resulted in the identification of 63 terms as significantly changed ($p \leq 0.05$). Most of the genes were located in the synapse, postsynaptic density, postsynaptic membrane, dendrite, axon, and neuron projection. Some of the significantly ($p \leq 0.05$) changed GO terms related to the cellular location are listed in Figure 2.2A and Table 2.3. The important biological processes enriched due to social play were GABA signaling, glutamate signaling, brain development, chemical synaptic transmission, and locomotor behavior. The significantly changed terms related to biological processes are listed in Figure 2.2B and Table 2.4.

2.4.2 Pathway analysis

The canonical pathways, molecular and cellular functions, and physiological functions associated with DEP were analyzed by IPA. The 170 proteins with a p-value of less than 0.05 along with their fold change value were uploaded into IPA. Based on protein expression, 87 canonical pathways were significantly ($p \leq 0.05$) altered by social play. Of those, 12 canonical pathways that play an important role in neurological function and are relevant to social play were listed in Figure 2.3A. IPA can predict whether the

pathway is activated or inhibited based on Z score, which is a statistical measure of the match between expected relationship direction and observed gene or protein expression. The Z score of less than -2 indicates the inhibition of canonical pathway, which is represented in blue color and the Z score of greater than 2 indicates the activation of the pathway, which is represented in orange color. The different pathways that were inhibited by social play included protein kinase A signaling, cAMP-mediated signaling, opioid signaling, and corticotropin-releasing hormone signaling. The activated pathways were Gαi signaling, Gαq signaling, and signaling by Rho family GTPases. The neurotransmitter pathways altered by social play were opioid signaling, dopamine receptor signaling, serotonin signaling, and GABA receptor signaling. The degradation pathways of dopamine, noradrenaline, and adrenaline were also altered and monoamine oxidase A (MAOA), which was downregulated by social play, was associated with most of the degradation pathways.

The 188 DEG were also uploaded into IPA to analyze the canonical pathways and functions altered due to social play. Based on differential gene expression, 55 canonical pathways were significantly ($p \leq 0.05$) altered by social play. Eight of those canonical pathways that are related to neurotransmitter signaling and G-protein coupled receptor (GPCR) signaling were shown in Figure 2.3B. The opioid signaling, CREB signaling in neurons, and G beta gamma signaling pathways were inhibited by social play. However, corticotropin-releasing hormone signaling and ERK/ MAPK signaling were activated by social play. The neurotransmitter pathways altered by social play were opioid signaling, glutamate receptor signaling, and GABA receptor signaling (Figure 2.3B).

IPA analysis showed that genes and proteins significantly altered by social play represented similar molecular and cellular functions (Figure 2.4A and Figure 2.4B). The top molecular functions identified from significant changes in gene/protein expression by social play include cell signaling, molecular transport, cellular movement, and cellular function and maintenance. Our results also showed that similar physiological functions were altered by social play at both gene and protein levels, including behavior, nervous system development, organ development, organ functions, and tissue development and functions. (Figure 2.5A and Figure 2.5B).

Network analysis in IPA identified a network of 19 interconnecting proteins, most of the proteins in the network were G-protein signaling-related proteins. Nodes shown in red in the network indicates upregulation while green indicates the downregulation of proteins in our dataset. The proteins in this network were associated with different canonical pathways such as the opioid signaling pathway, GABA receptor signaling, G-protein receptor signaling, serotonin receptor signaling, glutamate receptor signaling, and dopamine receptor signaling (Figure 2.6).

2.4.3 Western blotting

The expression of proteins which play an important role in different neurotransmitter signaling was confirmed by western blot analysis. The differential protein expression of regulatory G protein signaling 7 (RGS7), G protein alpha o (Gαo), monoamine oxidase A (MAOA), and GABA type A receptor in the amygdala of behavior and non-behavior rats was analyzed. All these proteins were downregulated by social play. There was a significant difference ($p \leq 0.05$) in protein levels between control behavioral and control nonbehavioral rats with respect to the expression of RGS7

(p=0.0037), Gαo (p=0.0001), and MAOA (p=0.0030) proteins (Figure 2.7A – 2.7C). However, the protein expression of GABA type A receptor in control behavioral rats was not statistically significantly different (p=0.068) from control non-behavior rats but demonstrated a trend towards significance (Figure 2.7D). The protein bands were shown in Figure 2.7E.

2.5 Discussion

Social play is a highly rewarding behavior, and the information about the neural substrates and the mechanisms that are involved in social play are limited. Therefore, to attempt to understand the neurobiology of social play, omics technology was utilized. This study presents the first proteomic and transcriptomic analysis of the amygdala of adolescent rats following participation in social play. The results suggest that a significant number of proteins and genes were differentially expressed due to participation in social play. Specifically, 67 proteins and 55 genes were upregulated and 103 proteins and 133 genes were downregulated indicating that more downregulation was observed compared to upregulation. These DEP and DEG are involved in a broad range of biological processes suggesting complex changes in the cellular proteome and transcriptome. However, these results only highlight the dynamic changes in protein and gene expression at one specific time point following social play.

DAVID analysis revealed that most of the proteins and genes were located in synapse-related regions such as the synapse, postsynaptic density, and synaptic vesicle suggesting changes in synaptic functions such as neurotransmission. This is also supported by the biological processes data where the significantly enriched biological processes included those that occur in the synapse such as neurotransmitter secretion and

transport and glutamate and GABA signaling. This indicates the importance of synaptic function and neurotransmission in social play. This is not surprising since many different neurotransmitters/neuromodulators play a role in social play including the opioids, dopamine, serotonin, and endocannabinoids (Trezza and Vanderschuren 2008a, Trezza and Vanderschuren 2008b, Trezza et al. 2012). In our study, signaling in multiple neurotransmitter systems, including the opioid, dopamine, serotonin, glutamate, and GABA systems, were predicted to be altered by social play. The opioid signaling pathway was predicted to be inhibited by social play based on analysis of both the protein expression and the gene expression. It has been demonstrated that the rewarding aspects of social play depend on brain opioid activity (Trezza and Vanderschuren 2008a). This reward can be dissociated into different components such as motivational (wanting), hedonic (liking), and cognitive (learning) properties (Berridge et al. 2009, Trezza et al. 2011a). The opioids increase social play by increasing hedonic properties of play. The literature suggest that opioids can have both positive and negative effects on social play depending on the type of receptor and the region of the brain involved (Trezza et al. 2010). However, in this study, the inhibition of the opioid signaling pathway that occurs following social play appears to be a response to the elevated signaling that occurred during the actual play and is an attempt to regulate the opioid-mediated reward involved in social play.

The dopamine and serotonin signaling were also represented by social play based on the altered protein expression. The role of the dopaminergic system in social play has been well described and dopamine modulates the motivational components of the reward associated with play. The general notion is that enhancing the dopaminergic

neurotransmission increases social play. However, the role of dopaminergic neurotransmission in the modulation of social play is less straightforward than expected. Although decreasing dopaminergic neurotransmission decreased social play (Beatty et al. 1984), increasing the neurotransmission both increased and decreased social play (Niesink and Van Ree 1989, Vanderschuren et al. 2016). This could be because of the involvement of other compensatory neurotransmitter signaling such as serotonin and nor-adrenaline in the modulation of social play (Homberg et al. 2007). In contrast to dopamine and opioids whose activity is required to increase the reward value of social play, the serotonin activity is usually increased due to reward. There is a large body of literature which describes the association between serotonin and aggression and sexual behavior but the information on the role of serotonin in reward is limited. Previously, it has been reported that increased serotonergic neurotransmission reduces social play behavior in peri-adolescent rats (Homberg et al. 2007). In contrast, the increase in serotonergic activity was observed in response to social rewards such as food, social interaction, and sex (Li et al. 2016). This suggests that an increase in serotonergic activity will decrease social play but social play will increase the activity of serotonin. We also observed the downregulation of MAOA, which plays an important role in the breakdown of monoamines including serotonin and dopamine. The protein expression of MAOA was also confirmed by western blot analysis. The downregulation of MAOA suggests the increased synaptic levels of dopamine and serotonin. Based on protein expression of MAOA, it can be hypothesized that the serotonergic and dopaminergic activity was increased by social play.

Glutamate (excitatory) and GABA (inhibitory) neurotransmitter signaling were identified by gene expression but not by protein expression when analyzed by DAVID. However, IPA predicted that signaling in both these neurotransmitter systems was altered with respect to both protein and gene expression. The data demonstrated changes in gene expression of the GABA type A receptor, the glutamate NMDA receptor, the kainate receptor, and the GABA transporter which were all downregulated by social play. Previously, a significant increase in GABA and glutamate levels was observed during social play in the lateral septum (Bredewold et al. 2015). Thus, the downregulation of GABA and glutamate receptors following social play could be a physiological adaptation to the increased synaptic levels of GABA and glutamate induced during social play and this decrease could be an effort to regulate the excitatory-inhibitory balance that has been altered during social play. Interestingly, the protein expression of GABA type A receptor was also decreased by social play. This decreased protein expression was confirmed by western blot analysis. The GABA type A receptor is known to regulate GABAergic inhibition in the amygdala. Maintaining GABAergic inhibition in the amygdala is critical for the appropriate expression of emotions such as fear and anxiety (Liu et al. 2017). It has been demonstrated that decreasing GABA signaling in the amygdala decreases sociability indicating the importance of GABAergic signaling in social play (Paine et al. 2017). In our study, both protein and gene expression of GABA type A receptor were downregulated by social play as a physiological response to an increase in synaptic GABA levels during social play.

The regulation of GTPase activity was another important biological process that was enriched based on differential protein expression. However, this process was not

enriched based on the DEG. The different GPCR signaling-related proteins that were associated with this process such as regulator of G-protein signaling 7 (RGS7), Rap1 GTPase activating protein (Rap 1 GAP), and G-protein subunit α o (Gαo). All these proteins were downregulated by social play. The protein expression of RGS7 and Gαo were confirmed by western blot analysis. However, no differential expression of the genes related to these proteins was identified in the transcriptomic analysis. It is very likely that the changes in gene expression that resulted in the changes in the protein levels of these components was a brief event and occurred during a window of time that did not correspond to the time we selected for determining gene expression. RGS7 regulates the strength and duration of GPCR signaling by acting as a GTPase activating protein for the G protein Gα subunit thereby terminating the GPCR signaling through deactivation (Ross and Wilkie 2000). It has been demonstrated that RGS7 negatively regulates reward behavior that is mediated by opioid signaling in the striatum and genetic deletion of RGS7 increases the rewarding effects induced by morphine administration (Sutton et al. 2016). If similar actions occur in the amygdala, the observed downregulation of RGS7 that occurs as a result of social play could be a process by which the opioid-mediated reward is regulated by indirectly increasing GPCR signaling.

Gα is the subunit of heterotrimeric guanine nucleotide binding protein (G protein), which is composed of three subunits Gα, Gβ, and Gγ. These G proteins are coupled to GPCR and mediate signaling upon binding of an endogenous ligand to the receptor (Hollmann et al. 2005, Zelek-Molik et al. 2012). Signal specificity is determined by the type of Gα subunit that interacts with the receptors. Mainly, there are four different types of Gα subunits involved in different signaling pathways: Gs (stimulates

the adenylyl cyclase (AC)), Gi/o (inhibits AC), Gq/11 (stimulates phospholipase C β), G 12/13 (modulates small G proteins such as Ras GTPases) (New and Wong 2007). In this study, G protein alpha o (Gαo) was downregulated by social play. Whenever there is downregulation of a particular isoform of a G protein such as Gαo, the other G proteins, including Gαi, provide functional compensation with or without an increase in the levels of these isoforms (Lamberts et al. 2011). This suggests the possibility that upregulation of other isoforms in the Gαi/o family occurred including Gαi. Interestingly, IPA predicted that Gαi signaling was activated by social play.

Rap GTPases are small G proteins involved in different cellular processes including cell proliferation, differentiation, and cell movement. In the nervous system, these GTPases play an important role in neuronal differentiation, neuronal polarity, and axon growth. Rap GTPase activating proteins (Rap GAPs) inactivate Rap signaling by accelerating the intrinsic GTP hydrolysis rate of Rap (Spilker and Kreutz 2010). The protein levels of Rap 1 GAP were downregulated by social play in our study. To date, no specific function of Rap1 GAP in social play has been proposed. Based on the present study, Rap 1 GAP appears to have a role in this behavior. This downregulation of Rap 1 GAP suggests that an increase in GPCR signaling is occurring. We also observed the downregulation of adenylate cyclase 5 (ADCY 5) which is the effector protein of Gαs and Gαi/o. This downregulation of G-protein signaling-related proteins (*e.g.,* RGS7, Rap 1 GAP, Gαo, and ADCY 5) suggests the inhibition of G-protein signaling or, in other words, the activation of the inhibitory pathway of GPCR signaling.

The other set of canonical pathways represented by social play were Protein Kinase A signaling, cAMP-mediated signaling, and Gαi signaling, which are part of

GPCR signaling. These pathways were identified based on only protein expression but not gene expression. The protein kinase A and cAMP signaling were inhibited, whereas Gαi signaling was activated suggesting the activation of the inhibitory pathway of GPCR signaling. As we mentioned earlier, Gαi inhibits adenylate cyclase, thereby decreases the levels of cAMP and PKA. In this study, downregulation of ADCY 5, Rap1 GAP, and RGS 7 support the activation of Gαi signaling. The Rap 1 GAP and RGS 7 inactivate the Gα subunit by increasing the GTP hydrolysis. However, these proteins were downregulated and thus suggest the activation of Gαi signaling. Most of the neurotransmitter systems contain metabotropic receptors that mediate their downstream signaling by GPCR signaling (Wettschureck and Offermanns 2005). All the neurotransmitter pathways can mediate both stimulatory (through stimulation of ADCY or increasing the ion current through ionotropic receptors) and inhibitory (through inhibition of ADCY) signaling. Here, the affected canonical pathways identified suggest that the inhibitory pathways of the neurotransmitter systems have been activated following social play possibly as a regulatory mechanism to control the neuronal activation induced by social play.

Another signaling pathway predicted to be altered by social play was corticotropin-releasing hormone (CRH) signaling which was activated 15 minutes following social play but inhibited three hours following social play. CRH signaling is also a GPCR signaling and is a key modulator of stress responses in the behavior. Previous studies have demonstrated that the amygdala is rich in CRH positive neurons (Broccoli et al. 2018). The activation of the CRH signaling pathway immediately after social play suggests an increase in the level of stress which might have been the result of

the high-intensity light and unfamiliar environment of behavioral test arena. These factors generally increase anxiety and it has previously been demonstrated that the expression of components related to CRH signaling was associated with anxiety-like behavior (Kentner et al. 2018). Based on that thought, these data suggest that social play increases CRH signaling due to increase in the levels of anxiety and stress during play. However, increased CRH signaling could be merely an outcome of the physical exertion that occurred during the actual play since physical exercise in rodents has been shown to increases plasma corticosterone, a down-stream product of CRH signaling (Kuoppasalmi et al. 1980, Coleman et al. 1998, Girard and Garland 2002). By three hours after social play, the CRH signaling pathway was inhibited suggesting that a physiological response by the body to the high levels of CRH signaling had occurred in order to maintain homeostasis.

Based on both protein and gene expression, two important physiological functions represented by social play based on both protein and gene expression were behavior and nervous system development and function. The same proteins that were associated with most of the neurotransmitter signaling pathways were also associated with behavior and nervous system development and function indicating that these proteins are the main downstream effectors of social play. These proteins included ADCY 5, Gαo, GABA type A receptor, monoamine oxidase A, RGS7, and Rap 1 GAP. However, the genes associated with these functions included ADCY 7, GABA type A receptor, and glutamate receptors.

In conclusion, previous studies have demonstrated the role of the various neurotransmitter systems in social play using pharmacological manipulation studies.

However, the effect of social play on these systems has not been elucidated. Our results clearly report the effect of social play on different neurotransmitter systems and the protein and genes that are associated with these systems. The alteration of opioid, dopaminergic, and serotonergic signaling suggest that the reward pathway is active for a long time even after cessation of social play. However, the alteration of GPCR signaling including the inhibition of PKA signaling and cAMP signaling and activation of Gαi signaling suggest the activation of inhibitory GPCR signaling which also suggest the inhibition of reward pathway three hours following social play as a physiological response by the body. Overall, the data suggest how long these neurotransmitters signaling are stimulated and when these signaling are started to inhibit to regulate the reward, stress, and excitatory-inhibitory balance.

Table 2.1 Significantly changed cellular location GO terms represented by differentially expressed proteins

Term	Count	%	P-value	Benjamini
Myelin sheath	25	14.79	6.96E-21	2.21E-18
Dendrite	18	10.65	1.59E-06	4.20E-05
Axon	15	8.87	4.83E-06	1.09E-04
Synaptic vesicle	9	5.32	2.14E-05	3.99E-04
Cell body	8	4.73	2.67E-05	4.71E-04
Growth cone	8	4.73	3.80E-04	0.0048
Proteasome complex	5	2.95	0.002	0.012
Synapse	9	5.33	0.005	0.042
Postsynaptic density	8	4.74	0.005	0.045

Number of differentially expressed proteins associated with enriched cellular component GO terms along with P-value and Benjamini values.

Table 2.2 Significantly changed biological process GO terms represented by differentially expressed proteins

Term	Count	%	P-value	Benjamini
Axon guidance	8	4.73	3.85E-04	0.186759
Adult behavior	4	2.37	0.004419	0.547766
Axonogenesis	6	3.55	0.00462	0.508923
Neuron projection development	6	3.55	0.011506	0.61596
Locomotory behavior	5	2.95	0.017375	0.592315
Regulation of axon extension	4	2.37	4.79E-04	0.6736
Neurotransmitter transport	3	1.77	0.039235	0.157623
Neurotransmitter secretion	3	1.77	0.041366	0.687425
Positive regulation of GTPase activity	9	5.32	0.031771	0.687912

Number of differentially expressed proteins associated with enriched biological process GO term along with P-value and Benjamini values.

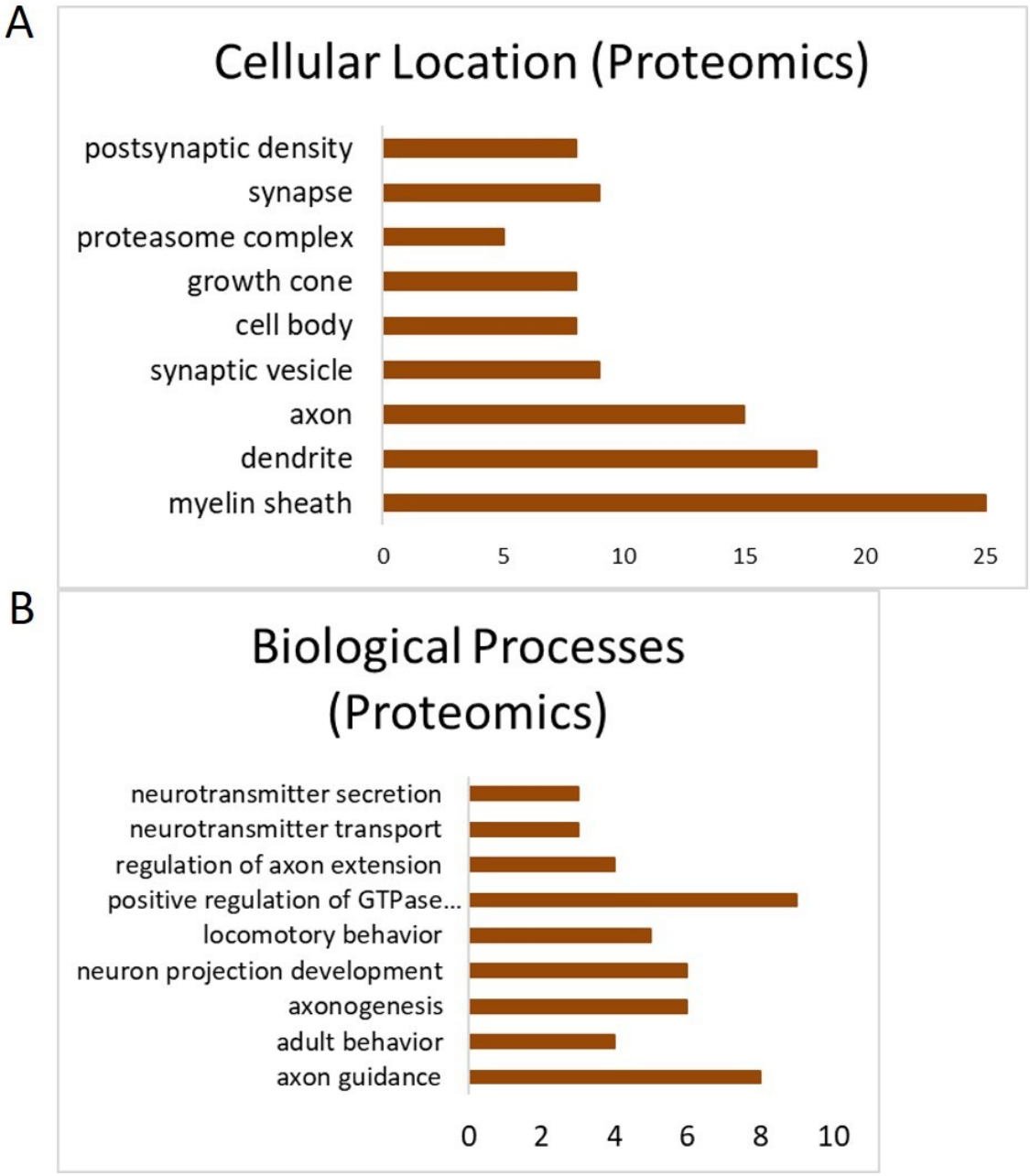

Figure 2.1 Significantly changed GO terms represented by differentially expressed proteins identified by DAVID

Cellular location (A) and biological processes (B) represented by differentially expressed proteins identified by DAVID. The x-axis indicates the number of proteins that are associated with each cellular component (a) or biological processes (B). P-value of ≤ 0.05 was considered while selecting enriched GO terms.

Table 2.3 Significantly changed cellular location GO terms represented by differentially expressed genes

Term	Count	%	P-value	Benjamini
Postsynaptic membrane	11	6.47	3.29E-06	3.39E-04
Cell junction	14	8.23	1.94E-05	0.001331
Neuron projection	13	7.64	5.89E-05	0.002425
Dendrite	14	8.23	9.95E-05	0.002923
Synapse	11	6.47	1.03E-04	0.00265
Neuronal cell body	12	7.05	0.003344	0.060795
Axon	8	4.70	0.022922	0.233089
Postsynaptic density	6	3.53	0.038472	0.332413

Number of differentially expressed genes associated with enriched cellular component GO terms along with P-value and Benjamini values.

Table 2.4 Significantly changed biological process GO terms represented by differentially expressed genes

Term	Count	%	P-value	Benjamini
Neuron development	5	2.94	0.00204	0.205
Response to cAMP	4	2.35	0.0269	0.584
Locomotory behavior	7	4.12	2.83E-04	0.062
Chemical synaptic transmission	6	3.53	0.015	0.480
Regulation of postsynaptic membrane potential	3	1.76	0.0185	0.514
GABA signaling pathway	3	1.76	0.0185	0.514
Glutamate receptor signaling pathway	3	1.76	0.0199	0.529
Brain development	7	4.12	0.0426	0.671

Number of differentially expressed genes associated with enriched biological process GO term along with P-value and Benjamini values.

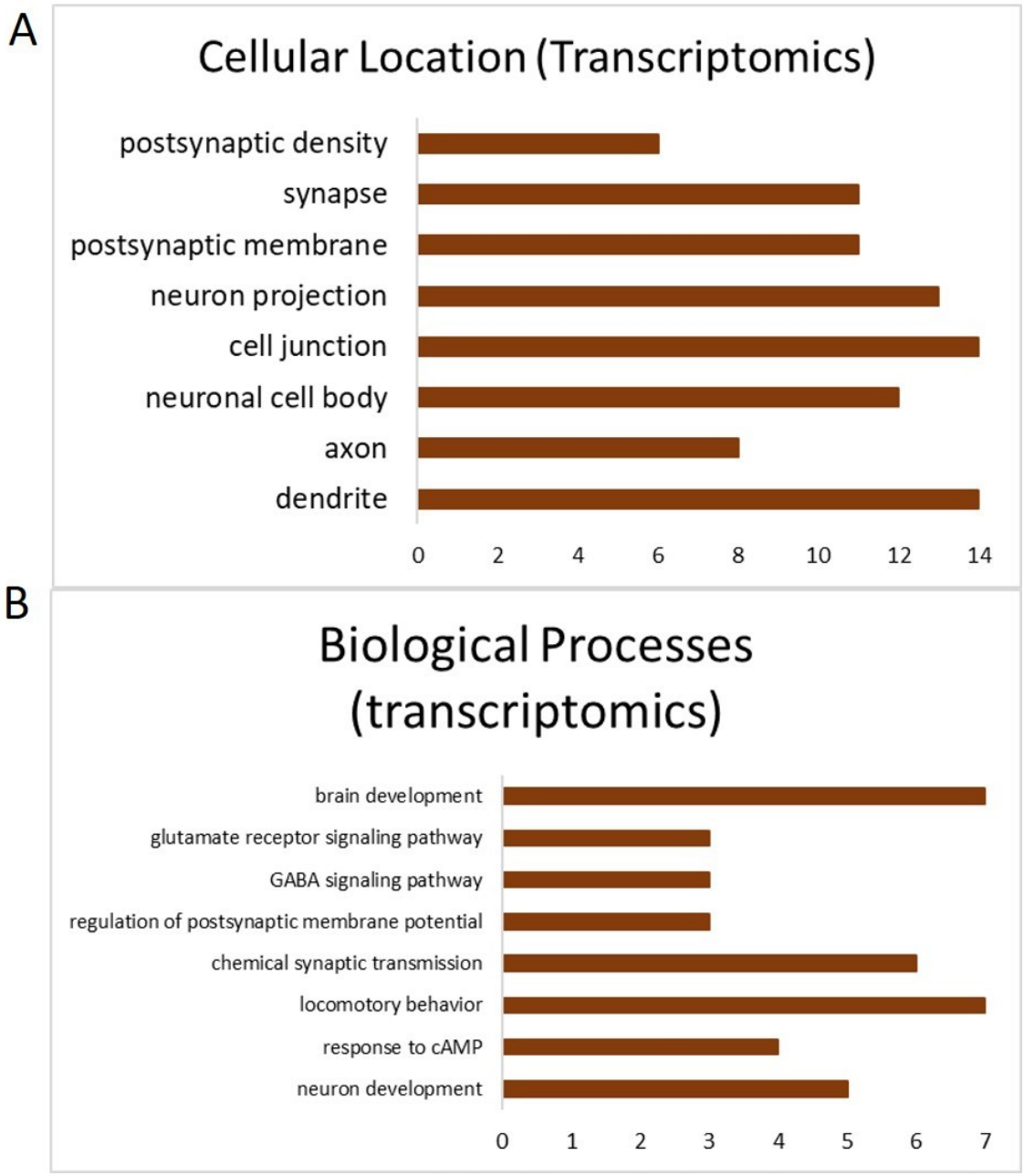

Figure 2.2 Significantly changed GO terms represented by differentially expressed genes identified by DAVID

Cellular location (A) and biological processes (B) represented by differentially expressed genes identified by DAVID. The x-axis indicates the number of genes that are associated with each cellular component (a) or biological processes (B). P-value of ≤ 0.05 was considered while selecting enriched GO terms.

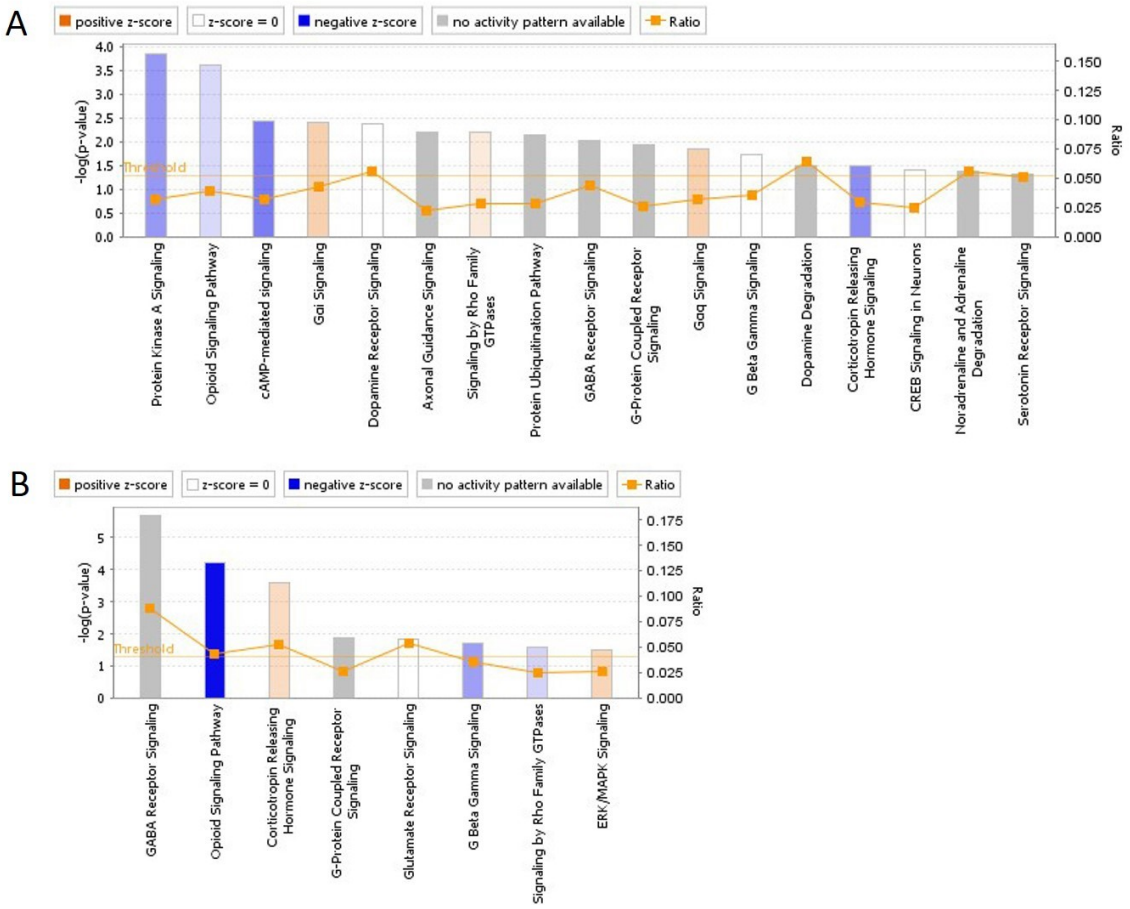

Figure 2.3 Canonical pathways represented by differentially expressed proteins (A) or genes (B) as identified by IPA

Ingenuity Pathway Analysis (IPA) identified canonical pathways represented by altered protein (A) and gene (B) expression during social play. The blue color indicates the inhibition of pathway, orange color indicates the activation of pathway, and white color indicates that there is no activation/ inhibition of the pathway. Gray color means IPA cannot predict about the activation state of that pathway. The color coding was given based on Z-score. Threshold (dot line) line indicates the p-value of 0.05 or -log (P-value) of 1.3. Ratio which is represented in orange solid line refers to the number of molecules from the dataset that map to the pathway listed divided by the total number of molecules that define the canonical pathway from within the IPA knowledgebase.

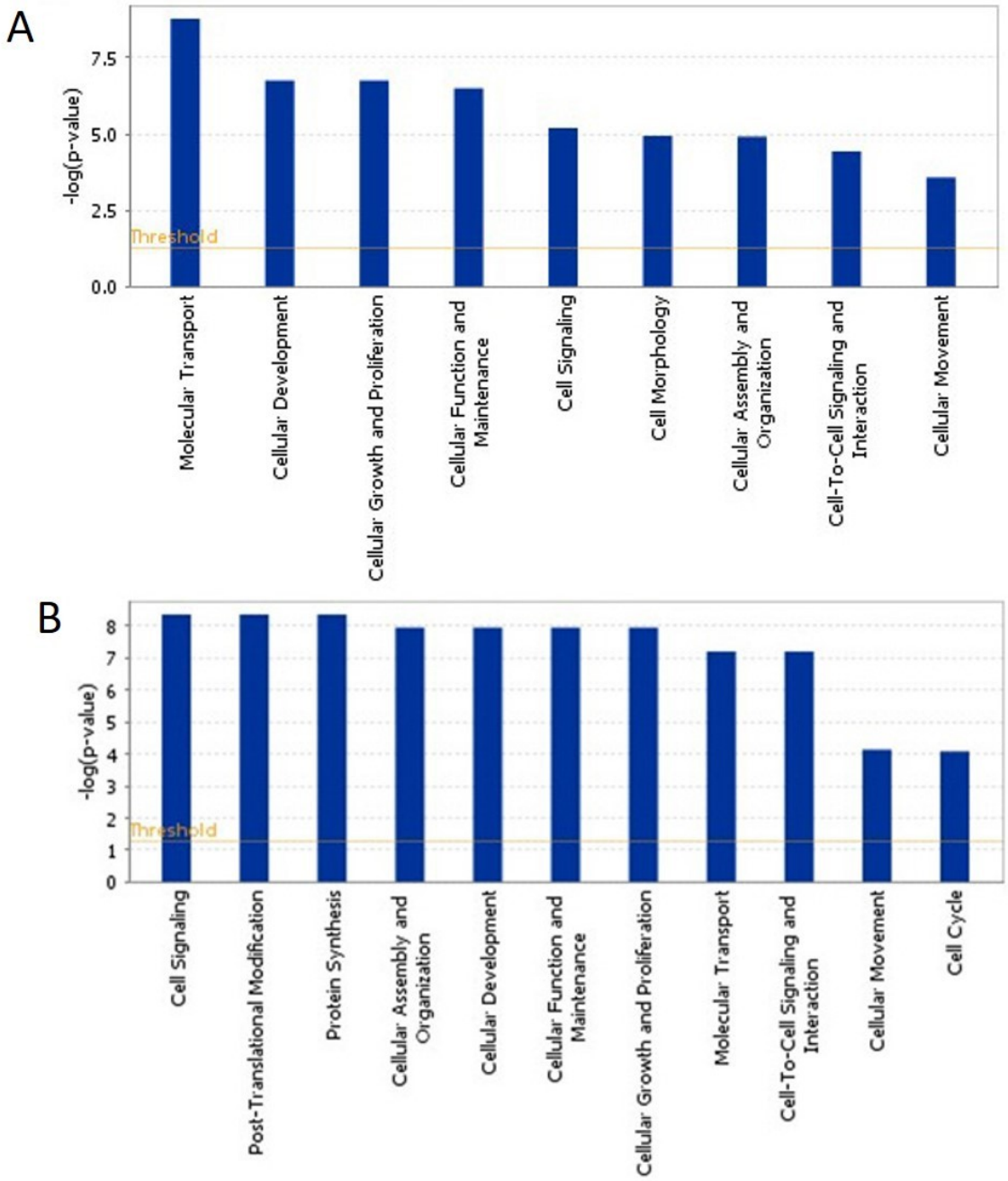

Figure 2.4 Molecular and cellular functions represented by altered protein (A) or gene (B) expression during social play

IPA identified molecular and cellular functions represented by altered protein (A) and gene (B) expression during social play. Threshold line indicates the p-value of 0.05 or -log (P-value) of 1.3.

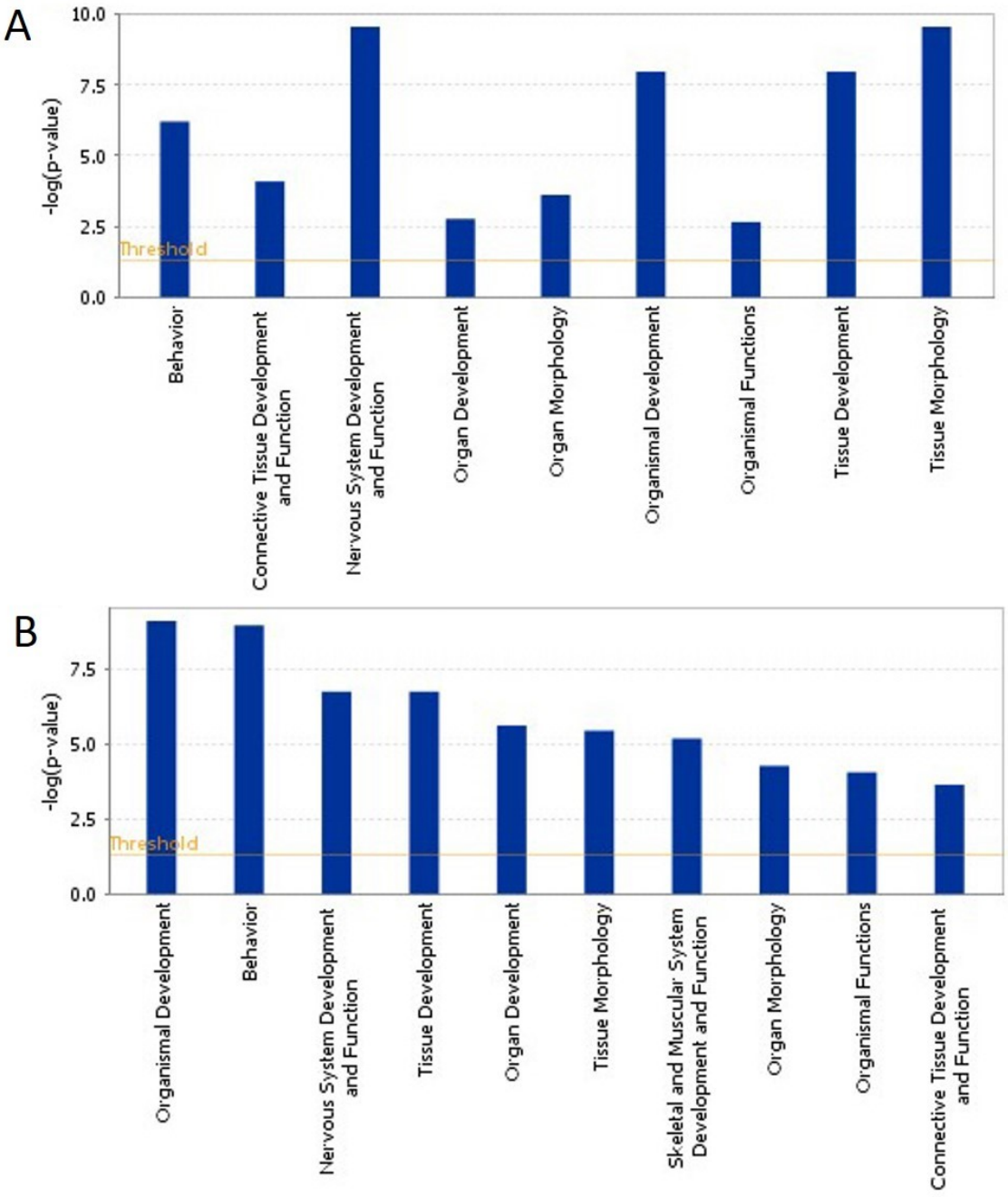

Figure 2.5 Physiological functions represented by altered protein (A) or gene (B) expression during social play

IPA identified physiological functions represented by protein (A) and gene (B) expression during social play. Threshold line indicates the p-value of 0.05 or -log (P-value) of 1.3.

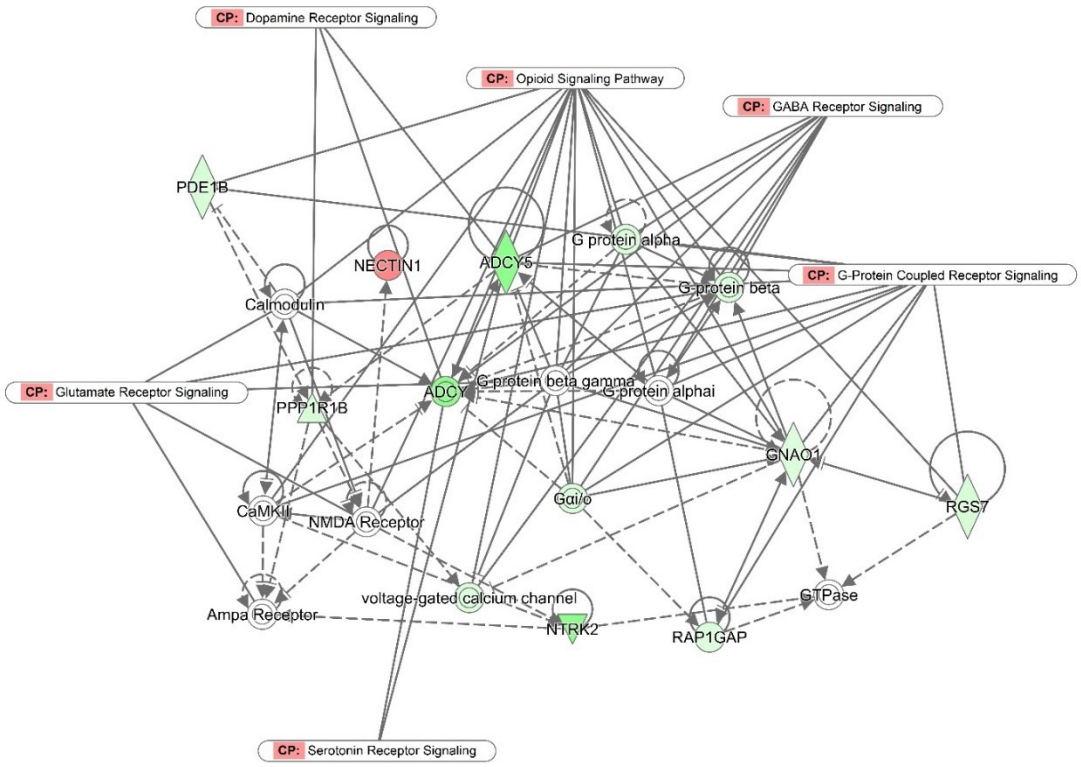

Figure 2.6 Top network identified by IPA based on differential protein expression

One of the top networks identified from differentially expressed proteins in social play is associated with different canonical pathways such as the dopamine receptor signaling, opioid signaling, GABA receptor signaling, G-protein coupled receptor signaling, serotonin receptor signaling, and glutamate receptor signaling. Differential expression of proteins is indicated by color: red color indicates the upregulation, green color indicates the down regulation, and white indicates that those proteins were not in the dataset. The intensity of color indicates the level of regulation i.e., fold change.

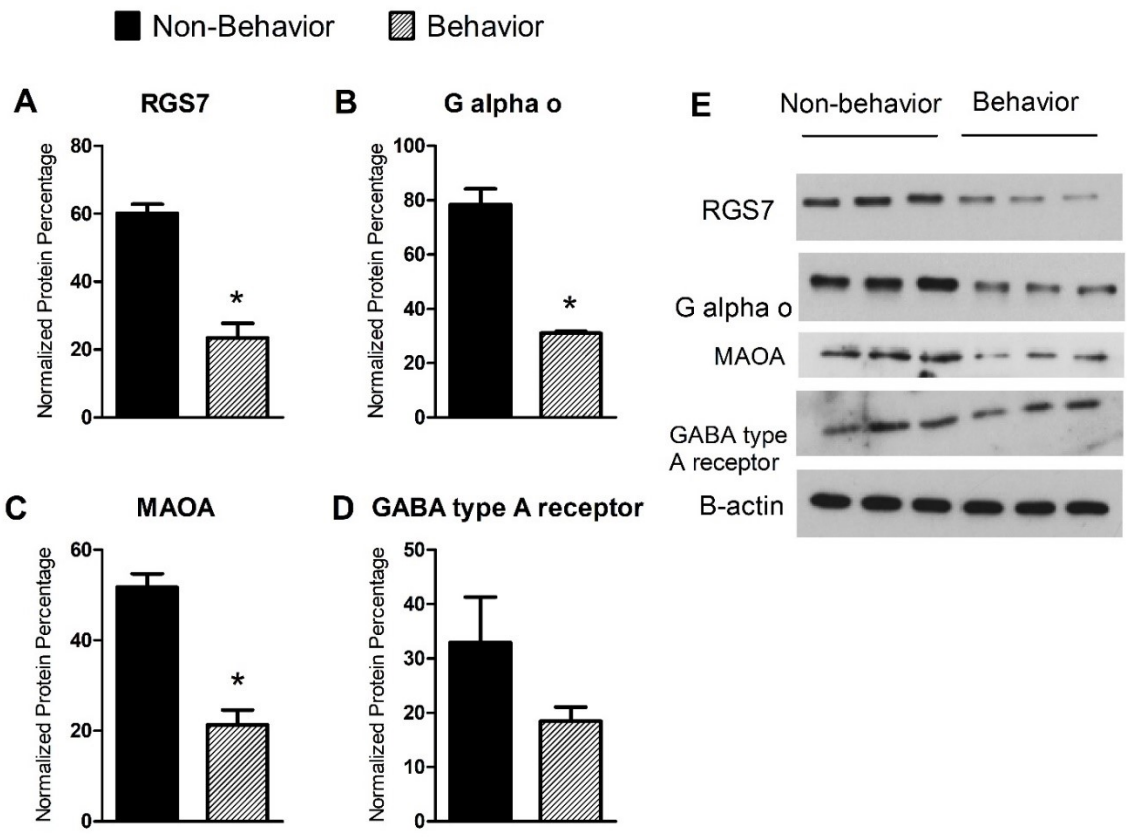

Figure 2.7 Western blot analysis of proteins that are differentially expressed by social play

The western blot analysis of protein expression of regulatory G-protein signaling 7 (RGS7) (A), G alpha o (Gαo) (B), Monoamine oxidase A (MAOA) (C), and GABA type A receptor (D) in adolescent rats who were either behaviorally naive or had completed a ten-minute interaction session with a play partner. The behavioral rats were sacrificed three hours following social play and protein expression in the amygdala was measured. The proteins levels were normalized to the β-actin levels. Values are expressed as mean ± SEM.

CHAPTER III

PERSISTENT CHANGES IN THE GLUTAMATERGIC AND GABAERGIC SIGNALING IN ADOLESCENT RATS EXPOSED DEVELOPMENTALLY TO CHLORPYRIFOS

3.1 Abstract

Organophosphorus insecticides (OPs) are the most widely used class of insecticides. Developmental exposure to OPs has long-lasting negative impacts, including abnormal emotional behavior. These negative impacts of OPs are observed at levels that cause only minimum inhibition of acetylcholinesterase, the canonical target of OPs. However, exposure to these levels results in the inhibition of endocannabinoid metabolizing enzyme fatty acid amide hydrolase (FAAH) but it is not clear what the long-term effects of this inhibition are. In this study, the male rat pups were exposed orally to either corn oil, 0.75 mg/kg chlorpyrifos (CPF), or 0.02 mg/kg PF-04457845 (PF; a specific inhibitor of FAAH) daily from postnatal day 10 (PND10) - PND16. This dosage of CPF does not alter brain cholinergic activity but inhibits FAAH. Once these rats reached adolescence (PND38), protein expression in the amygdala was determined using a label-free shotgun proteomic approach. The analysis of control vs CPF led to identification of a total of 1351 proteins, of which 44 proteins were statistically differentially regulated ($p \leq 0.05$) and the analysis of control vs PF led to identification of a total of 1111 proteins, of which 142 proteins were statistically differentially regulated

($p \leq 0.05$). DAVID analysis revealed that most of the proteins with altered expression in both CPF and PF treatment groups were localized in the synapse-related regions, such as presynaptic membrane, postsynaptic density, and synaptic vesicle. The different biological processes affected by both treatment groups included long-term synaptic potentiation, glutamate receptor signaling, protein phosphorylation, and chemical synaptic transmission. These results also indicated disturbances in the balance between glutamatergic (↓ Glutamate AMPA receptor 2, ↓ Excitatory amino acid transporter 2, and ↑vesicular glutamate transporter 2) and GABAergic signaling (↑ GABA transporter 3 and ↑ glutamate decarboxylase 2) suggesting hyperexcitation, which could be associated with abnormal emotional behavior. These results suggest that there is a similar pattern of expression between CPF and PF, and both these chemicals can persistently alter emotional behavior as a consequence of inhibition of FAAH.

3.2 Introduction

Chlorpyrifos (CPF) is a broad-spectrum organophosphate insecticide currently used to control insect pests in agriculture and is one of the most widely used insecticides in the USA. CPF was used for indoor pest control prior to June 2000, however, most household uses were canceled by 2001 because of the concern with chlorpyrifos that it elicits developmental neurotoxicity (EPA 2002). Despite the removal of CPF from home usage, its agricultural use involves the application of significant amounts in certain areas of the US and around the world. Thus, the children in agricultural and rural communities are at a higher risk for CPF exposure than children in other areas (Koch et al. 2002, Arcury et al. 2007). At high exposure levels, OPs cause neurotoxicity through the inhibition of acetylcholinesterase (AChE), an enzyme that degrades the widely

distributed neurotransmitter acetylcholine. The inhibition of AChE leads to accumulation of acetylcholine in the synapses and subsequent hyperactivity in the cholinergic system which eventually leads to respiratory failure resulting in death (Zheng et al. 2000, Gupta 2004). However, the real-world exposure scenario would involve application of low levels of OPs and exposure to these levels would not cause any overt signs of cholinergic toxicity thus giving the assumption that these low levels are safe. However, developmental exposure to low levels of OPs have produced long-lasting negative impacts including decreased cognitive abilities and motor skills (Engel et al. 2011), depressive-like behavior (Chen et al. 2014), increased occurrence of attention deficit hyperactivity disorder (Rauh et al. 2006), and reduced anxiety-like behavior (Chen et al. 2011a, Carr et al. 2017). Initially, the belief was that CPF caused developmental neurotoxicity through the same mechanism as it does at high exposures (*i.e.*, the inhibition of acetylcholinesterase). However, adverse effects on brain development have been observed at levels that cause only minimal or no inhibition of acetylcholinesterase suggesting the presence of non-cholinergic targets for OPs (Pope 1999, Slotkin 1999, Gupta 2004, Slotkin 2004a, Slotkin et al. 2006).

The adverse effects of developmental exposure to OP insecticides have been observed on different neurotransmitter systems including the serotonergic (Aldridge et al. 2003, Aldridge et al. 2004, Aldridge et al. 2005a, Aldridge et al. 2005c), dopaminergic (Aldridge et al. 2005a, Chen et al. 2011b, Zhang et al. 2015), and norepinephrine systems (Slotkin et al. 2002, Slotkin et al. 2015b). However, none of these studies identified an actual molecular target to which an OP binds. Our previous studies used dosages of CPF that caused no or minimal AChE inhibition and demonstrated that these low dosages

affect the endocannabinoid system (Carr et al. 2011, Carr et al. 2013, Carr et al. 2014, Carr et al. 2017). The endocannabinoid system is a neuromodulatory system that plays an important role in brain development. Fatty acid amide hydrolase (FAAH) and Monoacylglycerol lipase (MAGL) are the two metabolizing enzymes for the two most common endocannabinoids anandamide (AEA) and 2-arachidonoyl glycerol (2-AG), respectively (Devane et al. 1992, Di Marzo et al. 1994). In fact, developmental exposure to low levels of CPF inhibited FAAH and caused the subsequent accumulation of AEA without affecting the cholinergic system suggesting that the endocannabinoid system could be a potential non-cholinergic target of OPs (Carr et al. 2014).

The initial reports on effects of OPs on the endocannabinoid system demonstrated that acute high level exposure to CPF resulted in greater inhibition of FAAH than MAGL and AChE in adult mice (Quistad et al. 2001, Quistad et al. 2002, Quistad et al. 2006) and resulted in increased levels of AEA and 2-AG (Nomura et al. 2008, Nomura and Casida 2011). The authors concluded that the effects on the endocannabinoid system would not play a role in OP toxicity unless the exposure levels were very high. However, exposure to low levels of OPs is what is associated with agriculture application. Although adults are not affected by these low levels, the developing nervous system in children can be affected. In addition, since the endocannabinoid system plays an important role in brain development, any alteration in endocannabinoid system activity during development could be detrimental for the proper functioning of the brain.

The role of endocannabinoid system in brain development was first recognized by the observation that developmental exposure to exogenous cannabinoids altered the maturation of multiple neurotransmitter systems including the serotonergic (Molina-

Holgado et al. 1996, Molina-Holgado et al. 1997), opioid (Kumar et al. 1990, Fernandez-Ruiz et al. 2004), GABAergic (Garcia-Gil et al. 1999), glutamatergic (Suarez et al. 2004), and catecholaminergic systems (Garcia-Gil et al. 1997, Fernandez-Ruiz et al. 2000, Hernandez et al. 2000). Thus, it is possible that any alteration in the endocannabinoid system activity induced by developmental CPF exposure could affect the development of other neurotransmitter systems. In fact, neonatal or prenatal exposure to OPs can affect different neurotransmitter systems and these effects are observed during adolescence and adulthood suggesting that these adverse effects persist long after cessation of OP exposure (Slotkin et al. 2002, Aldridge et al. 2004, Aldridge et al. 2005a). Our previous studies reported that following the inhibition of FAAH and accumulation of AEA levels by CPF exposure, levels returned to normal after 48 hours following cessation of exposure (Carr et al. 2013). However, the long-term effects of FAAH inhibition caused by low levels of CPF are not known.

The objective of this study was to determine the persistent changes in protein expression and the associated neurotransmitter systems that are affected by early developmental exposure to CPF. For this purpose, juvenile male Sprague-Dawley neonatal rats were exposed to a dosage of CPF that causes no cholinesterase inhibition but inhibits FAAH by 33% and protein expression in the amygdala was measured during adolescence. The amygdala was selected because it is a complex structure in the brain and plays an important role in the processing of memory, learning, cognition, and emotional reactions (Tian et al. 2015). A label-free shotgun proteomic approach was utilized to identify the differentially expressed proteins (DEP). The gene ontology tool DAVID and the pathway analysis software Ingenuity Pathway Analysis (IPA) were

utilized to identify the functions and canonical pathways altered as a result of developmental CPF exposure. We also included a positive control, which is the specific inhibitor of FAAH PF-04457845 (PF) in the study to identify whether the long-term effects observed with CPF exposure are similar to those observed with PF exposure. If the effects were similar, the conclusion would be that the observed long-term effects observed during adolescence were the downstream effects of altered endocannabinoid activity induced by FAAH inhibition during the juvenile period.

3.3 Materials and Methods

3.3.1 Chemicals

Chlorpyrifos was a generous gift from DowElanco Chemical Company (Indianapolis, IN). PF-04457845 was purchased from MedChem Express (Monmouth Junction, NJ). All other chemicals were purchased from Sigma Chemical Co (St. Louis, MO).

3.3.2 Animal treatment

Adult male and female Sprague Dawley rats were obtained from Harlan Laboratories (Prattville, Al) and used for breeding. All rats were housed in an AAALAC-accredited temperature-controlled (22˚C) facility on a 12 h light and 12 h dark cycle with lights on between 7 am and 7 pm. Tap water and Lab Diet rodent chow were freely available during the experimentation. The procedures used in this project were approved by the Mississippi State University Institutional Animal Care and Use Committee. Females were separated from males once they appeared to be pregnant. The day of birth

was designated as PND0. Male rat pups within each litter were assigned to different treatments and the pups were marked for identification.

Male Sprague Dawley rats were treated daily by oral gavage from PND10-16 as previously described (Carr et al. 2011, Carr et al. 2013, Carr et al. 2014). This period would correspond to the postnatal age in humans in which significant brain maturation occurs (Tau and Peterson 2010). CPF and PF were dissolved in corn oil and delivered at a volume of 0.5 ml/kg body weight to the back of the throat using a 25 µl tuberculin syringe equipped with a 1-inch 24-gauge straight intubation needle (Popper and Sons, Inc., New Hyde Park, NY). The treatment groups selected for study were 1) corn oil (control); 2) 0.75 mg/kg CPF; and 3) 0.02 mg/kg PF. Our studies (Carr et al. 2017) and other previous studies (Zheng et al. 2000) also reported that the no observed effect level (NOEL) for CPF is 0.75 mg/kg CPF. This dosage of CPF does not inhibit brain AChE activity but results in 33% inhibition of FAAH activity (Carr et al. 2017). PF was used as a positive control because it is a very selective FAAH inhibitor and has been reported to be effective when administered orally (Ahn et al. 2011). Body weights were recorded during the treatment period. Rats were weaned on PND21 and marking was continued until sacrifice to allow identification. Rats were sacrificed on PND38. After sacrifice, brains were collected and stored at -80˚C. A total of three rat brains from each group were used for further analysis. Frozen brains were sliced using a manual tissue slicer to obtain 500-micron sections which were stored on microscopic slides until the amygdala was collected by punching using sharpened and blunted syringe needles (1mm size). The Paxinos and Watson (1998) atlas was used as a reference. The obtained amygdala tissue samples were processed for proteomic analysis.

3.3.3 Proteomic analyses

3.3.3.1 Protein extraction, fractionation and digestion

Each collected punch was lysed in NP-40 lysis buffer (150 mM NaCl, 20 mM $MgCl_2$, 50 mM Tris-HCl pH 7.4, 0.5% NP-40) supplemented with 1mM of the serine protease inhibitor, phenylmethylsulfonyl fluoride (PMSF) using a Microson™ ultrasonic cell disruptor. The debris was removed by centrifugation at 21,000g at 4˚C for 30 min. The protein concentration was measured using a Pierce™ BCA protein assay kit (Thermo Scientific). From each sample, 100 µg of protein was precipitated by chloroform/methanol extraction. Briefly, the sample volume was adjusted to 200 µl using NP-40 lysis buffer. To each sample, 600 µl of methanol, 150 µl of chloroform, and 450 µl of milliQ-H_20 were added, vortexed, and centrifuged at room temp for 1 min, at 21,000g. The upper aqueous phase was discarded and 450 µl of methanol was added to the lower phase, vortexed, and centrifuged under the same conditions for 2 min. The supernatant was discarded and protein digestion was performed by suspending the pellet in 33 µl of 100 mM Tris-HCl (pH 7.8) containing 6 M urea. The samples were reduced with 1.6 µl of 200 mM dithiothreitol (DTT) for 45min at room temperature and alkylated with 6.6 µl of 200 mM iodoacetamide (IAA) for 45 min at room temperature. The alkylation reaction was then quenched by adding 20 µl of 200 mM DTT for 45 min at room temperature. The urea concentration was reduced by adding 258 µl of milliQ-H_20. Finally, the proteins were digested with trypsin (sequencing grade modified trypsin, Promega) at 1:50 ratio for 18 hr at 37˚C. Protein digestion was terminated by lowering the pH of each sample to <6 by adding concentrated acetic acid. The samples were desalted using C18 SepPak columns (Waters, USA). The sample was then dried down in

speed vac. All samples were submitted to the University of Arizona Proteomic Consortium for analysis by in-line HPLC and a linear trap quadrupole mass spectrometer (LTQ Velos).

3.3.3.2 Mass spectrometry

The LC-MS/MS analysis of trypsin digested protein samples was carried out using a LTQ Orbitrap Velos mass spectrometer (Thermo Fisher Scientific, San Jose, CA) equipped with an Advion nanomate ESI source (Advion, Ithaca, NY. Peptides were eluted from a C18 precolumn (100-µm id × 2 cm, Thermo Fisher Scientific) onto an analytical column (75-µm ID × 10 cm, C18, Thermo Fisher Scientific) using a beginning concentration of 2% solvent B (acetonitrile, 0.1% formic acid) for 5 minutes, then a 2–7% gradient of solvent B over 5 minutes, followed by a 7-15 % gradient of solvent B over 50 minutes, a 15-35% gradient of solvent B over 60 minutes, a 35-40% gradient of solvent B over 28 minutes, a 40-85% gradient of solvent B over 5 minutes, held at solvent 85% B for 10 minutes, 85-2% gradient of solvent B for 1 minute then held at 2% solvent B for 16 min. All flow rates were at 400 nl/min. Solvent A consisted of water and 0.1% formic acid. Data dependent scanning was performed by the Xcalibur v 2.1.0 software using a survey mass scan at 60,000 resolutions in the Orbitrap analyzer scanning m/z 400–1600, followed by collision-induced dissociation (CID) tandem mass spectrometry (MS/MS) of the fourteen most intense ions in the linear ion trap analyzer. Precursor ions were selected by the monoisotopic precursor selection (MIPS) setting with selection or rejection of ions held to a +/− 10 ppm window. Dynamic exclusion was set to place any selected m/z on an exclusion list for 45 seconds after a single MS/MS.

3.3.3.3 Data processing and quantitation

The tandem mass spectra were extracted by Thermo Proteome Discoverer 1.3 (Thermo Scientific, USA) using the Sequest algorithm (Thermo Fisher Scientific, San Jose, CA, USA; version 1.3.0.339). Sequest was set up to search RattusNovergicus_UniprotKB assuming the digestion enzyme as trypsin. Fully tryptic peptides with up to 2 missed cleavage sites were selected. While searching with Sequest, fragment ion mass tolerance of 0.8 Da and a parent ion tolerance of 10.0 PPM were used. Oxidation of methionine and carbamidomethyl of cysteine were specified in Sequest as variable modifications. The results were also validated using X!Tandem, another search engine and displayed with Scaffold v 4.5.1 (Proteome Software Inc., Portland OR), a program that relies on various search engine results (i.e.: Sequest, X!Tandem, MASCOT) and uses Bayesian statistics to reliably identify more spectra (Keller et al. 2002). Peptide identifications were accepted if they could be established at greater than 91.0% probability by the Scaffold Local FDR algorithm. Protein identifications were accepted if they could be established at greater than 91.0% probability and contained at least 2 identified peptides. Protein probabilities were assigned by the Protein Prophet algorithm (Nesvizhskii et al. 2003). Proteins that contain similar peptides and cannot be differentiated based on MS/MS analysis alone were grouped to satisfy the principles of parsimony. Proteins sharing significant peptide evidence were grouped into clusters. Label-free protein quantitation using the sum of weighted spectra associated with a protein was performed in Scaffold. The proteins that passed the Fisher's exact test with a p-value of ≤ 0.05 were used for biological interpretation. Differentially expressed proteins (DEP) were identified based on a fold change value, which was calculated by

applying normalization in Scaffold. A minimum value of 0.2 was used for the samples in which a protein was not identified.

3.3.4 Gene ontology analysis

The database for Annotation, Visualization and Integrated Discovery (DAVID) was used for obtaining functional annotation of differentially expressed proteins and to perform GO enrichment analysis. GO terms with a p-value < 0.1 were considered to be enriched in our protein lists. Statistical significance of these enriched GO terms was determined by EASE Score Threshold, which is a modified Fisher exact p-value along with FDR correction. The cellular location and biological processes enriched among DEP were identified (Dennis et al. 2003). The number of molecules for each GO term was calculated and plotted in Excel.

3.3.5 Pathway analysis

Functional annotations, canonical pathways, and networks of DEP were analyzed using Ingenuity Pathway Analysis software (IPA, QIAGEN Inc., https://www.qiagenbioinformatics.com/products/ingenuity-pathway-analysis). Fisher's exact test was utilized in all those analyses to identify the overrepresented proteins with a p-value of less than 0.05. Functional annotation tool in IPA was used to classify the DEP based on their physiological and molecular functions. Network analysis is a visual representation of the interactions among identified proteins. The main focus was to identify the canonical pathways associated with different neurotransmitter systems including the endocannabinoid, GABAergic, glutamatergic, and dopaminergic systems. However, other functions associated with DEP including behavior, nervous system

development and function, cell signaling, tissue development, post-translational modifications, and protein synthesis were also identified.

3.3.6 Western blot analysis

The rats were sacrificed, brains were extracted and frozen on dry ice. Frozen brains were sliced at 500-micron increments, and the amygdala was collected by punching. The collected tissue was lysed in NP-40 lysis buffer (150 mM NaCl, 20 mM $MgCl_2$, 50 mM Tris-HCl pH 7.4, 0.5% NP-40) supplemented with 1mM of the serine protease inhibitor, phenylmethylsulfonyl fluoride (PMSF) using a Microson™ ultrasonic cell disruptor. The debris was removed by centrifugation at 21,000g at 4˚C for 30 min. The protein concentration was measured using a Pierce™ BCA protein assay kit (Thermo Scientific). The protein extracts containing the same amount of protein were resolved by 7.5% polyacrylamide gel electrophoresis and then transferred to a polyvinylidene difluoride (PVDF) membrane. The proteins of interest were detected using primary antibodies against excitatory amino acid transporter 2 (1:500 dilution, Santa Cruz Biotechnology, USA), glutamate decarboxylase 2 (1:1000 dilution, Santa Cruz Biotechnology, USA), neurabin 1 (1:500 dilution, Santa Cruz Biotechnology, USA), GABA transporter 3 (1:1000 dilution, Santa Cruz Biotechnology, USA), and glutamate receptor 2 (1:500 dilution, Santa Cruz Biotechnology, USA), and followed by a mouse IgGk light chain binding protein conjugate to horseradish peroxidase (1:5000 dilution, Santa Cruz Biotechnology, USA) and visualized using SuperSignal West Pico PLUS Chemiluminescent substrate. The bands were then quantified using ImageJ software (National Institute of Health). Anti-beta actin antibody was used as a loading control (1:20,000 dilution, Sigma Aldrich, USA) (n=3).

3.3.7 Statistical Analysis

Statistical analysis was performed on western blot data using GraphPad Prism version 7.00 for Windows, GraphPad Software, California, USA. One-way ANOVA followed by Tukey multiple comparison test was used to identify the statistically significant differences between control, CPF, and PF groups. Prior to analysis, the data were normalized by log transformation in Excel. The criterion for significance was set at $p < 0.05$.

3.4 Results

The proteomic analysis of three treatment groups, control, CPF, and PF resulted in two comparisons control vs CPF and control vs PF. The analysis of control vs CPF led to the identification of 1351 proteins. Of these, 147 proteins were identified only in the control samples and 108 proteins were identified only in the CPF treated samples (Figure 3.1). Of these, 44 proteins were identified as differentially expressed ($p \leq 0.05$) with 19 being upregulated and 25 being downregulated (Table A.3). Similarly, the analysis of control vs PF led to the identification of 1111 proteins. Of these, 132 proteins were identified only in the control samples and 169 proteins were identified only in the PF treated samples (Figure 3.1). Of these, 142 proteins were identified as differentially expressed ($p \leq 0.05$) with 58 proteins being upregulated and 84 proteins being downregulated (Table A.4).

3.4.1 Gene ontology analysis

The statistically significant proteins from both comparisons were further analyzed by DAVID software. DAVID is a gene ontology tool which gives information about

cellular location, biological processes, and molecular functions. In the C vs CPF analysis, DAVID could read 40 of 44 DEP and analysis using DAVID functional annotation tool, GOTERM_CC_DIRECT, resulted in the identification of 24 terms and using GOTERM_BP_DIRECT resulted in the identification of 10 terms as significantly changed ($p \leq 0.1$). In the C vs PF analysis, DAVID could read 138 of 142 DEP and GOTERM_CC_DIRECT analysis resulted in the identification of 63 terms and GOTERM_BP_DIRECT resulted in the identification of 73 terms as significantly changed ($p \leq 0.1$). A significant number of DEP in both the comparisons were located in synapse-related regions such as postsynaptic density, presynaptic membrane, and synaptic vesicle. Some of the significantly changed terms related to the cellular location were shown in Figure 3.2 and Table 3.1. The proteins located in synaptic regions were listed in Table 3.3. The significant biological processes enriched among DEP in both comparisons were protein phosphorylation, glutamate receptor signaling, substantia nigra development, and dendrite morphogenesis. Some of the significantly changed terms related to biological processes were shown in Figure 3.3 and Table 3.2. The commonly expressed proteins in both the comparisons were shown in Table 3.4. These proteins have similar direction of expression in both comparisons. Also, significant cellular location and biological process GO terms altered by both CPF and PF were similar suggesting the similar molecular mechanisms for both CPF and PF.

3.4.2 Pathway analysis

The DEP with a p-value of less than 0.05 of both comparisons along with their fold change values were uploaded into IPA. The canonical pathways, molecular and cellular functions, and physiological functions associated with the DEP were analyzed.

The canonical pathways altered with CPF exposure were protein ubiquitination pathway, choline degradation I, neuropathic pain signaling in dorsal horn neurons, synaptic long-term potentiation, and amyotrophic lateral sclerosis signaling (Figure 3.4A). IPA can predict whether the pathway is activated or inhibited based on the Z score, which is a statistical measure of the match between expected relationship direction and observed gene or protein expression. The Z score of less than -2 indicates the inhibition of canonical pathway, which is represented in blue color and the Z score of greater than 2 indicates the activation of the pathway, which is represented in orange color. The pathway in gray indicates IPA could not predict the activation state of that pathway. The pathway in white indicates that the pathway was neither activated nor inhibited. In this analysis, IPA predicted that CPF altered five pathways but the activation state of two pathways was not predicted. The pathways altered with PF exposure were axonal guidance signaling, GABA receptor signaling, protein ubiquitination pathway, serotonin degradation, dopamine degradation, protein kinase A signaling, choline degradation I, and calcium signaling (Figure 3.4B). Protein ubiquitination pathway and choline degradation I were altered with both CPF and PF. Although synaptic long-term potentiation was not identified by IPA in PF samples, DAVID analysis indicated that this process was altered with PF.

Similar molecular and physiological functions were altered with both CPF and PF. The most significant functions were protein synthesis, posttranslational modifications, behavior, nervous system development and function, cell signaling, molecular transport, and tissue development (Figure 3.5). Using network analysis feature, a network of 19 interconnecting proteins were identified by IPA in C vs CPF comparison.

Glutamate and GABA receptors were present in the network. The network was associated with different canonical pathways, such as glutamate receptor signaling, GABA receptor signaling, synaptic long-term potentiation, axonal guidance signaling, and protein kinase A signaling (Figure 3.6). Interestingly, the network identified in C vs PF comparison was also associated with the same canonical pathways as in C vs CPF comparison suggesting that similar functional pathways were altered by both treatments (Figure 3.7). Specifically, the network data confirms that GABA and glutamate signaling were altered with both CPF and PF exposure.

3.4.3 Western blot analysis

The expression of proteins that play an important role in glutamatergic and GABAergic signaling was confirmed by western blot analysis. The differential protein expression of excitatory amino acid transporter 2 (EAAT2), glutamate decarboxylase 2 (GAD2), neurabin 1, GABA transporter 3 (GAT3), and glutamate receptor 2 (GRIA2) in the amygdala of control, CPF, and PF treated rats was analyzed. GAD65 and GAT3 were upregulated, whereas EAAT2, GRIA2, and neurabin 1 were downregulated due to CPF and PF treatments. There was a significant difference ($p \leq 0.05$) in EAAT2 protein levels between control and CPF ($p=0.0027$) treated rats but the EAAT2 levels between control and PF treated rats ($p=0.0726$) only trended towards significance (Figure 3.8A). The significant difference in GAD2 levels was observed between control and CPF ($p=0.0005$) and control and PF ($p=0.0006$) treated rats (Figure 3.8B). A significant difference in neurabin 1 levels was also observed between control and CPF ($p=0.0001$) and control and PF ($p=0.0077$) treated rats and there was also a significant difference observed between CPF and PF ($p=0.0033$) treated rats (Figure 3.8C). A significant difference in GAT3

levels was observed between control and CPF (p=0.0047) and control and PF (p=0.0036) treated rats (Figure 3.8D) as was a significant difference in GRIA2 levels between control and CPF (p=0.0003) and control and PF (p=0.0016) treated rats (Figure 3.8E). The protein bands are presented in Figure 8F.

3.5 Discussion

Although the long-term effects of developmental exposure to OP insecticides have been described, the persistent effects of developmental exposure to low levels of OPs, which do not cause AChE inhibition, have not been thoroughly investigated. The adverse effects of CPF on different neurotransmitter systems have been observed at exposure levels that cause minimal AChE inhibition (Aldridge et al. 2005a, Slotkin et al. 2015b, Zhang et al. 2015). However, these studies could not identify a non-cholinergic target to which an OP binds. We demonstrated that developmental exposure to low levels of CPF inhibits FAAH but not AChE (Carr et al. 2014). The effects on endocannabinoid metabolism in the absence of effects on AChE activity suggest that the endocannabinoid system may be a non-cholinergic target. However, the long-term effects of FAAH inhibition caused by low levels of CPF are not known. Thus, the present study investigated the long-term proteomic changes in the amygdala of adolescent rats exposed developmentally to either CPF or PF. The major finding of this study is that a similar pattern of protein expression was observed between CPF and PF treatments, which strongly supports the hypothesis that long-term adverse effects observed following developmental CPF exposure occur as a result of the inhibition of FAAH that occurs during the exposure period.

In the present study, half of the DEP identified in CPF treated rats were also present in PF treated rats and these proteins had similar direction of expression in both treatment groups. In addition, more downregulation was observed as compared to upregulation in both groups. This study strongly suggests that the developmental exposure to CPF produces similar changes in the amygdala proteome as that of PF. Also, these changes can be linked to different biological processes including neurotransmitter signaling. DAVID analysis revealed that many of the downregulated proteins in both the comparisons, such as neurabin 1, neuroplastin, and serine/threonine protein kinase, were located in different synaptic regions such as the presynaptic membrane, postsynaptic density, and synaptic vesicle suggesting alterations in the synaptic function. Neurabin 1 is an F-actin binding protein implicated in synapse formation, synaptic function, and synaptic transmission and stabilization (Nakanishi et al. 1997). Neurabin also regulate the function of protein phosphatase1 which plays a critical role in the glutamatergic signaling (Nakanishi et al. 1997). The association of neurabin and protein phosphatase I initiate the dephosphorylation of glutamate receptors thereby regulating the glutamatergic signaling (Terry-Lorenzo et al. 2005). However, neurabin was downregulated by both CPF and PF which suggests an alteration in glutamatergic signaling. The protein expression of neurabin 1 was also confirmed by western blot analysis. Neuroplastin is a cell adhesion molecule (CAM) that acts as messengers between the intracellular and extracellular events of neurons. CAM's play an important role in the formation, maturation, maintenance, and plastic modulation of synaptic contacts between neurons (Owczarek and Berezin 2012). Specifically, neuroplastins have been known to regulate the formation and functional organization of excitatory and inhibitory synapses (Beesley et

al. 2014). Maintaining the organization and proper activity of excitatory and inhibitory synapses is necessary for neuronal network function. In neuroplastin knockout mice, the ratio of glutamatergic versus GABAergic synapses was perturbed and the transmission at both inhibitory and excitatory synapses was altered (Herrera-Molina et al. 2014). Thus, the downregulation of neuroplastin by both CPF and PF treatment suggests an alteration in the excitatory-inhibitory balance in this study.

Other synaptic proteins, such as glutamate receptor AMPA subunit 2 (GRIA2), excitatory amino acid transporter 2 (EAAT2), vesicular glutamate transporter 2 (VGLUT2), GABA type A receptor alpha 1 subunit (GABRA1), and GABA transporter 3 (GAT3), were associated with different biological processes including chemical synaptic transmission, GABAergic signaling, or glutamate receptor signaling. Glutamate is a major excitatory neurotransmitter in the brain that plays an important role in signaling (Zhou and Danbolt 2014). Glutamate receptor signaling was affected by both treatments and different glutamate transporters and receptor were associated with the process. VGLUT2, which was upregulated by PF treatment, transports the glutamate into synaptic vesicles in the presynaptic neuron. However, EAAT2, which was downregulated by PF treatment, clears excitatory amino acids, specifically glutamate, from the synapse into glial cells. EAAT2 is the vital transporter for limiting glutamate signaling (Danbolt 2001, Zhou and Danbolt 2013). The increased expression of VGLUT2 and decreased expression of EAAT2 suggest an increase in glutamatergic signaling. Our results are in agreement with previous studies where paraoxon and chlorpyrifos exposure increased glutamatergic signaling by enhancing the release of glutamate from hippocampus and corticostriatal terminals respectively (Kozhemyakin et al. 2010, Torres-Altoro et al.

2011). In contrast to our results, increased mRNA and protein levels of glial glutamate transporters such as EAAT1 and EAAT 2 have been observed with paraoxon exposure in the hippocampus (Mohammadi et al. 2016) and cerebral cortex (Zare et al. 2017) when measured 4 hours following exposure. The levels of paraoxon used in these studies spanned the threshold for AChE inhibition. However, in our study, we used levels of CPF that do not cause AChE inhibition and we measured the persistent effects of CPF during adolescence. Thus, the difference in the levels of OPs used and the time of testing could be the reasons for contrasting results. Although glutamate plays an important role in brain development and normal brain functions, excessive levels of glutamate in the synapse is toxic. Therefore, control of the extracellular concentration of glutamate is crucial for normal brain functioning.

The other glutamate signaling-related proteins are GRIA2 and calcium/ calmodulin-dependent protein kinase 2 (CaMKII). GRIA2 was downregulated and CaMKII was upregulated by CPF treatment. GRIA2 is a regulatory subunit of the AMPA type of glutamate receptor that regulates glutamatergic transmission. AMPA receptors are heteromeric molecules comprising various combinations of GRIA1, GRIA2, GRIA3, and GRIA4 subunits. In contrast to other subunits, GRIA2 contains an arginine at a critical position in its structure. Thus, the incorporation of GRIA2 into AMPA receptor reduces the Ca^{+2} entry and thereby controls glutamatergic signaling (Wang et al. 2010). Whereas, CaMKII increases glutamatergic transmission by phosphorylating glutamate receptors (Mao et al. 2014). However, the increased expression of CaMKII and decreased expression of GRIA2 by CPF treatment could lead to an increased glutamatergic signaling. These two proteins also play an important role in long-term synaptic

potentiation (LTP). The LTP in the amygdala plays a pivotal role in different forms of emotional memory (Suvrathan et al. 2014). LTP is a process in which brief periods of synaptic activity can produce a long-lasting increase in synapse strength. The process of LTP starts by releasing of glutamate in the synapse, which acts on glutamate receptors and thereby increases the Ca^{+2} entry into the postsynaptic neuron, which in turn activates CaMKII. Upon activation, CaMKII translocates to the synapse and phosphorylates the AMPA receptor subunits to produce potentiation by increasing glutamatergic signaling (Lisman et al. 2012). However, CaMKII was upregulated and the regulatory subunit GRIA2 was downregulated by CPF, which could lead to an abnormal increase in glutamatergic signaling resulting in hyperexcitation. Although long-term synaptic potentiation was not identified by DAVID, IPA identified that this process was altered by CPF treatment. In addition, DAVID identified that PF also altered the long-term synaptic potentiation process even though CaMKII and GRIA2 expression were not significantly altered as a result of PF treatment. Nevertheless, GRIA2 was downregulated by PF treatment but this expression was not statistically significant ($p = 0.089$). However, western blot analysis confirmed that this protein was significantly altered by both CPF and PF. Together, these data suggest that both developmental exposure to CPF and PF treatments persistently increased glutamatergic signaling possibly resulting in hyperexcitation which could be associated with abnormal emotional behavior (Li et al. 2011).

Interestingly, GABAergic signaling was also altered by both CPF and PF. GABA is a major inhibitory neurotransmitter in the brain that plays a key role in modulating neuronal activity (Jewett and Sharma 2018). GAT3, which transports GABA from

synapse into glial cells (Zhou and Danbolt 2013), was upregulated by both CPF and PF treatments. Glutamate decarboxylase 2 (GAD2), which is an enzyme that converts glutamate into GABA, was also upregulated. The protein expression of GAT3 and GAD2 was confirmed by western blot analysis. However, GABRA1 was downregulated by PF (Martin 1987). The differential expression of these GABA signaling proteins suggests an alteration in the GABAergic signaling. IPA predicted that the GABA signaling canonical pathway was altered as a result of PF treatment. Contrasting reports on the effects of OPs on GABAergic signaling exist. An increase (Fosbraey et al. 1990), a decrease (Kar and Matin 1972), or no change (Lallement et al. 1991) in GABA levels has been reported when GABA was measured immediately following OP exposure. In addition, the alterations in GABA signaling functional components have been observed by OP exposure. Specifically, a decrease in GABA uptake by decreasing the velocity of GABA uptake through GABA transporter 1 was observed with paraoxon exposure (Ghasemi et al. 2007). The increase in GABAergic signaling as evidenced by increased expression of GAD was observed with methyl parathion exposure when measured immediately after exposure (Basha and Nayeemunnisa 1992). In this study, we demonstrated that developmental exposure to CPF affects GABAergic signaling during adolescence by affecting GABA uptake and synthesis components. Together, the alteration in glutamatergic and GABAergic signaling suggest the deregulation of excitatory-inhibitory balance.

The efficient network connectivity in the brain requires homeostatic control of excitatory-inhibitory balance. It is a process established during brain development and maintained by a balance between glutamatergic and GABAergic activity. The altered

excitatory-inhibitory balance is observed in several neuropsychological disorders such as autism, schizophrenia, depression, and personality disorders (Dickinson et al. 2016). Altered emotional behavior associated with neuropsychological and psychiatric impairments have been reported in occupational groups exposed to OP intoxication (Salvi et al. 2003, Mackenzie Ross et al. 2010, Parron et al. 2011). The deregulation of excitatory-inhibitory balance could explain the alterations in emotional behavior induced by developmental OP exposure. OP pesticide exposure could cause a deficit in inhibitory control behaviors associated with emotion (Montes de Oca et al. 2013). IPA identified that behavioral function was altered by both CPF and PF treatments. We have also demonstrated that developmental exposure to CPF alters socio-emotional behavior during adolescence, specifically decreased anxiety-like behavior and increased social play behavior (Carr et al. 2017). In this study, the altered GABA and glutamate components may indicate perturbed excitatory-inhibitory balance which could be associated with altered emotional behaviors. The role of excitatory-inhibitory imbalance in OP-induced altered emotional behavior will be studied in future investigations.

In conclusion, we have demonstrated previously that the developmental exposure to low levels of CPF inhibits endocannabinoid metabolism through the inhibition of FAAH which results in excessive signaling in the endocannabinoid system. This leads to the disruption of anxiety-like behavior in preadolescent rats and altered social play in adolescent rats. In this study, a proteomic approach was utilized to determine the persistent effects of developmental exposure to either CPF or PF. We observed long-term effects on glutamatergic signaling-related proteins (such as GRIA2, VGLUT2, and EAAT2) and GABAergic signaling-related proteins (such as GAD2, and GAT3)

following developmental exposure to CPF and to PF. The protein expression of some of these proteins was also confirmed by western blot analysis. We suggest that developmental exposure to CPF perturbs the excitatory-inhibitory balance by altering the glutamatergic and GABAergic signaling during adolescence. Similar effects were observed with PF exposure suggesting that there is a similar pattern of protein expression between CPF and PF. This similarity suggests that these long-term effects observed following developmental CPF exposure are downstream effects of altered endocannabinoid signaling, occurring as a result of FAAH inhibition.

Table 3.1 Significantly changed cellular location GO terms represented by differentially expressed proteins

Term	Count	%	P-value	Benjamini
C vs CPF comparison				
Postsynaptic density	6	14.28	1.53E-04	0.0089
Myelin sheath	5	11.9	7.49E-04	0.029
Proteasome complex	3	7.14	0.007	0.19
Presynaptic membrane	3	7.14	0.011	0.232
Neuronal cell body	5	11.90	0.028	0.315
Growth cone	3	7.14	0.040	0.358
Dendrite cytoplasm	2	4.76	0.046	0.350
Synaptic membrane	2	4.76	0.068	0..358
C vs PF comparison				
Myelin sheath	17	12.14	7.72E-13	1.07E-10
Neuronal cell body	18	12.85	4.62E-07	1.60E-05
Growth cone	10	7.14	1.47E-06	4.08E-05
Post synaptic density	10	7.14	6.68E-05	0.0011
Synaptic vesicle	7	5	3.81E-04	0.0047
Proteasome complex	4	2.85	0.009	0.067
Synapse	7	5	0.021	0.139
Postsynaptic membrane	5	3.57	0.057	0.270

Number of differentially expressed proteins associated with enriched cellular component GO terms along with P-value and Benjamini values.

Table 3.2 Significantly changed biological process GO terms represented by differentially expressed proteins

Term	Count	%	P-value	Benjamini
C vs CPF comparison				
Dendrite morphogenesis	3	7.14	0.0038	0.652
Substantia nigra development	3	7.14	0.0043	0.451
Regulation of actin cytoskeleton organization	3	7.14	0.005	0.373
Response to toxic substance	3	7.14	0.024	0.821
Chemical synaptic transmission	3	7.14	0.048	0.858
Glutamate receptor signaling	2	4.76	0.052	0.840
Protein phosphorylation	4	9.52	0.082	0.928
Regulation of circadian rhythm	2	4.76	0.094	0.933
C vs PF comparison				
Phosphorylation	6	4.28	0.0042	0.25
Neuron differentiation	6	4.28	0.0067	0.304
Dendrite morphogenesis	3	2.14	0.045	0.692
Regulation of synaptic plasticity	3	2.14	0.048	0.702
Substantia nigra development	3	2.14	0.050	0.707
Long term synaptic potentiation	3	2.14	0.056	0.721
Brain development	6	4.28	0.079	0.747
Glutamate transmembrane transport	2	1.42	0.079	0.744

Number of differentially expressed proteins associated with each enriched biological process GO term along with P-value and Benjamini values.

Table 3.3 List of proteins located in different synaptic regions

Protein name	ID	Fold change		Synaptic regions
		C vs CPF	C vs PF	
Neuroplastin	NPTN_RAT	-1.42	-1.67	PSD, PSM
Neurabin	NEB1_RAT	-10	-10	PSD, S
Serine/threonine protein kinase	BRSK1_RAT	-1.67	-10	PSD, SV
Glutamate receptor AMPA subunit 2	G3V914_RAT	-16.7	-2	PSD, PSM
Vesicular glutamate transporter 2	VGLU2_RAT	-1.67	2.5	SV
Excitatory amino acid transporter 2	EAA2_RAT	-1.11	-1.42	S
GABA type A receptor alpha 1 subunit	GBRA1_RAT	NP	-10	PSD
GABA transporter 3	S6A11_RAT	2.1	3	PSD

List of proteins located in different synaptic regions such as postsynaptic density (PSD), presynaptic membrane (PSM), synapse (S), and synaptic vesicle (SV). NP = not present

Table 3.4 Some of the commonly expressed proteins in CPF and PF treated samples

Protein name	C vs CPF		C vs PF	
	Fold change	P-value	Fold change	P-value
GABA transporter 3	2.1	0.013	3	0.0001
Proteasome subunit beta type	12	0.0072	9.6	0.027
Neurofilament light polypeptide	1.6	0.02	1.7	0.011
Rho associated protein kinase	11	0.015	7.1	0.05
Glutamate decarboxylase 2	1.5	0.072	1.7	0.039
Glutamate receptor AMPA subunit 2	-16.7	0.0022	-2	0.089
Neurabin 1	-10	0.033	-10	0.019
Neuroplastin	-1.42	0.036	-1.67	0.0044
Vesicular glutamate transporter 2	-1.67	NS	2.5	0.04
Excitatory amino acid transporter 2	-1.11	NS	-1.42	0.01
Sideroflexin 5	-14.3	0.0022	-5	0.015

NS = not significant ($p \geq 0.1$)

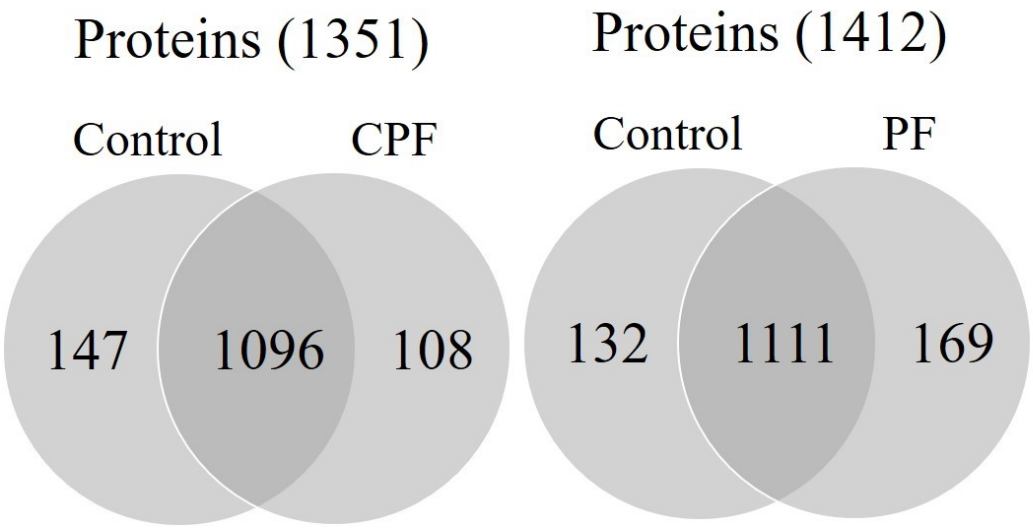

Figure 3.1 Number of unique proteins in each treatment group

Venn diagram illustrates the number of unique proteins in each treatment group and proteins that are present in both treatments in each comparison

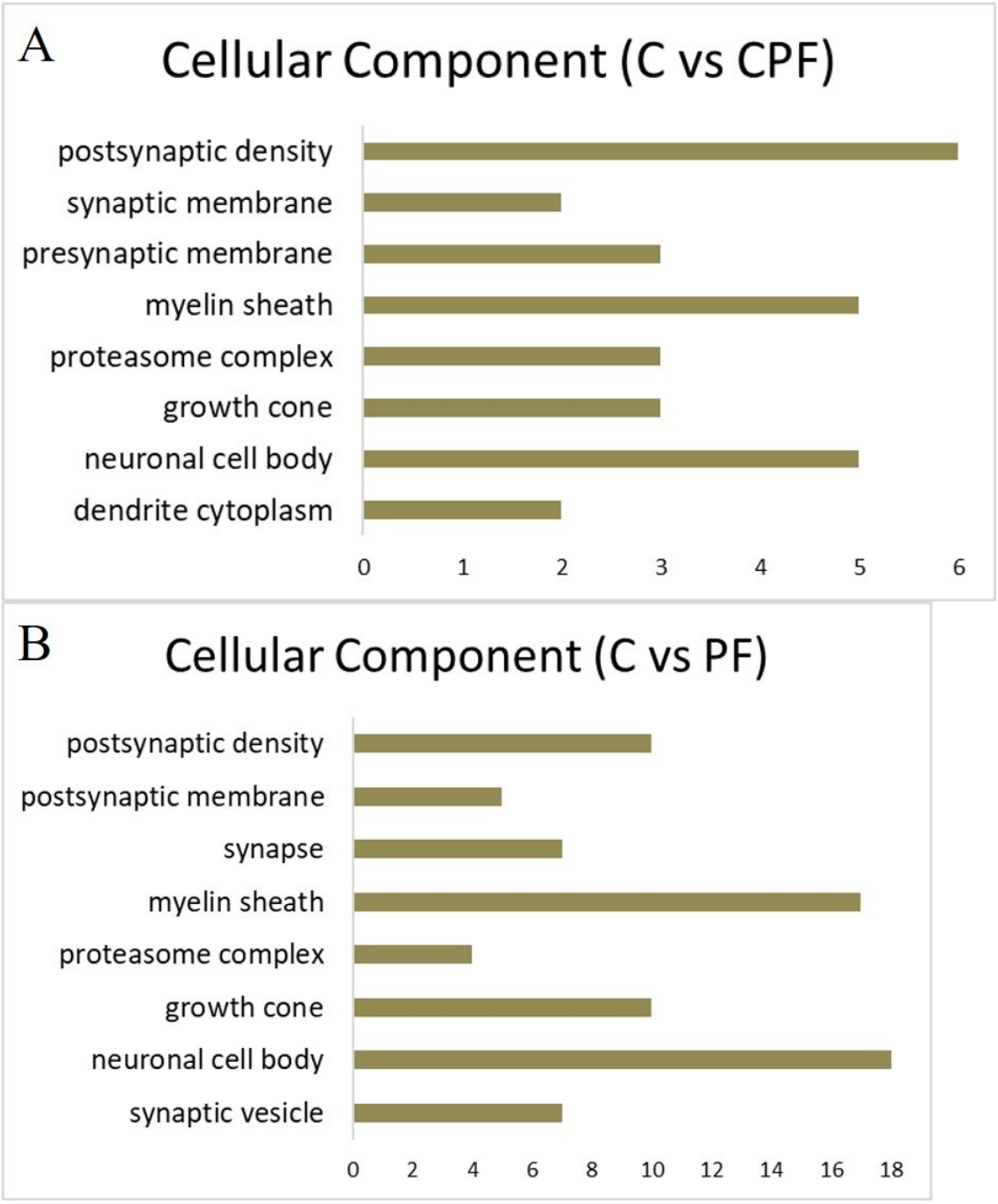

Figure 3.2 Significantly changed cellular location GO terms represented by differentially expressed proteins identified by DAVID

Cellular location of the differentially expressed proteins of A) C vs CPF B) C vs PF comparison identified by DAVID gene ontology tool. The x-axis indicates the number of proteins that are associated with each cellular component. P-value of ≤ 0.1 was considered while selecting the GO terms.

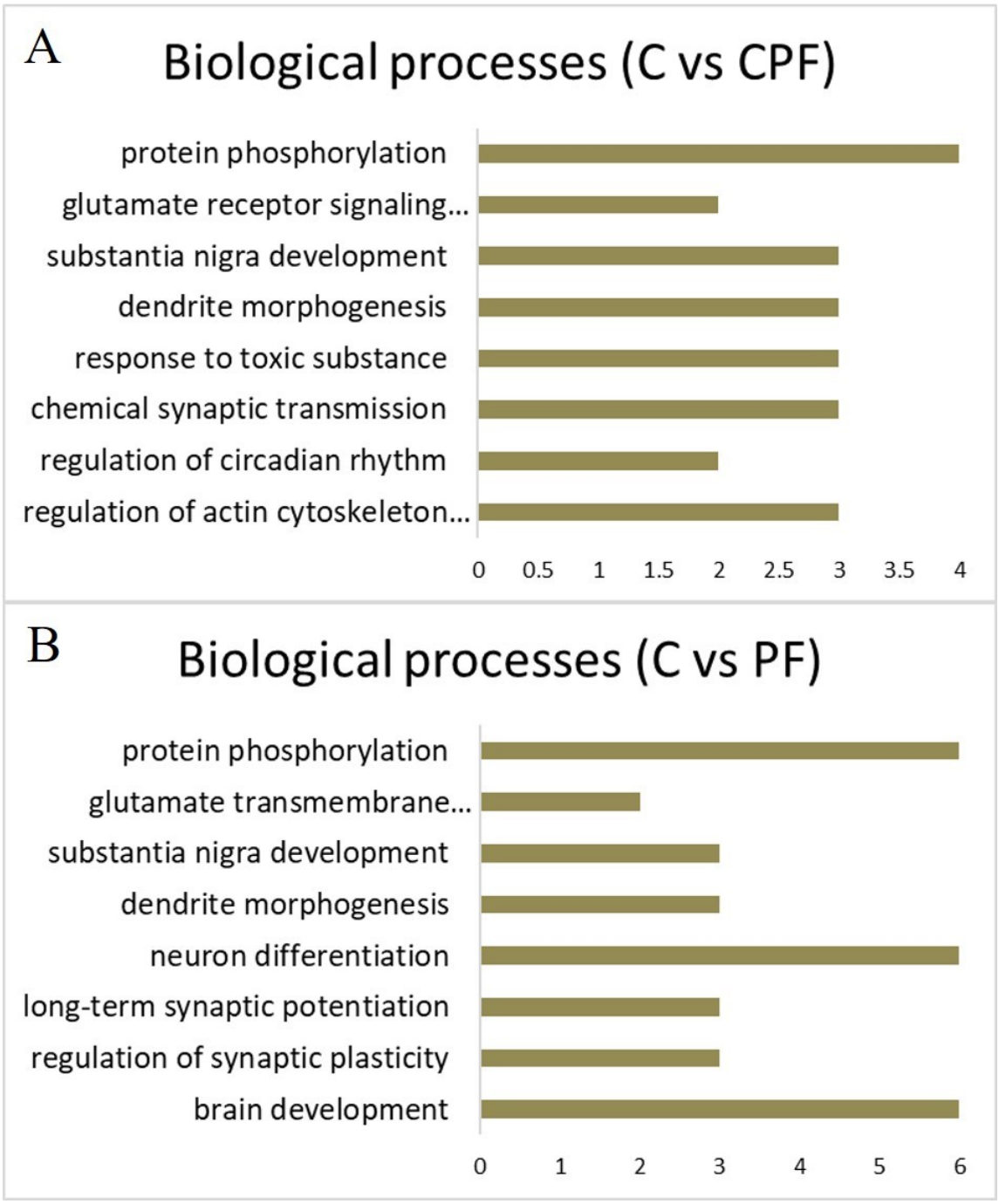

Figure 3.3 Significantly changed biological process GO terms represented by differentially expressed proteins identified by DAVID.

Biological processes that are associated with differentially expressed proteins of A) C vs CPF B) C vs PF comparison identified by DAVID gene ontology tool. The x-axis indicates the number of proteins that are associated with each biological process. P-value of ≤ 0.1 was considered while selecting the GO terms.

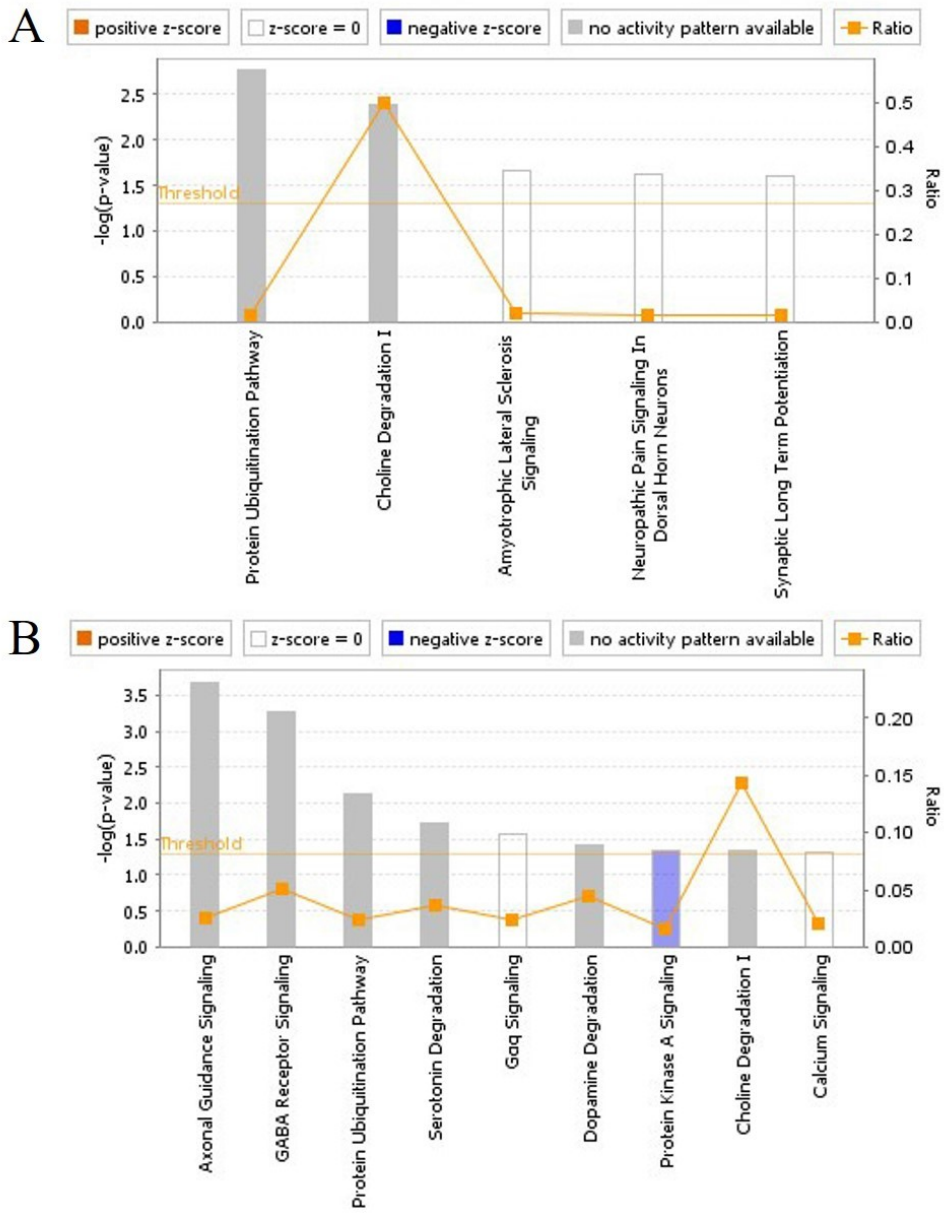

Figure 3.4 Canonical pathways altered by CPF (A) or PF (B)

Ingenuity Pathway Analysis (IPA) identified the canonical pathways that are altered by both CPF (A) and PF (B) treatments. The blue color indicates the inhibition of the pathway, the orange color indicates the activation of the pathway, and the white color indicates that there is no activation/ inhibition of the pathway. Gray color means IPA cannot predict about the activation state of that pathway. Threshold (dot line) line indicates the p-value of 0.05 or -log (P-value) of 1.3. The ratio which is represented in orange solid line refers to the number of molecules from the dataset that map to the pathway listed divided by the total number of molecules that define the canonical pathway from within the IPA knowledge base.

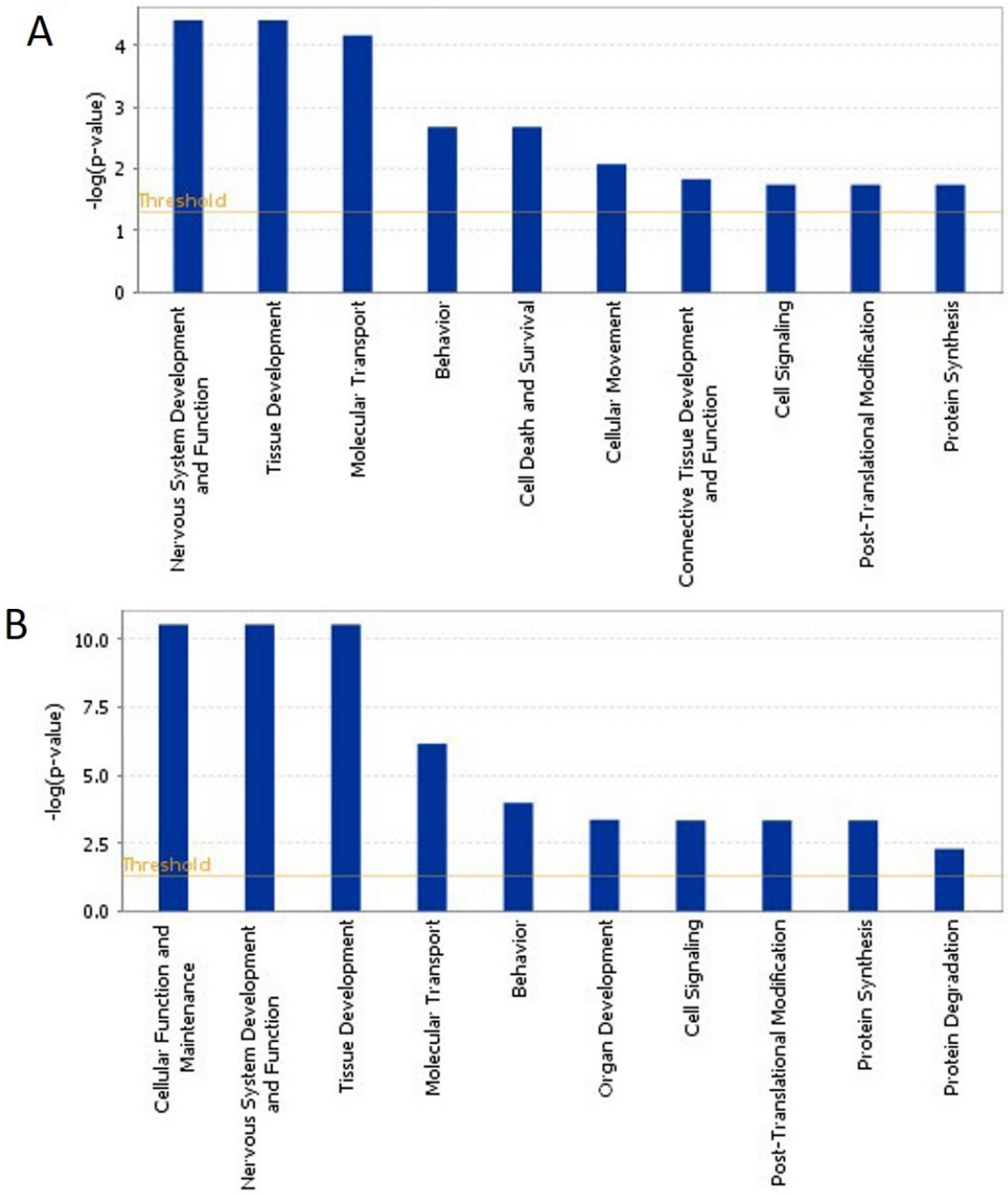

Figure 3.5 Molecular and physiological functions altered by CPF (A) or PF (B)

IPA identified the molecular and physiological functions that are altered by both (A) CPF and (B) PF. Threshold line indicates the p-value of 0.05 or -log (P-value) of 1.3

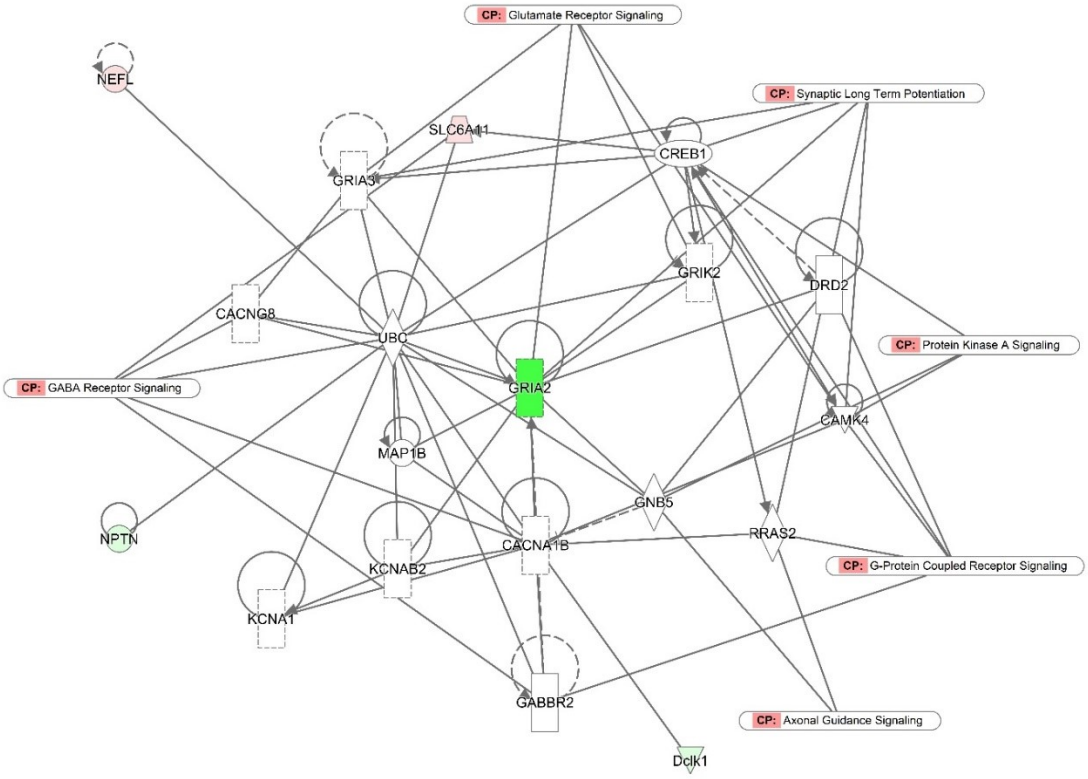

Figure 3.6 A network identified by IPA for C vs CPF comparison

The network of differentially expressed proteins identified in C vs CPF comparison is associated with different canonical pathways such as the GABA receptor signaling, glutamate receptor signaling, G-protein coupled receptor signaling, synaptic long-term potentiation, axonal guidance signaling, and protein kinase A signaling. Differential expression of proteins is indicated by color: red color indicates the upregulation, green color indicates the down-regulation, and white indicates that those proteins were not in the dataset. The intensity of color indicates the level of regulation.

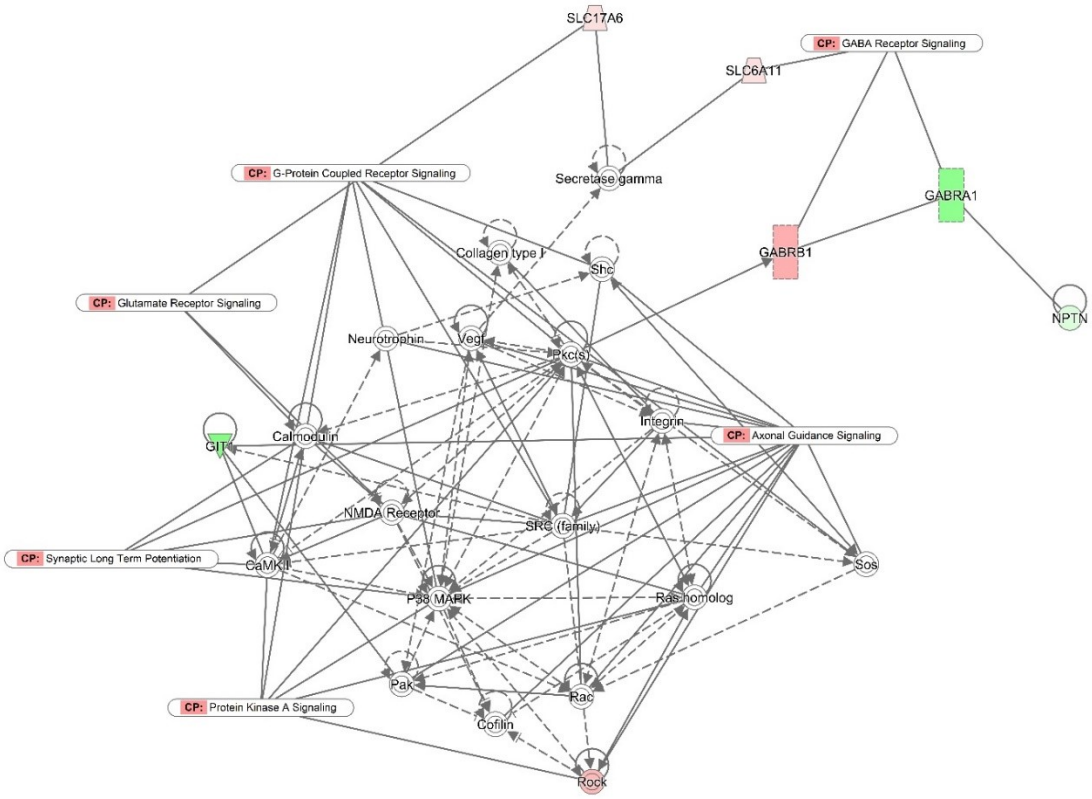

Figure 3.7 A network identified by IPA for C vs PF comparison

The network of differentially expressed proteins identified in C vs PF comparison is associated with different canonical pathways such as the GABA receptor signaling, glutamate receptor signaling, G-protein coupled receptor signaling, long-term potentiation, axonal guidance signaling, and protein kinase A signaling. Differential expression of proteins is indicated by color: red color indicates the upregulation, green color indicates the down-regulation, and white indicates that those proteins were not in the dataset. The intensity of color indicates the level of regulation.

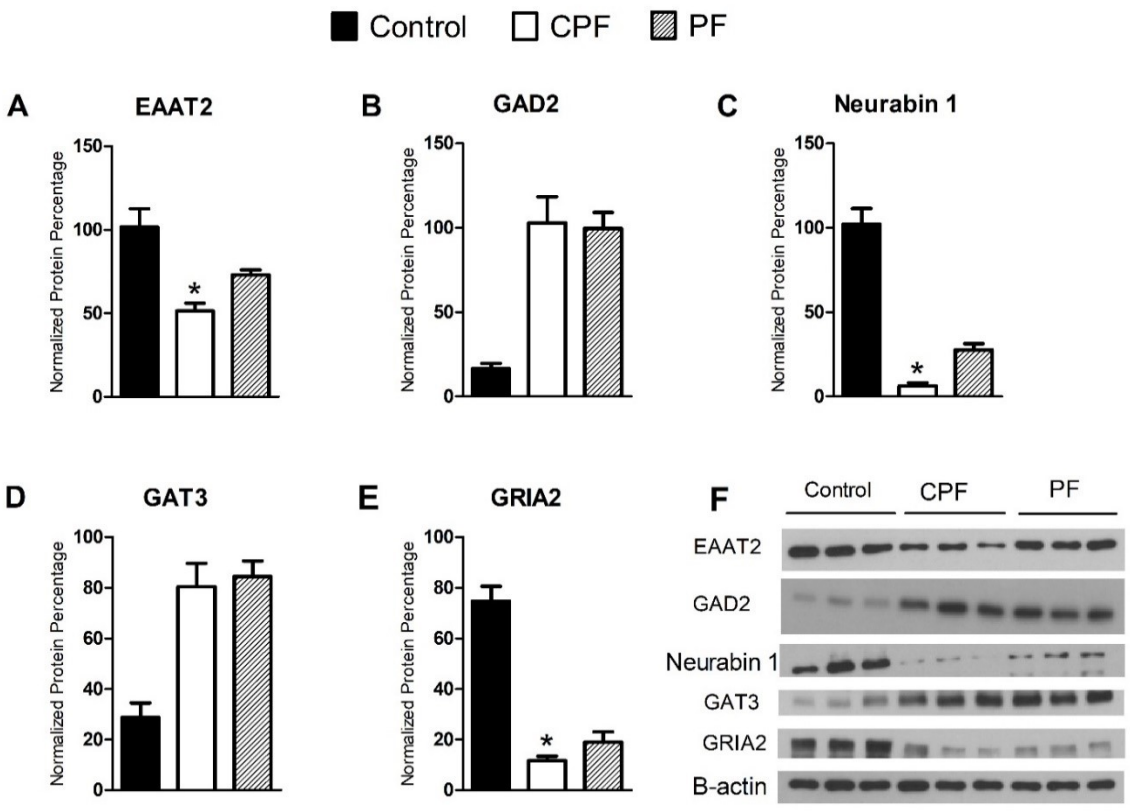

Figure 3.8 Western blot analysis of proteins that are differentially expressed by CPF and PF treatments

The western blot analysis of protein expression of glutamatergic signaling related proteins such as excitatory amino acid transporter 2 (EAAT2) (A), glutamate receptor 2 (GRIA2) (E), and Neurabin 1 (C), and GABAergic signaling related proteins such as glutamate decarboxylase (GAD 65) (B) and GABA transporter 3 (GAT3) (D) in adolescent rats developmentally exposed to either corn oil (control), 0.75 mg/kg CPF, or 0.02 mg/kg PF-04457845, a specific inhibitor of FAAH.

CHAPTER IV

ALTERATIONS IN THE NEUROTRANSMITTER SIGNALING ARE RESPONSIBLE FOR INCREASED SOCIAL PLAY BEHAVIOR IN ADOLESCENT RATS DEVELOPMENTALLY EXPOSED TO CHLORPYRIFOS

4.1 Abstract

Developmental neurotoxicity of widely used insecticide chlorpyrifos (CPF) at high doses has been well studied. However, the developmental exposure to low doses also demonstrated negative effects, including disruption of endocannabinoid metabolism through the inhibition of fatty acid amide hydrolase (FAAH), and increased social play behavior without affecting the cholinergic system. In this study, we utilized a proteomic approach to identify the neurotransmitter systems that are responsible for increased social play behavior in adolescent rats developmentally exposed to CPF. The male rat pups were exposed orally to either corn oil, 0.75 mg/kg CPF, or 0.02 mg/kg PF-04457845 (PF; a specific inhibitor of FAAH) daily from postnatal day 10 (PND10) - PND16. Social play was performed on PND38 and protein expression in the amygdala was measured 3 hrs following social play. The obtained differentially expressed proteins were analyzed by DAVID and Ingenuity Pathway Analysis (IPA). DAVID analysis revealed that the glutamate receptor signaling was altered due to behavior. These data suggest that alteration of glutamatergic signaling in the amygdala enhances reward resulting in increased social play behavior. IPA confirmed the alterations in the glutamatergic

signaling. IPA also revealed that the opioid signaling was activated due to play suggesting the increased levels of reward that can lead to increased social play behavior. IPA also revealed that the alterations in the GABAergic signaling might play a role in the social play.

4.2 Introduction

CPF is one of the most widely used organophosphate (OP) insecticide worldwide in both agriculture and urban communities. It has been established that CPF causes neurotoxicity by inhibiting the enzyme acetylcholinesterase (AChE), which breakdowns the neurotransmitter acetylcholine. The inhibition of AChE leads to the accumulation of acetylcholine at cholinergic synapses which results in systemic toxicity (Eaton et al. 2008, Burke et al. 2017). The domestic use of CPF was banned in 2000 in the USA because of the concern that OPs elicit greater neurotoxicity in children than in adults (Whitney et al. 1995b, Whyatt et al. 2004). OP-induced neurotoxicity in children was supported by epidemiological studies that demonstrated that childhood OP exposure adversely affects growth, neurodevelopment, and behavior. Also, children that were highly exposed to CPF displayed attentional problems, impaired cognitive and motor functions, deficits in working memory and full-scale intelligent quotient, and brain anomalies (Rauh et al. 2006, Rauh et al. 2011, Rauh et al. 2012). CPF was originally thought to interfere with brain development by inhibiting AChE. However, CPF exposure at doses below the threshold for systemic toxicity and with minimal AChE inhibition exerted disruptive effects on DNA synthesis, axonogenesis, and synaptogenesis suggesting that there was an unknown non-cholinergic mechanisms (Dam et al. 1998, Crumpton et al. 2000). Several animal studies demonstrated that CPF targets other

neurotransmitter systems including the serotonergic (Aldridge et al. 2003, Aldridge et al. 2004, Aldridge et al. 2005a), dopaminergic (Chen et al. 2011b, Zhang et al. 2015), and norepinephrine systems (Slotkin et al. 2002, Slotkin et al. 2015b) in addition to the cholinergic system. Furthermore, previous studies reported alterations in behavior such as decreased cognitive abilities and motor skills (Engel et al. 2011), reduced anxiety (Chen et al. 2011a, Carr et al. 2017), anhedonia (Aldridge et al. 2005a), and depression (Chen et al. 2014). These behaviors were reported to be associated with alterations in the synaptic functions of different neurotransmitter systems. However, these studies failed to identify the non-cholinergic target to which CPF binds that causes all these alterations.

Our previous studies demonstrated that developmental exposure to low levels of CPF disrupts endocannabinoid metabolism without affecting AChE activity (Carr et al. 2014). The endocannabinoid system is a neuromodulatory system that plays a vital role in mood, emotion, brain maturation, and synaptogenesis. The two most common endocannabinoids are 2-arachidonyl glycerol (2-AG) and anandamide (AEA) which are degraded primarily by monoacylglycerol lipase (MAGL) and fatty acid amide hydrolase (FAAH), respectively (Devane et al. 1992, Di Marzo et al. 1994). It was also reported that developmental exposure to low levels of CPF inhibited FAAH and resulted in the accumulation of AEA in the brain without affecting the cholinergic system suggesting that FAAH could be a potential non-cholinergic target of CPF (Carr et al. 2014, Carr et al. 2017). Although these studies demonstrated biochemical disruption in the endocannabinoid system, the effects of this disruption at the level of the whole animal are not clear. Since the endocannabinoid system plays an important role in modulating emotionality and anxiety, the effect of developmental exposure to CPF on emotional

behavior was measured by performing an emergence test. Decreased anxiety-like behavior was observed in both male and female rats exposed developmentally to levels of CPF that did not inhibit brain AChE activity but did inhibit brain FAAH activity (Carr et al. 2017). However, a single behavioral test is not sufficient to measure an animal's emotional reactivity so additional behavioral tests were performed to confirm the effects of CPF on emotional behavior.

Social play behavior was measured in adolescent rats exposed developmentally to low levels of CPF. Social play is a non-mother directed behavior which involves social interaction between play partners that is very rewarding. Social play is important for proper cognitive, emotional, and social development of adolescents (Pellis and Pellis 1991, Pellis and Pellis 1998, Vanderschuren and Trezza 2014). The play is measured by analyzing different parameters, including social grooming, body and genital sniffing, crawling over/under, chasing, nape attacks, time spent playing, and pinning (Panksepp and Beatty 1980, Vanderschuren et al. 2016). The developmental exposure to CPF increased social play behavior in adolescent rats. An additional treatment group that was exposed to a specific inhibitor of FAAH (PF-04457845 or PF) was included in this study to determine if the behavioral effects observed following developmental CPF exposure were similar to those induced by the inhibition of FAAH by PF during development (Ahn et al. 2011). Developmental exposure to PF also increased social play similarly to that of CPF. These data suggest that developmental exposure to CPF inhibits FAAH resulting in altered endocannabinoid signaling which leads to persistent alterations in emotional behavior (*i.e.,* increased social play). However, the altered endocannabinoid signaling is not persistent since FAAH activity and AEA levels recover to normal levels by 48h post

exposure. Therefore, it is not clear how this altered endocannabinoid signaling during development led to altered social behavior during adolescence.

The objective of this study is to determine the CPF and PF induced changes in the expression of proteins and determine the associated pathways that are responsible for the increased level of social play observed in adolescent rats exposed as juveniles to CPF and PF. Male Sprague Dawley rats were developmentally exposed to CPF and PF and social play was measured during adolescence. Protein expression in the amygdala of the rat brain was assessed following social play using a shotgun label-free proteomics. The amygdala was chosen for study because the amygdala is a complex structure in the brain and plays an important role in the processing of memory, learning, cognition, and emotional reactions (Tian et al. 2015). The identified differentially expressed proteins (DEP) were further analyzed using DAVID and Ingenuity Pathway Analysis (IPA) software.

4.3 Materials and methods

4.3.1 Chemicals

Chlorpyrifos was a generous gift from DowElanco Chemical Company (Indianapolis, IN). PF-04457845 was purchased from MedChem Express (Monmouth Junction, NJ). All other chemicals were purchased from Sigma Chemical Co (St. Louis, MO).

4.3.2 Animal treatment

Adult male and female Sprague Dawley rats were used for breeding. These rats were housed in an AAALAC-accredited facility under constant temperature (22˚C), on a

12 h light and 12 h dark cycle with lights on between 7 am and 7 pm. Tap water and Lab Diet rodent chow were freely available during the experimentation. The procedures used in this project were approved by the Mississippi State University Institutional Animal Care and Use Committee. Females were separated from males once they appeared to be pregnant. The date of birth was designated as PND0. Male rat pups within each litter were assigned to different treatments and the pups were marked for identification.

Male Sprague Dawley rats were treated daily by oral gavage from PND10-16 as previously described (Carr et al. 2011, Carr et al. 2013, Carr et al. 2017). CPF and PF were dissolved in corn oil and delivered at a volume of 0.5 ml/kg body weight to the back of the throat using a 25 µl tuberculin syringe equipped with a 1-inch 24-gauge straight intubation needle (Popper and Sons, Inc., New Hyde Park, NY). There were two cohorts: a behavioral cohort and a non-behavioral cohort. Each cohort contain three treatment groups: 1) corn oil (control); 2) 0.75 mg/kg CPF; and 3) 0.02 mg/kg PF-04457845 (a specific inhibitor of FAAH). According to Zheng et al. (2000), the no observed effect level (NOEL) for CPF is 0.75 mg/kg. We have reported that 0.75 mg/kg CPF does not inhibit brain AChE but results in 33% inhibition of FAAH activity (Carr et al. 2017). PF was used as a positive control because it is a very selective FAAH inhibitor and has been reported to be effective when administered orally (Ahn et al. 2011). Body weights were recorded during the treatment period. Rats were weaned on PND21 and marking was continued until behavioral testing.

4.3.3 Behavioral testing

The behavioral arena was a clear empty litter-cage with bright light (~700 lux). Each test session was filmed and recorded using a remotely operated Canon EOS Rebel

camera. Testing was performed on PND38. Following a 24-hour isolation period, two rats of the same treatment, sex, age, and size but from different litters were placed into different corners of the behavioral apparatus. The rats remained in the arena together for 600s. After each test, the cage was emptied, cleaned with 70% ethanol, dried, and refilled with fresh litter. The behavioral cohort was sacrificed 3 hours following social play. The non-behavioral cohort was also sacrificed on PND 38. After sacrifice, brains were collected and stored at -80˚C. A total of three rat brains from each group were used for proteomic analysis. Frozen brains were sliced using a manual tissue slicer to obtain 500-micron sections which were stored on microscopic slides until the amygdala was collected by punching using sharpened and blunted syringe needles (1mm size). The Paxinos and Watson (1998) atlas was used as a reference. The obtained amygdala tissue samples were processed for proteomic analysis.

4.3.4 Proteomic analyses

4.3.4.1 Protein extraction, fractionation and digestion

Collected amygdala tissue was lysed in NP-40 lysis buffer (150 mM NaCl, 20 mM $MgCl_2$, 50 mM Tris-HCl pH 7.4, 0.5% NP-40) supplemented with 1mM of the serine protease inhibitor, phenylmethylsulfonyl fluoride (PMSF) using a Microson™ ultrasonic cell disruptor. The debris was removed by centrifugation at 21,000g at 4˚C for 30 min. The protein concentration was measured using a Pierce™ BCA protein assay kit (Thermo Scientific). From each sample, 100 µg of protein was precipitated by chloroform/methanol extraction. Briefly, the sample volume was adjusted to 200 µl using NP-40 lysis buffer. To each sample, 600 µl of methanol, 150 µl of chloroform, and 450 µl of milliQ-H_20 were added, vortexed, and centrifuged at room temp for 1 min, at

21,000g. The upper aqueous phase was discarded and 450 µl of methanol was added to the lower phase, vortexed, and centrifuged under the same conditions for 2 min. The supernatant was discarded and protein digestion was performed by suspending the pellet in 33 µl of 100 mM Tris-HCl (pH 7.8) containing 6 M urea. The samples were reduced with 1.6 µl of 200 mM dithiothreitol (DTT) for 45min at room temperature and alkylated with 6.6 µl of 200 mM iodoacetamide (IAA) for 45 min at room temperature. The alkylation reaction was then quenched by adding 20 µl of 200 mM DTT for 45 min at room temperature. The urea concentration was reduced by adding 258 µl of milliQ-H_20. Finally, the proteins were digested with trypsin (sequencing grade modified trypsin, Promega) at 1:50 ratio for 18 hr at 37˚C. Protein digestion was terminated by lowering the pH of each sample to <6 by adding concentrated acetic acid. The samples were desalted using C18 SepPak columns (Waters, USA). The sample was then dried down in speed vac. All samples were submitted to the University of Arizona Proteomic Consortium for analysis by in-line HPLC and a linear trap quadrupole mass spectrometer (LTQ Velos).

4.3.4.2 Mass spectrometry

The LC-MS/MS analysis of trypsin digested protein samples was carried out using a LTQ Orbitrap Velos mass spectrometer (Thermo Fisher Scientific, San Jose, CA) equipped with an Advion nanomate ESI source (Advion, Ithaca, NY. Peptides were eluted from a C18 precolumn (100-µm id × 2 cm, Thermo Fisher Scientific) onto an analytical column (75-µm ID × 10 cm, C18, Thermo Fisher Scientific) using a beginning concentration of 2% solvent B (acetonitrile, 0.1% formic acid) for 5 minutes, then a 2–7% gradient of solvent B over 5 minutes, followed by a 7-15 % gradient of solvent B

over 50 minutes, a 15-35% gradient of solvent B over 60 minutes, a 35-40% gradient of solvent B over 28 minutes, a 40-85% gradient of solvent B over 5 minutes, held at solvent 85% B for 10 minutes, 85-2% gradient of solvent B for 1 minute then held at 2% solvent B for 16 min. All flow rates were at 400 nl/min. Solvent A consisted of water and 0.1% formic acid. Data dependent scanning was performed by the Xcalibur v 2.1.0 software using a survey mass scan at 60,000 resolutions in the Orbitrap analyzer scanning m/z 400–1600, followed by collision-induced dissociation (CID) tandem mass spectrometry (MS/MS) of the fourteen most intense ions in the linear ion trap analyzer. Precursor ions were selected by the monoisotopic precursor selection (MIPS) setting with selection or rejection of ions held to a +/− 10 ppm window. Dynamic exclusion was set to place any selected m/z on an exclusion list for 45 seconds after a single MS/MS.

4.3.4.3 Data processing and quantitation

The tandem mass spectra were extracted by Thermo Proteome Discoverer 1.3 (Thermo Scientific, USA) using the Sequest algorithm (Thermo Fisher Scientific, San Jose, CA, USA; version 1.3.0.339). Sequest was set up to search RattusNovergicus_UniprotKB assuming the digestion enzyme as trypsin. Fully tryptic peptides with up to 2 missed cleavage sites were selected. While searching with Sequest, fragment ion mass tolerance of 0.8 Da and a parent ion tolerance of 10.0 PPM were used. Oxidation of methionine and carbamidomethyl of cysteine were specified in Sequest as variable modifications. The results were also validated using X!Tandem, another search engine and displayed with Scaffold v 4.5.1 (Proteome Software Inc., Portland OR), a program that relies on various search engine results (i.e.: Sequest, X!Tandem, MASCOT) and uses Bayesian statistics to reliably identify more spectra (Keller et al. 2002). Peptide

identifications were accepted if they could be established at greater than 91.0% probability by the Scaffold Local FDR algorithm. Protein identifications were accepted if they could be established at greater than 91.0% probability and contained at least 2 identified peptides. Protein probabilities were assigned by the Protein Prophet algorithm. (Nesvizhskii et al. 2003). Proteins that contain similar peptides and cannot be differentiated based on MS/MS analysis alone were grouped to satisfy the principles of parsimony. Proteins sharing significant peptide evidence were grouped into clusters. Label-free protein quantitation using the sum of weighted spectra associated with a protein was performed in Scaffold. The proteins that passed the Fisher's exact test with a p-value of ≤ 0.05 were used for biological interpretation. Differentially expressed proteins (DEP) were identified based on a fold change value, which was calculated by applying normalization in Scaffold. A minimum value of 0.2 was used for the samples in which a protein was not identified.

4.3.5 Gene ontology analysis

The database for Annotation, Visualization and Integrated Discovery (DAVID) was used for obtaining functional annotation of differentially expressed proteins and to perform GO enrichment analysis. GO terms with a p-value < 0.1 were considered to be enriched in our protein lists. Statistical significance of these enriched GO terms was determined by EASE Score Threshold, which is a modified Fisher exact p-value along with FDR correction. The cellular location and biological processes enriched among DEP were identified (Dennis et al. 2003). The number of molecules for each GO term was calculated and plotted in Excel.

4.3.6 Pathway analysis

Functional annotations, canonical pathways, and networks of DEP were analyzed using Ingenuity Pathway Analysis software (IPA, QIAGEN Inc., https://www.qiagenbioinformatics.com/products/ingenuity-pathway-analysis). Fisher's exact test was utilized in all those analyses to identify the overrepresented proteins with a p-value of less than 0.05. Different canonical pathways associated with DEP were identified.

4.4 Results

In this study, from all the treatment groups, four different comparisons such as 1) C behavior vs CPF behavior (C B vs CPF B) 2) C behavior vs PF behavior (C B vs PF B) 3) CPF non-behavior vs CPF behavior (CPF NB vs CPF B) 4) PF non-behavior vs PF behavior (PF NB vs PF B) were evaluated to identify the proteins and associated pathways that are altered by CPF that are responsible for altered social play in CPF treated rats. We first analyzed differences in basal protein levels between different groups. We then employed gene ontology and IPA tools to identify the functions and pathways altered due to treatment and behavior. The number of total proteins and statistically significant proteins identified in each comparison were shown in Table 4.1 and DEP for each comparison are listed in Tables A.5-A.6. The C B vs CPF B comparison was used to identify the effect of CPF on behavior and C B vs PF B was used to confirm that the effects on behavior were due to altered endocannabinoid signaling. The commonly expressed proteins in these two comparisons were shown in Table 4.2. The other two comparisons such as CPF NB vs CPF B and PF NB vs PF B were used to

identify the proteins and pathways that were altered due to both behavior and treatment. The commonly expressed proteins in these two comparisons were shown in Table 4.3.

4.4.1 Gene ontology analysis

The statistically significant proteins from all the comparisons were further analyzed by a gene ontology tool DAVID. In C B vs CPF B analysis, DAVID could read all 33 DEP that were submitted. The analysis resulted in the identification of 10 cellular location GO terms and 5 biological processes GO terms as significantly changed ($p \leq 0.1$). In C B vs PF B analysis, DAVID could read 47 of 49 DEP. The analysis resulted in the identification of 22 cellular location GO terms and 14 biological processes GO terms as significantly changed ($p \leq 0.1$). The biological processes that were altered by both treatments following social behavior testing include cAMP catabolic process and cGMP catabolic process. The proteins associated with these processes were calcium/calmodulin-dependent 3',5'-cyclic nucleotide phosphodiesterase 1B and phosphodiesterase 10A, both proteins were upregulated due to treatment and were located in the cytoplasm and neuronal cell body regions. Interestingly, glutamate receptor signaling was also altered by PF treatment. Some of the significantly changed GO terms in these two comparisons were shown in Table 4.4.

Similarly, other comparisons CPF NB vs CPF B and PF NB vs PF B were also analyzed by DAVID. In CPF NB vs CPF B analysis, DAVID could read 150 of 153 DEP and the analysis resulted in the identification of 76 cellular location GO terms and 63 biological processes GO terms as significantly changed ($p \leq 0.1$). In PF NB vs PF B analysis, DAVID could read 116 of 118 DEP and the analysis resulted in the identification of 66 cellular location GO terms and 66 biological processes GO terms as

significantly changed ($p \leq 0.1$). The biological processes that were altered by behavior in CPF and PF treated rats include glutamate transport, glutamate receptor signaling, brain development, axon development, and locomotor behavior. The glutamate receptor signaling was associated with different proteins including excitatory amino acid transporter 2, glutamate receptor 2, and vesicular glutamate transporter 2. These proteins were located in synapse-related regions such as synaptic vesicle, synapse, postsynaptic density, and presynaptic membrane. Some of the significantly changed GO terms in these two comparisons were shown in Table 4.5.

4.4.2 Pathway analysis

The DEP with a p-value of less than 0.05 from all the comparisons along with their fold change values were uploaded into IPA. The canonical pathways, molecular and cellular functions, and physiological functions associated with DEP were analyzed. The canonical pathways altered due to CPF following social behavior testing (C B vs CPF B) were cAMP mediated signaling, opioid signaling pathway, protein kinase A signaling, and mitochondrial dysfunction (Figure 4.1A). The pathways altered in PF treated rats following social play (C B vs PF B) were mitochondrial dysfunction, protein kinase A signaling, actin cytoskeleton signaling, and G-protein coupled receptor signaling (Figure 4.1B). The protein kinase A signaling and mitochondrial dysfunction pathways were altered by both CPF and PF.

Similarly, some of the canonical pathways altered due to behavior in CPF treated rats (CPF NB vs CPF B) were G-protein coupled receptor signaling, protein kinase A signaling, cAMP signaling, glutamate receptor signaling, CREB signaling in neurons, and opioid signaling (Figure 4.2A). The protein kinase A signaling and cAMP signaling were

inhibited; whereas, opioid signaling was activated due to behavior in CPF treated rats. The canonical pathways altered due to behavior in PF treated rats (PF NB vs PF B) include different neurotransmitter signaling such as glutamate receptor signaling, GABA signaling, opioid signaling, and serotonin receptor signaling (Figure 4.2B). These neurotransmitter pathways are known to be altered due to behavior as described in the Chapter II. The other canonical pathways altered due to behavior in PF treated rats were cAMP signaling, corticotropin-releasing hormone signaling, and CREB signaling in neurons. The pathways altered due to behavior in both CPF and PF treated rats were opioid signaling, glutamate receptor signaling, CREB signaling in neurons, and cAMP mediated signaling.

4.5 Discussion

We previously reported that developmental exposure to 0.75 mg/kg of CPF persistently affects the glutamatergic and GABAergic signaling during adolescence (Chapter III). We have also observed that repeated developmental exposure to 0.75 mg/kg of CPF increases social play behavior in adolescent rats (preliminary data). This dosage of CPF does not inhibit AChE, but inhibits FAAH suggesting the alteration in the endocannabinoid signaling. However, developmental exposure to CPF did not persistently affect endocannabinoid system during adolescence further evidenced by the fact that we did not observe any changes in the endocannabinoid-related proteins in any of our analyses. This suggests that altered endocannabinoid signaling may not be directly responsible for increased levels of social play. Therefore, the objective of this study was to determine how the CPF-induced inhibition of FAAH in juvenile rats leads to increased levels of social play during adolescence. The proteins and neurotransmitter systems

responsible for increased social play behavior were identified in this study. We demonstrated that altered signaling of different neurotransmitter systems, such as glutamatergic, GABAergic, and opioid systems, could be responsible for increased levels of social play in adolescent rats developmentally exposed to CPF.

DAVID analysis revealed that most of the proteins located in synaptic related regions were associated with glutamate receptor signaling. The glutamate signaling was affected by both behavior and treatment. IPA also predicted that the glutamate signaling is altered by behavior in both CPF and PF treated rats (CPF NB vs CPF B and PF NB vs PF B). Previous studies reported that exposure to paraoxon and chlorpyrifos increased glutamatergic signaling by enhancing the release of glutamate form hippocampus and corticostriatal terminals respectively (Kozhemyakin et al. 2010, Torres-Altoro et al. 2011). Our studies also indicated that glutamatergic signaling is altered in adolescent rats developmentally exposed to either CPF or PF (Chapter III). These data suggest a hypothesis that the developmental exposure to CPF or PF affects the glutamatergic signaling, which could be responsible for increased levels of social play. The increased levels of social play are associated with enhanced reward. The reward is mediated by corticolimbic circuits comprising the dopaminergic, GABAergic, and glutamatergic interconnections between nucleus accumbens, ventral tegmental area, prefrontal cortex, and amygdala (Berridge and Kringelbach 2008, Haber and Knutson 2010). The reward input to the nucleus accumbens, a region of the ventral striatum that integrates reward input, mainly comes from the dopaminergic neurons in the ventral tegmental area (Haber and Knutson 2010). Under normal conditions, the excitatory input from the amygdala and prefrontal cortex to the nucleus accumbens controls the inhibitory output from nucleus

accumbens to the ventral tegmental area and thereby controlling the reward (Kandel and Kandel 2014). However, in our study, the altered glutamatergic signaling in the amygdala that is present as a result of either CPF or PF exposure could have decreased the inhibitory output from the nucleus accumbens to the ventral tegmental area and thus enhanced the reward by means of disinhibition. This enhanced reward signaling may be responsible for increased levels of social play.

It has been reported that social play is associated with a significant increase in the extracellular release of GABA and glutamate in the lateral septum (Bredewold et al. 2015). The lateral septum also plays a critical role in modulating social, motivational, and rewarding behaviors which are mediated through extensive connections of lateral septum with regions that play a major role in reward including the amygdala (Luo et al. 2011, McDonald et al. 2012, Veenema et al. 2012). The GABA input to the lateral septum mainly originates from the nucleus accumbens (Zahm et al. 2013), whereas, the glutamatergic input to the lateral septum originates from the hippocampus and amygdala (Chee et al. 2015). As mentioned earlier, the glutamate signaling input from the amygdala to the nucleus accumbens is crucial in regulating the reward associated with social play. GABAergic signaling was also altered due to behavior in PF treated rats (PF NB vs PF B). Previous studies also reported that GABAergic signaling was altered due to OP exposure (Basha and Nayeemunnisa 1992, Ghasemi et al. 2007). GABA transporter 3 (GAT3) protein was associated with GABA signaling and this protein was downregulated due to behavior in PF treated rats (PF NB vs PF B). GAT3 transports GABA from synapse into glial cells and controls the GABA levels in the synapse (Zhou and Danbolt 2013). This protein was also reported to be down-regulated by both CPF and PF (Chapter

III). This suggests that alterations in GABAergic signaling also play a role in the altered social behavior. Maintaining a physiological balance between excitatory and inhibitory neurotransmission is critical for social behavior (Dickinson et al. 2016). The alteration of both glutamatergic and GABAergic signaling suggests the presence of an excitatory-inhibitory imbalance which could be responsible for altered social behavior.

IPA suggested that opioid signaling was activated as a result of participating in behavior in the CPF treated rats (CPF NB vs CPF B). This signaling was also enriched in the PF NB vs PF B comparison and the C B vs CPF B comparison. In control behavioral rats, opioid signaling was inhibited as a regulatory mechanism to regulate the reward mediated by social play (Chapter II). This suggests that the inhibition of opioid signaling plays a major role in controlling the levels of social play under normal conditions. However, activation of the opioid signaling due to behavior (CPF NB vs CPF B) suggests that there is no regulation of reward activity in CPF treated rats. In addition, the increased levels of social play were observed in CPF and PF treated rats suggesting the increased levels of reward, which could have been mediated by increased opioid signaling. Social play is rewarding for adolescent rats and it is mediated by neural systems involved in reward and motivation such as the opioid and dopaminergic systems (Vanderschuren et al. 1997a, Trezza and Vanderschuren 2008b). The opioid system has been known to play an important role in mediating reward aspects of play (Trezza et al. 2011b, Manduca et al. 2016). The involvement of the opioid system in the modulation of social play emerged from the "opioid theory of social behavior" which was postulated in the 1980's (Panksepp et al. 1980). This theory postulated that the pleasurable aspects of social play are mediated by increased endogenous opioid activity. Subsequent studies provided

experimental support to this theory and demonstrated that treatment with opioid agonist, morphine, enhances; whereas, treatment with opioid antagonist, naloxone, decreases social play behavior (Normansell and Panksepp 1990, Vanderschuren et al. 1995a, Vanderschuren et al. 1997a, Trezza and Vanderschuren 2008a, Trezza and Vanderschuren 2008b). In our study, the activation of opioid signaling suggests the enhanced levels of reward which could possibly lead to an increase in social play behavior.

In conclusion, we have previously reported that developmental exposure to low levels of CPF inhibits the endocannabinoid metabolizing enzyme FAAH resulting in accumulation of endocannabinoids and that these animals exhibit increased levels of social play during adolescence. In the earlier Chapters, we observed that developmental exposure to CPF persistently affects the glutamatergic and GABAergic signaling. In this study, we identified the neurotransmitter systems that are responsible for the increased levels of social play in CPF treated rats. Here, we report that the activation of opioid signaling and alteration of glutamatergic and GABAergic signaling might be responsible for increased levels of social play. These neurotransmitters signaling were also altered in PF treatment suggesting that the alterations in these signaling are downstream effects of altered endocannabinoid signaling occurred due to FAAH inhibition.

Table 4.1 Summary of proteomic analyses for all comparisons

Comparison	Total number of proteins	Unique proteins		Statistically significant proteins ($p \leq 0.05$)	Upregulated proteins	Downregulated proteins
		Control	**CPF**			
C vs CPF behavior	1441	132	124	33	19	14
		Control	**PF**			
C vs PF behavior	1426	149	95	49	26	23
		CPF non-behavior	**CPF-behavior**			
CPF NB vs CPF B	1398	205	96	153	63	90
		PF non-behavior	**PF-behavior**			
PF NB vs PF B	1436	146	167	118	64	54

Total number of proteins, number of unique proteins, upregulated and downregulated proteins identified in different comparisons.

Table 4.2 Comparison of protein expression between different groups such as C B vs CPF B and C B vs PF B

Name of the protein	C B vs CPF B		C B vs PF B	
	Fold change	**P-value**	**Fold change**	**P-value**
Proteasome subunit beta type	17 (up)	0.00095	16 (up)	0.0014
Annexin	8.5 (up)	0.031	4.2 (up)	0.0007
Calcium/calmodulin-dependent 3',5'-cyclic nucleotide phosphodiesterase	4 (up)	0.032	6.1 (up)	0.0025

List of proteins that are commonly expressed in different comparisons along with fold change value and p-value.

Table 4.3 Comparison of protein expression between different groups such as CPF NB vs CPF B and PF NB vs PF B

Name of the protein	CPF NB vs CPF B		PF NB vs PF B	
	Fold change	**P-value**	**Fold change**	**P-value**
Monoamine oxidase A	-2.5 (down)	0.032	-5 (down)	0.022
Excitatory amino acid transporter 2	-1.42 (down)	0.0026	-1.42 (down)	0.01
G alpha o	-1.42 (down)	0.0028	-1.42 (down)	0.017
GABA transporter 3	NP		-2 (down)	0.0044
Vesicular glutamate transporter 2	NP		-25 (down)	0.0001
Glutamate receptor 2	18 (up)	0.00099	-11.1 (down)	0.0087
Adenylate cyclase 5	NP		-11.1 (down)	0.017
Regulator of G-protein signaling 7	-16.7 (down)	0.0006	-11.1 (down)	0.0087
Proteasome subunit beta type	-10 (down)	0.037	NP	
Annexin	-3.3 (down)	0.0099	NP	
Flotillin-1	-14.3 (down)	0.0031	-14.3(down)	0.0022

NP = not present

Table 4.4 Number of differentially expressed proteins in different GO term categories in two different comparisons such as C B vs CPF B and C B vs PF B

Term	Count	%	P-value	Benjamini
C B vs CPF B comparison				
GOTERM_CC_DIRECT				
Cytoplasm	22	66.66667	2.44E-06	2.42E-04
Neuronal cell body	5	15.15152	0.010737	0.413944
Extracellular vesicle	2	6.060606	0.07796	0.637
GOTERM_BP_DIRECT				
cGMP catabolic process	2	6.060606	0.014059	0.978441
cAMP catabolic process	2	6.060606	0.022748	0.955753
Nervous system development	3	9.090909	0.048051	0.964431
C B vs PF B comparison				
GOTERM_CC_DIRECT				
Cytoplasm	30	63.82979	4.56E-07	5.70E-05
Neuronal cell body	11	23.40426	5.20E-07	3.25E-05
Postsynaptic density	4	8.510638	0.020005	0.154983
Synaptic membrane	2	4.255319	0.077207	0.366527
Myelin sheath	5	10.6383	0.001174	0.020754
GOTERM_BP_DIRECT				
cGMP catabolic process	2	4.255319	0.020351	0.855246
cAMP catabolic process	2	4.255319	0.032864	0.876817
Ionotropic glutamate receptor signaling pathway	2	4.255319	0.064671	0.876912

List of enriched GO term categories in two different comparisons

Table 4.5 Number of differentially expressed proteins in different GO term categories in two different comparisons such as CPF NB vs CPF B and PF NB vs PF B

Term	Count	%	P-value	Benjamini
CPF NB vs CPF B comparison				
GOTERM_CC_DIRECT				
Myelin sheath	30	20	3.17E-29	9.26E-27
Postsynaptic density	14	9.333333	5.26E-08	1.54E-06
Neuronal cell body	18	12	1.27E-06	2.65E-05
Synaptic vesicle	7	4.666667	5.56E-04	0.008511
Synapse	9	6	0.002338	0.026965
Presynaptic membrane	4	2.666667	0.020707	0.138447
GOTERM_BP_DIRECT				
Ionotropic glutamate receptor signaling pathway	3	2	0.018884	0.606342
Brain development	7	4.666667	0.038027	0.729491
Axon development	2	1.333333	0.071063	0.82767
L-glutamate transport	2	1.333333	0.078642	0.844778
L-glutamate transmembrane transport	2	1.333333	0.08616	0.846621
Adult locomotory behavior	3	2	0.098578	0.852668
PF NB vs PF B comparison				
GOTERM_CC_DIRECT				
Myelin sheath	21	18.10345	1.85E-19	4.89E-17
Synaptic vesicle	8	6.896552	1.33E-05	3.52E-04
Neuronal cell body	13	11.2069	1.04E-04	0.002119
Postsynaptic density	8	6.896552	6.12E-04	0.008933
Synapse	8	6.896552	0.002073	0.021678
Synaptic vesicle membrane	4	3.448276	0.005473	0.041719
GOTERM_BP_DIRECT				
Chemical synaptic transmission	7	6.034483	7.53E-04	0.122896
L-glutamate transmembrane transport	3	2.586207	0.002067	0.181283
Brain development	8	6.896552	0.002999	0.21146
Axon development	2	1.724138	0.055075	0.775411
L-glutamate transport	2	1.724138	0.061005	0.800245
Adult locomotory behavior	3	2.586207	0.062834	0.800733

List of enriched GO term categories in two different comparisons

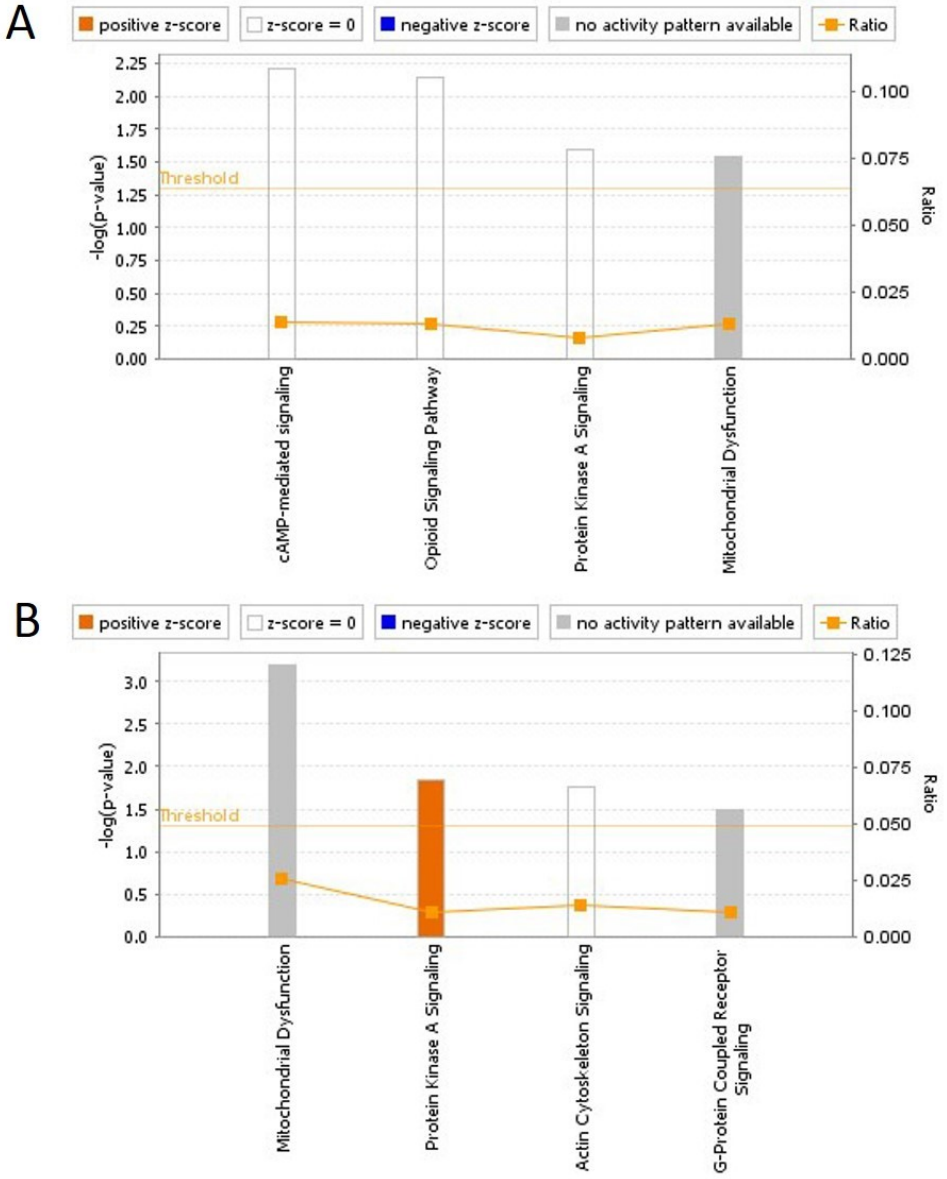

Figure 4.1 Canonical pathways altered in C vs CPF B (A) and C vs PF B (B) comparisons

Ingenuity Pathway Analysis (IPA) identified the canonical pathways that are altered in C vs CPF B (A) and C vs PF B (B) comparisons. The blue color indicates the inhibition of the pathway, the orange color indicates the activation of the pathway, and the white color indicates that there is no activation/ inhibition of the pathway. Gray color means IPA cannot predict the activation state of that pathway. Threshold (dot line) line indicates the p-value of 0.05 or -log (P-value) of 1.3. The ratio which is represented in orange solid line refers to the number of molecules from the dataset that map to the pathway listed divided by the total number of molecules that define the canonical pathway from within the IPA knowledge base.

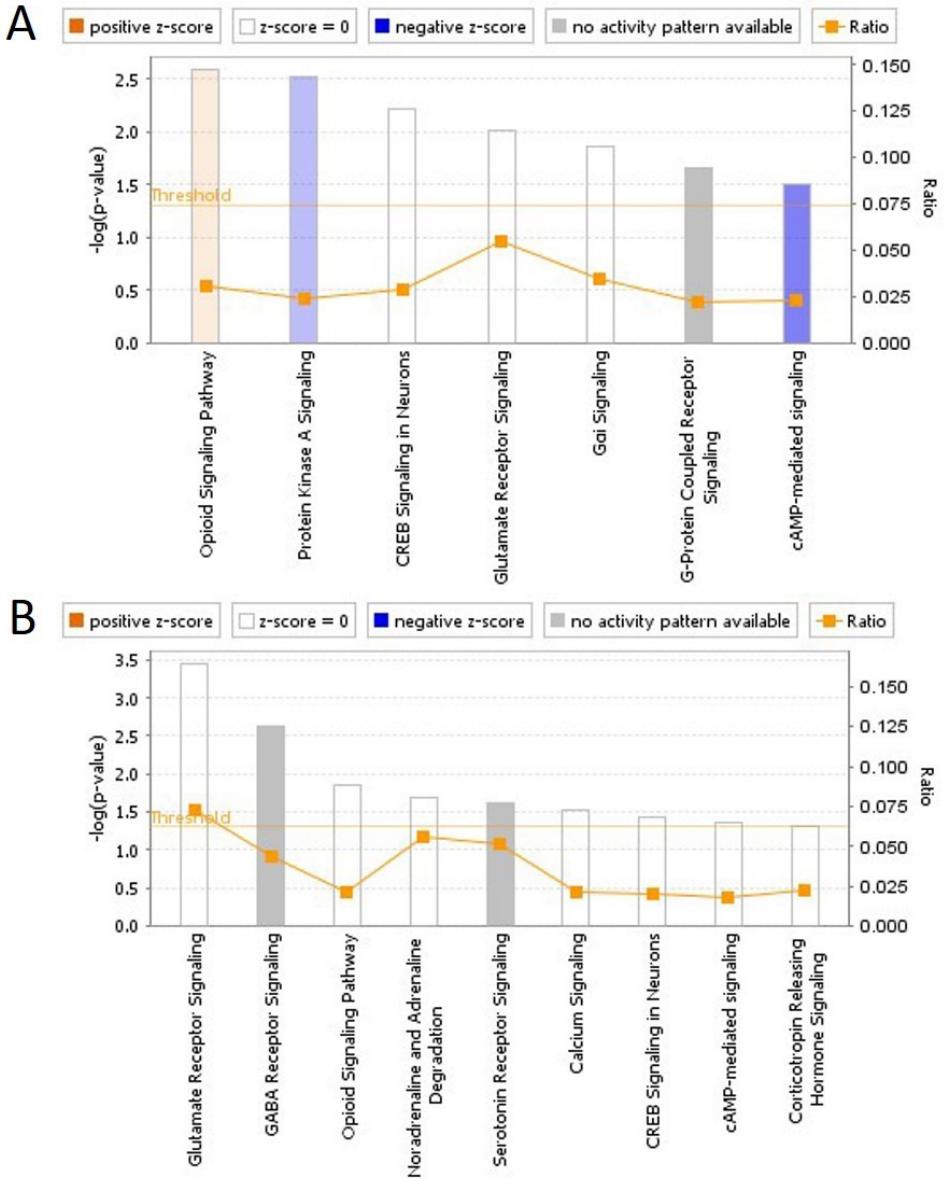

Figure 4.2 Canonical pathways altered in CPF NB vs CPF B (A) and PF NB vs PF B (B) comparisons

Ingenuity Pathway Analysis (IPA) identified the canonical pathways that are altered in CPF NB vs CPF B (A) and PF NB vs PF B (B) comparisons. The blue color indicates the inhibition of the pathway, the orange color indicates the activation of the pathway, and the white color indicates that there is no activation/ inhibition of the pathway. Gray color means IPA cannot predict the activation state of that pathway. Threshold (dot line) line indicates the p-value of 0.05 or -log (P-value) of 1.3. The ratio which is represented in orange solid line refers to the number of molecules from the dataset that map to the pathway listed divided by the total number of molecules that define the canonical pathway from within the IPA knowledge base.

CHAPTER V

CONCLUSION

The developmental neurotoxicity of organophosphorus (OP) insecticides is well established and these insecticides are more toxic to children than to adults due to the greater susceptibility of the developing nervous system. Although the household use of many OP insecticides, such as chlorpyrifos (CPF) and diazinon, was eliminated in 2000, the developmental toxicity of these compounds is still observed at low concentrations that are detected in the environment through agricultural use (Whyatt et al. 2004). However, these low concentrations of OPs do not inhibit acetylcholinesterase (AChE) which is the canonical target of OPs. Our previous studies observed that low-level CPF exposure inhibits the endocannabinoid metabolizing enzyme fatty acid amide hydrolase (FAAH) in the absence of any AChE inhibition and results in the accumulation of anandamide in the brain (Carr et al. 2013, Carr et al. 2014). Following that early life exposure to low CPF levels, anxiety-like behavior is reduced in preadolescent rats (Carr et al. 2017). Our preliminary data demonstrates that this early life exposure to CPF also alters social behavior, specifically increased social play. These data suggest that disruption of endocannabinoid system function during early life may be responsible for the altered behavior observed in adolescence. However, it appears that CPF does not exert any persistent effects on endocannabinoid system function suggesting that alterations in

the endocannabinoid system may not be directly responsible for the altered social behavior (unpublished data). In fact, current literature indicate that OPs negatively impact several other neurotransmitter systems including the serotonergic (Aldridge et al. 2003, Aldridge et al. 2004, Aldridge et al. 2005b), and dopaminergic systems (Aldridge et al. 2005a, Chen et al. 2011b) and these alterations are reported to play an important role in behavioral abnormalities. In addition, the dopaminergic, endocannabinoid, and opioid systems are known to modulate social behavior (Trezza and Vanderschuren 2008a, Trezza and Vanderschuren 2008b, Trezza et al. 2012). However, it is not clear which neurotransmitter system(s) are perturbed as a result of CPF toxicity that is responsible for the observed altered social behavior.

This research identified the neurotransmitter systems and their downstream pathways that are perturbed as a result of CPF toxicity, with a central hypothesis that "Developmental exposure to CPF inhibits FAAH resulting in altered endocannabinoid signaling, which further leads to alterations in functions of other neurotransmitter systems that are required for normal social behavior".

First, the changes in protein and gene expression between play and non-play rats were determined in order to identify the neurotransmitter systems and downstream pathways that were altered by social play in adolescent rats. The synaptic levels of GABA and glutamate were suggested to be increased in the amygdala as a result of participating in social play because of the imbalance in the glutamatergic and GABAergic signaling. Previous studies have demonstrated that social behavior is associated with a significant increase in the extracellular release of GABA and glutamate in the lateral septum (Bredewold et al. 2015). We observed alterations in the opioid, serotonin, and

dopamine systems which suggest that play alters the systems involved in the regulation of reward. Previous studies have demonstrated that opioid and dopaminergic systems modulate social play (Trezza and Vanderschuren 2008a, Trezza and Vanderschuren 2008b). However, we report for the first time how social play alters these systems. In addition, corticotropin-releasing hormone signaling was activated at 15 min following social play possibly indicating an increased level of stress occurred during play. This signaling was inhibited three hours following social play as a physiological response by the body to regulate the stress levels. Our data suggest that increased inhibitory GPCR signaling in these neurotransmitter pathways occurs following social play as a physiological response to regulate the induced level of reward and to maintain the excitatory-inhibitory balance in the neurotransmitter systems. However, these results only highlight the dynamic changes in protein and gene expression and associated neurotransmitter systems at a specific time point following social play. Future studies should investigate the changes in the neurotransmitter systems at different time points to get a complete picture of the different neural substrates involved in the social play.

Second, the long-term effects of developmental inhibition of FAAH in adolescent rats were identified. CPF, at a dosage that does not inhibit AChE but inhibits FAAH (0.75 mg/kg), was used. In addition, PF-04457845, which is a specific inhibitor of FAAH, was also included (Ahn et al. 2011). This allowed us to determine if the long-term effects observed following developmental CPF exposure were similar to those induced by the inhibition of FAAH during development. One major finding of this study was that there are persistent changes in glutamatergic and GABAergic signaling in adolescent rats developmentally exposed to FAAH inhibitors. Specifically, the altered expression of

glutamatergic signaling-related proteins (such as glutamate receptor 2, vesicular glutamate transporter 2, and excitatory amino acid transporter 2) and GABAergic signaling-related proteins (such as GABA type A receptor, glutamate decarboxylase 2, and GABA transporter 3) were observed with both CPF and PF treatments. This alteration of glutamatergic and GABAergic signaling suggested the presence of an excitatory-inhibitory imbalance in signaling. This imbalance could be the basis for the altered emotional behaviors that we have previously demonstrated to be altered following developmental exposure to CPF. However, how this FAAH inhibition by developmental exposure to CPF persistently changes glutamatergic and GABAergic signaling, which could result in altered emotional behavior, remains a question. To clarify this, future studies should investigate the events that occur during the actual exposure period in order to match those effects with the long-term altered expression of glutamatergic and GABAergic signaling-related proteins that we observed in this study.

Third, the CPF and PF induced changes in the expression of proteins and associated neurotransmitter pathways that are responsible for increased levels of social play were identified. In Chapter II, the persistent effects of CPF on glutamatergic and GABAergic signaling were determined. In this study, the possible role of glutamatergic and GABAergic signaling in altering social play behavior was addressed. Our data suggest that altered glutamatergic signaling in the amygdala causes disinhibition of the reward circuit resulting in enhanced reward and increased social play behavior. In addition, our data suggest that the activation of opioid signaling could be responsible for the increased social play behavior since it has been postulated that the pleasurable aspects of social play are mediated by increased endogenous opioid activity. In order to get a

complete picture of the mechanisms responsible for increased social play behavior, further studies should identify the steps involved between FAAH inhibition and altered social play behavior. One way is to identify the receptor(s) involved in mediating the changes in the behavior observed. In previous studies, we demonstrated increased brain AEA levels immediately following developmental inhibition of FAAH by CPF or PF. This suggests the activation of either the CB1 receptor or the peroxisome proliferator-activated receptor alpha (PPARα) receptor or both is occurring since AEA is an agonist to these receptors. Using knockout models for these two receptors, it may be possible to determine the role that improper activation of each of these receptors plays in the increased social play.

In summary, this dissertation study identified 1) the different neurotransmitter systems that play a regulatory role in social play 2) the neurotransmitter systems that were persistently affected by developmental CPF exposure 3) the neurotransmitter systems that are responsible for increased levels of social play. The new knowledge gained from this research can be utilized to develop better preventive and therapeutic strategies for socio-emotional behavioral problems. The findings in this dissertation also provided insights into the long-term effects of FAAH inhibition and how this leads to altered behavior.

REFERENCES

Ahn, K. et al. (2011). "Mechanistic and pharmacological characterization of PF-04457845: a highly potent and selective fatty acid amide hydrolase inhibitor that reduces inflammatory and noninflammatory pain." *J Pharmacol Exp Ther* **338**(1): 114-124.

Aldridge, J. E. et al. (2005a). "Developmental Exposure of Rats to Chlorpyrifos Leads to Behavioral Alterations in Adulthood, Involving Serotonergic Mechanisms and Resembling Animal Models of Depression." *Environ Health Perspect* **113**(5): 527-531.

Aldridge, J. E. et al. (2005b). "Alterations in Central Nervous System Serotonergic and Dopaminergic Synaptic Activity in Adulthood after Prenatal or Neonatal Chlorpyrifos Exposure." *Environ Health Perspect* **113**(8): 1027-1031.

Aldridge, J. E. et al. (2005c). "Developmental exposure to terbutaline and chlorpyrifos: pharmacotherapy of preterm labor and an environmental neurotoxicant converge on serotonergic systems in neonatal rat brain regions." *Toxicol Appl Pharmacol* **203**(2): 132-144.

Aldridge, J. E. et al. (2003). "Serotonergic systems targeted by developmental exposure to chlorpyrifos: effects during different critical periods." *Environ Health Perspect* **111**(14): 1736-1743.

Aldridge, J. E. et al. (2004). "Developmental exposure to chlorpyrifos elicits sex-selective alterations of serotonergic synaptic function in adulthood: critical periods and regional selectivity for effects on the serotonin transporter, receptor subtypes, and cell signaling." *Environ Health Perspect* **112**(2): 148-155.

Alessandri, S. M. (1992). "Attention, play, and social behavior in ADHD preschoolers." *J Abnorm Child Psychol* **20**(3): 289-302.

Arcury, T. A. et al. (2007). "Pesticide urinary metabolite levels of children in eastern North Carolina farmworker households." *Environ Health Perspect* **115**(8): 1254-1260.

Atwood, D. and C. Paisley-Jones (2017). Pesticides industry sales and usage. 2008-2012 market estimates. U. S. E. P. Agency. Washington D.C.

Balali-Mood, M. and K. Balali-Mood (2008). "Neurotoxic disorders of organophosphorus compounds and their managements." *Arch Iran Med* **11**(1): 65-89.

Barone, S., Jr. et al. (2000). "Vulnerable processes of nervous system development: a review of markers and methods." *Neurotoxicology* **21**(1-2): 15-36.

Barrett, C. E. et al. (2017). "Developmental disruption of amygdala transcriptome and socioemotional behavior in rats exposed to valproic acid prenatally." *Mol Autism* **8**: 42.

Basha, M. P. and Nayeemunnisa (1992). "Methyl parathion induced alterations in GABAergic system during critical stage of central nervous system development in albino rat pups " *Indian Journal of Experimental Biology* **31**: 369-372.

Beatty, W. W. et al. (1984). "Suppression of play fighting by amphetamine: effects of catecholamine antagonists, agonists and synthesis inhibitors." *Pharmacol Biochem Behav* **20**(5): 747-755.

Beesley, P. W. et al. (2014). "The Neuroplastin adhesion molecules: key regulators of neuronal plasticity and synaptic function." *J Neurochem* **131**(3): 268-283.

Berridge, K. C. (2007). "The debate over dopamine's role in reward: the case for incentive salience." *Psychopharmacology (Berl)* **191**(3): 391-431.

Berridge, K. C. and M. L. Kringelbach (2008). "Affective neuroscience of pleasure: reward in humans and animals." *Psychopharmacology (Berl)* **199**(3): 457-480.

Berridge, K. C. et al. (2009). "Dissecting components of reward: 'liking', 'wanting', and learning." *Curr Opin Pharmacol* **9**(1): 65-73.

Bredewold, R. et al. (2015). "Dynamic changes in extracellular release of GABA and glutamate in the lateral septum during social play behavior in juvenile rats: Implications for sex-specific regulation of social play behavior." *Neuroscience* **307**: 117-127.

Broccoli, L. et al. (2018). "Targeted overexpression of CRH receptor subtype 1 in central amygdala neurons: effect on alcohol-seeking behavior." *Psychopharmacology (Berl)* **235**(6): 1821-1833.

Brown, T. P. et al. (2006). "Pesticides and Parkinson's disease--is there a link?" *Environ Health Perspect* **114**(2): 156-164.

Buratti, F. M. et al. (2002). "Kinetic parameters of OPT pesticide desulfuration by c-DNA expressed human CYPs." *Environ Toxicol Pharmacol* **11**(3-4): 181-190.

Buratti, F. M. et al. (2003). "CYP-specific bioactivation of four organophosphorothioate pesticides by human liver microsomes." *Toxicol Appl Pharmacol* **186**(3): 143-154.

Burke, R. D. et al. (2017). "Developmental neurotoxicity of the organophosphorus insecticide chlorpyrifos: from clinical findings to preclinical models and potential mechanisms." *J Neurochem* **142 Suppl 2**: 162-177.

Bushnell, P. J. et al. (1991). "Behavioral and neurochemical changes in rats dosed repeatedly with diisopropylfluorophosphate." *J Pharmacol Exp Ther* **256**(2): 741-750.

Cardona, D. et al. (2011). "Impulsivity as long-term sequelae after chlorpyrifos intoxication: time course and individual differences." *Neurotox Res* **19**(1): 128-137.

Carr, R. L. et al. (2013). "Induction of endocannabinoid levels in juvenile rat brain following developmental chlorpyrifos exposure." *Toxicol Sci* **135**(1): 193-201.

Carr, R. L. et al. (2017). "Decreased anxiety in juvenile rats following exposure to low levels of chlorpyrifos during development." *Neurotoxicology* **59**: 183-190.

Carr, R. L. et al. (2011). "Effect of developmental chlorpyrifos exposure, on endocannabinoid metabolizing enzymes, in the brain of juvenile rats." *Toxicol Sci* **122**(1): 112-120.

Carr, R. L. et al. (2014). "Low level chlorpyrifos exposure increases anandamide accumulation in juvenile rat brain in the absence of brain cholinesterase inhibition." *Neurotoxicology* **43**: 82-89.

Casida, J. E. and G. B. Quistad (2004). "Organophosphate toxicology: safety aspects of nonacetylcholinesterase secondary targets." *Chem Res Toxicol* **17**(8): 983-998.

Chee, M. J. et al. (2015). "Melanin-concentrating hormone neurons release glutamate for feedforward inhibition of the lateral septum." *J Neurosci* **35**(8): 3644-3651.

Chen, W. Q. et al. (2011a). "Repeated exposure to chlorpyrifos alters the performance of adolescent male rats in animal models of depression and anxiety." *Neurotoxicology* **32**(4): 355-361.

Chen, W. Q. et al. (2014). "Neurobehavioral evaluation of adolescent male rats following repeated exposure to chlorpyrifos." *Neurosci Lett* **570**: 76-80.

Chen, X. et al. (2015). "Quantitative proteomics using SILAC: Principles, applications, and developments." *Proteomics* **15**(18): 3175-3192.

Chen, X. P. et al. (2011b). "Different reaction patterns of dopamine content to prenatal exposure to chlorpyrifos in different periods." *J Appl Toxicol* **31**(4): 355-359.

Coleman, M. A. et al. (1998). "Glucocorticoid response to forced exercise in laboratory house mice (Mus domesticus)." *Physiol Behav* **63**(2): 279-285.

Crumpton, T. L. et al. (2000). "Developmental neurotoxicity of chlorpyrifos in vivo and in vitro: effects on nuclear transcription factors involved in cell replication and differentiation." *Brain Research* **857**(1): 87-98.

Dam, K. et al. (1998). "Developmental neurotoxicity of chlorpyrifos: delayed targeting of DNA synthesis after repeated administration." *Developmental Brain Research* **108**(1): 39-45.

Danbolt, N. C. (2001). "Glutamate uptake." *Progress in Neurobiology* **65**(1): 1-105.

Davies, S. (2016). Evidence too thin to support chlorpyrifos regulation, panel concludes. Agri-Pulse communications, INC. **https://www.agri-pulse.com/articles/7319-evidence-too-thin-to-support-chlorpyrifos-regulation-panel-concludes**.

De Felice, A. et al. (2014). "Sex-dimorphic effects of gestational exposure to the organophosphate insecticide chlorpyrifos on social investigation in mice." *Neurotoxicol Teratol* **46**: 32-39.

Dennis, G., Jr. et al. (2003). "DAVID: Database for Annotation, Visualization, and Integrated Discovery." *Genome Biol* **4**(5): P3.

Devane, W. A. et al. (1992). "Isolation and structure of a brain constituent that binds to the cannabinoid receptor." *Science* **258**(5090): 1946-1949.

Di Marzo, V. et al. (1994). "Formation and inactivation of endogenous cannabinoid anandamide in central neurons." *Nature* **372**(6507): 686-691.

Dickinson, A. et al. (2016). "Measuring neural excitation and inhibition in autism: Different approaches, different findings and different interpretations." *Brain Res* **1648**(Pt A): 277-289.

Dobin, A. et al. (2013). "STAR: ultrafast universal RNA-seq aligner." *Bioinformatics* **29**(1): 15-21.

Eaton, D. L. et al. (2008). "Review of the toxicology of chlorpyrifos with an emphasis on human exposure and neurodevelopment." *Crit Rev Toxicol* **38 Suppl 2**: 1-125.

Engel, S. M. et al. (2011). "Prenatal exposure to organophosphates, paraoxonase 1, and cognitive development in childhood." *Environ Health Perspect* **119**(8): 1182-1188.

EPA, U. S. (2002). "Interim Registration eligibility decision: Chlorpyrifos. washington D.C. ." *U.S. Environmental Protection Agency. Office of Prevention, Petsticides and Toxic substances*.

Eskenazi, B. et al. (2004). "Association of in utero organophosphate pesticide exposure and fetal growth and length of gestation in an agricultural population." *Environ Health Perspect* **112**(10): 1116-1124.

Eskenazi, B. et al. (2007). "Organophosphate pesticide exposure and neurodevelopment in young Mexican-American children." *Environ Health Perspect* **115**(5): 792-798.

Fattore, L. et al. (2005). "Endocannabinoid system and opioid addiction: behavioural aspects." *Pharmacol Biochem Behav* **81**(2): 343-359.

Fernandez-Ruiz, J. et al. (2000). "The endogenous cannabinoid system and brain development." *Trends Neurosci* **23**(1): 14-20.

Fernandez-Ruiz, J. et al. (2004). "Cannabinoids and gene expression during brain development." *Neurotox Res* **6**(5): 389-401.

Forsyth, C. S. and J. E. Chambers (1989). "Activation and degradation of the phosphorothionate insecticides parathion and EPN by rat brain." *Biochem Pharmacol* **38**(10): 1597-1603.

Fosbraey, P. et al. (1990). "Neurotransmitter changes in guinea-pig brain regions following soman intoxication." *J Neurochem* **54**(1): 72-79.

Francis, H. M. et al. (2013). "Proteomic analysis of the dorsal and ventral hippocampus of rats maintained on a high fat and refined sugar diet." *Proteomics* **13**(20): 3076-3091.

Franklin, J. L. et al. (2016). "Quantitative Proteomic Analysis of the Orbital Frontal Cortex in Rats Following Extended Exposure to Caffeine Reveals Extensive Changes to Protein Expression: Implications for Neurological Disease." *J Proteome Res* **15**(5): 1455-1471.

Garcia-Gil, L. et al. (1997). "Perinatal delta(9)-tetrahydrocannabinol exposure alters the responsiveness of hypothalamic dopaminergic neurons to dopamine-acting drugs in adult rats." *Neurotoxicol Teratol* **19**(6): 477-487.

Garcia-Gil, L. et al. (1999). "Perinatal delta9-tetrahydrocannabinol exposure augmented the magnitude of motor inhibition caused by GABA(B), but not GABA(A), receptor agonists in adult rats." *Neurotoxicol Teratol* **21**(3): 277-283.

George, J. and Y. Shukla (2011). "Pesticides and cancer: insights into toxicoproteomic-based findings." *J Proteomics* **74**(12): 2713-2722.

George, J. et al. (2010). "Toxicoproteomics: new paradigms in toxicology research." *Toxicol Mech Methods* **20**(7): 415-423.

Ghasemi, A. et al. (2007). "Paraoxon inhibits GABA uptake in brain synaptosomes." *Toxicol In Vitro* **21**(8): 1499-1504.

Giesy, J. P. et al. (1999). "Chlorpyrifos: ecological risk assessment in North American aquatic environments." *Rev Environ Contam Toxicol* **160**: 1-129.

Girard, I. and T. Garland, Jr. (2002). "Plasma corticosterone reponse to acute and chronic voluntary exercise in female house mice." *Journal of Applied Physiology* **92**: 1553-1561.

Gordon, N. S. et al. (2003). "Socially-induced brain 'fertilization': play promotes brain derived neurotrophic factor transcription in the amygdala and dorsolateral frontal cortex in juvenile rats." *Neurosci Lett* **341**(1): 17-20.

Gunnell, D. et al. (2007). "The global distribution of fatal pesticide self-poisoning: systematic review." *BMC Public Health* **7**: 357.

Gupta, R. C. (2004). "Brain regional heterogeneity and toxicological mechanisms of organophosphates and carbamates." *Toxicol Mech Methods* **14**(3): 103-143.

Haber, S. N. and B. Knutson (2010). "The reward circuit: linking primate anatomy and human imaging." *Neuropsychopharmacology* **35**(1): 4-26.

Hayden, K. M. et al. (2010). "Occupational exposure to pesticides increases the risk of incident AD: the Cache County study." *Neurology* **74**(19): 1524-1530.

Hernandez, M. et al. (2000). "Cannabinoid CB(1) receptors colocalize with tyrosine hydroxylase in cultured fetal mesencephalic neurons and their activation increases the levels of this enzyme." *Brain Res* **857**(1-2): 56-65.

Herrera-Molina, R. et al. (2014). "Structure of excitatory synapses and GABAA receptor localization at inhibitory synapses are regulated by neuroplastin-65." *J Biol Chem* **289**(13): 8973-8988.

Hodgson, E. and R. L. Rose (2007). "The importance of cytochrome P450 2B6 in the human metabolism of environmental chemicals." *Pharmacol Ther* **113**(2): 420-428.

Hollmann, H. W. et al. (2005). "Receptors, G proteins, and their interactions." *Anesthesiology* **103**(5): 1066-1078.

Homberg, J. R. et al. (2007). "Acute and constitutive increases in central serotonin levels reduce social play behaviour in peri-adolescent rats." *Psychopharmacology (Berl)* **195**(2): 175-182.

Huen, K. et al. (2012). "Organophosphate pesticide levels in blood and urine of women and newborns living in an agricultural community." *Environ Res* **117**: 8-16.

Iyer, R. et al. (2015). "Developments in alternative treatments for organophosphate poisoning." *Toxicol Lett* **233**(2): 200-206.

Jamal, G. A. et al. (2002). "Low level exposures to organophosphorus esters may cause neurotoxicity." *Toxicology* **181-182**: 23-33.

Jewett, B. E. and S. Sharma (2018). Physiology, GABA. StatPearls. Treasure Island (FL), StatPearls Publishing LLC.

Jordan, R. (2003). "Social play and autistic spectrum disorders: a perspective on theory, implications and educational approaches." *Autism* **7**(4): 347-360.

Kandel, E. R. and D. B. Kandel (2014). "Shattuck Lecture. A molecular basis for nicotine as a gateway drug." *N Engl J Med* **371**(10): 932-943.

Kar, P. P. and M. A. Matin (1972). "Possible role of gamma-aminobutyric acid in paraoxon-induced convulsions." *J Pharm Pharmacol* **24**(12): 996-997.

Keller, A. et al. (2002). "Empirical statistical model to estimate the accuracy of peptide identifications made by MS/MS and database search." *Anal Chem* **74**(20): 5383-5392.

Kentner, A. C. et al. (2018). "Complex Environmental Rearing Enhances Social Salience and Affects Hippocampal Corticotropin Releasing Hormone Receptor Expression in a Sex-Specific Manner." *Neuroscience* **369**: 399-411.

Kim, J. H. et al. (2010). "Identification and characterization of biomarkers of organophosphorus exposures in humans." *Adv Exp Med Biol* **660**: 61-71.

King, A. M. and C. K. Aaron (2015). "Organophosphate and carbamate poisoning." *Emerg Med Clin North Am* **33**(1): 133-151.

Koch, D. et al. (2002). "Temporal association of children's pesticide exposure and agricultural spraying: report of a longitudinal biological monitoring study." *Environ Health Perspect* **110**(8): 829-833.

Kolarich, D. et al. (2008). "Glycoproteomic characterization of butyrylcholinesterase from human plasma." *Proteomics* **8**(2): 254-263.

Kozhemyakin, M. et al. (2010). "Central cholinesterase inhibition enhances glutamatergic synaptic transmission." *J Neurophysiol* **103**(4): 1748-1757.

Kumar, A. M. et al. (1990). "Effect of early exposure to delta-9-tetrahydrocannabinol on the levels of opioid peptides, gonadotropin-releasing hormone and substance P in the adult male rat brain." *Brain Res* **525**(1): 78-83.

Kuoppasalmi, K. et al. (1980). "Plasma cortisol, androstenedione, testosterone and luteinizing hormone in running exercise of different intensities." *Scand J Clin Lab Invest* **40**(5): 403-409.

Kwong, T. C. (2002). "Organophosphate pesticides: biochemistry and clinical toxicology." *Ther Drug Monit* **24**(1): 144-149.

Lallement, G. et al. (1991). "Effects of soman-induced seizures on different extracellular amino acid levels and on glutamate uptake in rat hippocampus." *Brain Res* **563**(1-2): 234-240.

Lamberts, J. T. et al. (2011). "mu-Opioid receptor coupling to Galpha(o) plays an important role in opioid antinociception." *Neuropsychopharmacology* **36**(10): 2041-2053.

Lari, P. et al. (2014). "Alteration of protein profile in rat liver of animals exposed to subacute diazinon: a proteomic approach." *Electrophoresis* **35**(10): 1419-1427.

Lassiter, T. L. et al. (1998). "Gestational exposure to chlorpyrifos: apparent protection of the fetus?" *Toxicol Appl Pharmacol* **152**(1): 56-65.

Lauder, J. M. (1985). "Roles for neurotransmitters in development: possible interaction with drugs during the fetal and neonatal periods." *Prog Clin Biol Res* **163c**: 375-380.

Lehotzky, K. et al. (1989). "Behavioral consequences of prenatal exposure to the organophosphate insecticide sumithion." *Neurotoxicol Teratol* **11**(3): 321-324.

Levin, E. D. et al. (2002). "Prenatal chlorpyrifos exposure in rats causes persistent behavioral alterations." *Neurotoxicol Teratol* **24**(6): 733-741.

Levin, E. D. et al. (2001). "Persistent behavioral consequences of neonatal chlorpyrifos exposure in rats." *Brain Res Dev Brain Res* **130**(1): 83-89.

Levin, E. D. et al. (2010). "Early postnatal parathion exposure in rats causes sex-selective cognitive impairment and neurotransmitter defects which emerge in aging." *Behav Brain Res* **208**(2): 319-327.

Li, C. Y. et al. (2011). "Bilirubin enhances neuronal excitability by increasing glutamatergic transmission in the rat lateral superior olive." *Toxicology* **284**(1-3): 19-25.

Li, Y. et al. (2016). "Serotonin neurons in the dorsal raphe nucleus encode reward signals." *Nat Commun* **7**: 10503.

Lima, C. S. et al. (2013). "Methamidophos exposure during the early postnatal period of mice: immediate and late-emergent effects on the cholinergic and serotonergic systems and behavior." *Toxicol Sci* **134**(1): 125-139.

Lin, X. et al. (2011). "Changes of protein expression profiles in the amygdala during the process of morphine-induced conditioned place preference in rats." *Behav Brain Res* **221**(1): 197-206.

Lisman, J. et al. (2012). "Mechanisms of CaMKII action in long-term potentiation." *Nat Rev Neurosci* **13**(3): 169-182.

Liu, Z. P. et al. (2017). "Delta Subunit-Containing Gamma-Aminobutyric Acid A Receptor Disinhibits Lateral Amygdala and Facilitates Fear Expression in Mice." *Biol Psychiatry* **81**(12): 990-1002.

Luo, A. H. et al. (2011). "Linking context with reward: a functional circuit from hippocampal CA3 to ventral tegmental area." *Science* **333**(6040): 353-357.

Lupica, C. R. and A. C. Riegel (2005). "Endocannabinoid release from midbrain dopamine neurons: a potential substrate for cannabinoid receptor antagonist treatment of addiction." *Neuropharmacology* **48**(8): 1105-1116.

Mackenzie Ross, S. J. et al. (2010). "Neuropsychological and psychiatric functioning in sheep farmers exposed to low levels of organophosphate pesticides." *Neurotoxicol Teratol* **32**(4): 452-459.

Manduca, A. et al. (2016). "Interacting Cannabinoid and Opioid Receptors in the Nucleus Accumbens Core Control Adolescent Social Play." *Front Behav Neurosci* **10**: 211.

Mao, L. M. et al. (2014). "Phosphorylation and regulation of glutamate receptors by CaMKII." *Sheng Li Xue Bao* **66**(3): 365-372.

Martin, D. L. (1987). "Regulatory properties of brain glutamate decarboxylase." *Cell Mol Neurobiol* **7**(3): 237-253.

Maurer, M. H. (2012). "Genomic and proteomic advances in autism research." *Electrophoresis* **33**(24): 3653-3658.

McDonald, M. M. et al. (2012). "GABAA receptor activation in the lateral septum reduces the expression of conditioned defeat and increases aggression in Syrian hamsters." *Brain Res* **1439**: 27-33.

Meaney, M. J. and J. Stewart (1981). "A descriptive study of social development in rat *(Rattus Norvegicus)*." *Anim. Behav.* **29**: 34-45.

Meaney, M. J. et al. (1985). "Sex differneces in social play, the socialization of sex roles." *Adv. Study behav* **15**: 1-58.

Merrick, B. A. (2008). "The plasma proteome, adductome and idiosyncratic toxicity in toxicoproteomics research." *Brief Funct Genomic Proteomic* **7**(1): 35-49.

Middlemore-Risher, M. L. et al. (2011). "Effects of chlorpyrifos and chlorpyrifos-oxon on the dynamics and movement of mitochondria in rat cortical neurons." *J Pharmacol Exp Ther* **339**(2): 341-349.

Middlemore-Risher, M. L. et al. (2010). "Repeated exposures to low-level chlorpyrifos results in impairments in sustained attention and increased impulsivity in rats." *Neurotoxicol Teratol* **32**(4): 415-424.

Miller, I. et al. (2014). "The added value of proteomics for toxicological studies." *J Toxicol Environ Health B Crit Rev* **17**(4): 225-246.

Mohammadi, M. et al. (2016). "Alterations in mRNA and protein expression of glutamate transporters in rat hippocampus after paraoxon exposure." *Neurotoxicology* **57**: 251-257.

Molina-Holgado, F. et al. (1997). "Maternal exposure to delta 9-tetrahydrocannabinol (delta 9-THC) alters indolamine levels and turnover in adult male and female rat brain regions." *Brain Res Bull* **43**(2): 173-178.

Molina-Holgado, F. et al. (1996). "Effect of maternal delta 9-tetrahydrocannabinol on developing serotonergic system." *Eur J Pharmacol* **316**(1): 39-42.

Moller, P. and R. Husby (2000). "The initial prodrome in schizophrenia: searching for naturalistic core dimensions of experience and behavior." *Schizophr Bull* **26**(1): 217-232.

Montes de Oca, L. et al. (2013). "Long term compulsivity on the 5-choice serial reaction time task after acute Chlorpyrifos exposure." *Toxicol Lett* **216**(2-3): 73-85.

Moretto, A. and C. Colosio (2013). "The role of pesticide exposure in the genesis of Parkinson's disease: epidemiological studies and experimental data." *Toxicology* **307**: 24-34.

Moulder, R. et al. (2017). "Analysis of the plasma proteome using iTRAQ and TMT-based Isobaric labeling." *Mass Spectrom Rev*.

Mowry, J. B. et al. (2014). "2013 Annual Report of the American Association of Poison Control Centers' National Poison Data System (NPDS): 31st Annual Report." *Clinical Toxicology* **52**(10): 1032-1283.

Nakanishi, H. et al. (1997). "Neurabin: A Novel Neural Tissue–specific Actin Filament–binding Protein Involved in Neurite Formation." *The Journal of Cell Biology* **139**(4): 951-961.

Nesvizhskii, A. I. et al. (2003). "A statistical model for identifying proteins by tandem mass spectrometry." *Anal Chem* **75**(17): 4646-4658.

New, D. C. and Y. H. Wong (2007). "Molecular mechanisms mediating the G protein-coupled receptor regulation of cell cycle progression." *J Mol Signal* **2**: 2.

Niesink, R. J. and J. M. Van Ree (1989). "Involvement of opioid and dopaminergic systems in isolation-induced pinning and social grooming of young rats." *Neuropharmacology* **28**(4): 411-418.

Nomura, D. K. et al. (2008). "Activation of the endocannabinoid system by organophosphorus nerve agents." *Nature Chemical Biology* **4**: 373.

Nomura, D. K. and J. E. Casida (2011). "Activity-Based Protein Profiling of Organophosphorus and Thiocarbamate Pesticides Reveals Multiple Serine Hydrolase Targets in Mouse Brain." *Journal of Agricultural and Food Chemistry* **59**(7): 2808-2815.

Normansell, L. and J. Panksepp (1990). "Effects of morphine and naloxone on play-rewarded spatial discrimination in juvenile rats." *Dev Psychobiol* **23**(1): 75-83.

O'Shea, M. et al. (2006). "Repeated cannabinoid exposure during perinatal, adolescent or early adult ages produces similar longlasting deficits in object recognition and reduced social interaction in rats." *J Psychopharmacol* **20**(5): 611-621.

O'Shea, M. et al. (2004). "Chronic cannabinoid exposure produces lasting memory impairment and increased anxiety in adolescent but not adult rats." *J Psychopharmacol* **18**(4): 502-508.

Owczarek, S. and V. Berezin (2012). "Neuroplastin: cell adhesion molecule and signaling receptor." *Int J Biochem Cell Biol* **44**(1): 1-5.

Paine, T. A. et al. (2017). "Decreasing GABA function within the medial prefrontal cortex or basolateral amygdala decreases sociability." *Behav Brain Res* **317**: 542-552.

Panksepp, J. and W. W. Beatty (1980). "Social deprivation and play in rats." *Behav Neural Biol* **30**(2): 197-206.

Panksepp, J. et al. (1980). "Endogenous opioids and social behavior." *Neurosci Biobehav Rev* **4**(4): 473-487.

Panksepp, J. et al. (1984). "The psychobiology of play: theoretical and methodological perspectives." *Neurosci Biobehav Rev* **8**(4): 465-492.

Parron, T. et al. (2011). "Association between environmental exposure to pesticides and neurodegenerative diseases." *Toxicol Appl Pharmacol* **256**(3): 379-385.

Patel, S. et al. (2007). "Identification of differentially expressed proteins in striatum of maneb-and paraquat-induced Parkinson's disease phenotype in mouse." *Neurotoxicol Teratol* **29**(5): 578-585.

Pellis, S. M. and V. C. Pellis (1991). "Attack and defense during play fighting appear to be motivationally independant behaviors in muroid rodents." *Psychol. Rec.* **41**: 175-184.

Pellis, S. M. and V. C. Pellis (1998). "Play fighting of rats in comparative perspective: a schema for neurobehavioral analyses." *Neurosci Biobehav Rev* **23**(1): 87-101.

Pellis, S. M. and V. C. Pellis (2007). "Rough - and - Tumble Play and the Development of the Social brain." *Current directions in psychological science* **16**(2): 95-98.

Peris-Sampedro, F. et al. (2014). "Impaired retention in AbetaPP Swedish mice six months after oral exposure to chlorpyrifos." *Food Chem Toxicol* **72**: 289-294.

Plonsky, M. and P. R. Freeman (1982). "The effects of methadone on the social behavior and activity of the rat." *Pharmacol Biochem Behav* **16**(4): 569-571.

Pope, C. N. (1999). "Organophosphorus pesticides: do they all have the same mechanism of toxicity?" *J Toxicol Environ Health B Crit Rev* **2**(2): 161-181.

Quistad, G. B. et al. (2006). "Monoacylglycerol lipase inhibition by organophosphorus compounds leads to elevation of brain 2-arachidonoylglycerol and the associated hypomotility in mice." *Toxicology and Applied Pharmacology* **211**(1): 78-83.

Quistad, G. B. et al. (2001). "Fatty Acid Amide Hydrolase Inhibition by Neurotoxic Organophosphorus Pesticides." *Toxicology and Applied Pharmacology* **173**(1): 48-55.

Quistad, G. B. et al. (2002). "Selective Inhibitors of Fatty Acid Amide Hydrolase Relative to Neuropathy Target Esterase and Acetylcholinesterase: Toxicological Implications." *Toxicology and Applied Pharmacology* **179**(1): 57-63.

Rauh, V. et al. (2011). "Seven-year neurodevelopmental scores and prenatal exposure to chlorpyrifos, a common agricultural pesticide." *Environ Health Perspect* **119**(8): 1196-1201.

Rauh, V. A. et al. (2015). "Prenatal exposure to the organophosphate pesticide chlorpyrifos and childhood tremor." *Neurotoxicology* **51**: 80-86.

Rauh, V. A. et al. (2006). "Impact of prenatal chlorpyrifos exposure on neurodevelopment in the first 3 years of life among inner-city children." *Pediatrics* **118**(6): e1845-1859.

Rauh, V. A. et al. (2012). "Brain anomalies in children exposed prenatally to a common organophosphate pesticide." *Proc Natl Acad Sci U S A* **109**(20): 7871-7876.

Ricceri, L. et al. (2003). "Developmental exposure to chlorpyrifos alters reactivity to environmental and social cues in adolescent mice." *Toxicol Appl Pharmacol* **191**(3): 189-201.

Ricceri, L. et al. (2006). "Developmental neurotoxicity of organophosphorous pesticides: fetal and neonatal exposure to chlorpyrifos alters sex-specific behaviors at adulthood in mice." *Toxicol Sci* **93**(1): 105-113.

Ross, E. M. and T. M. Wilkie (2000). "GTPase-activating proteins for heterotrimeric G proteins: regulators of G protein signaling (RGS) and RGS-like proteins." *Annu Rev Biochem* **69**: 795-827.

Ross, S. M. et al. (2013). "Neurobehavioral problems following low-level exposure to organophosphate pesticides: a systematic and meta-analytic review." *Crit Rev Toxicol* **43**(1): 21-44.

Ruckart, P. Z. et al. (2004). "Long-term neurobehavioral health effects of methyl parathion exposure in children in Mississippi and Ohio." *Environ Health Perspect* **112**(1): 46-51.

Salazar, J. G. et al. (2011). "Amyloid β peptide levels increase in brain of AβPP Swedish mice after exposure to chlorpyrifos." *Current Alzheimer Research* **8**(7): 732-740.

Salvi, R. M. et al. (2003). "Neuropsychiatric evaluation in subjects chronically exposed to organophosphate pesticides." *Toxicol Sci* **72**(2): 267-271.

Singh, A. K. et al. (2011). "Nigrostriatal proteomics of cypermethrin-induced dopaminergic neurodegeneration: microglial activation-dependent and -independent regulations." *Toxicol Sci* **122**(2): 526-538.

Singh, S. and N. Sharma (2000). "Neurological syndromes following organophosphate poisoning." *Neurol india* **48**(4): 308-313.

Siviy, S. M. and J. Panksepp (1985). "Energy balance and play in juvenile rats." *Physiol. Behav.* **35**: 435-441.

Slotkin, T. A. (1999). "Developmental cholinotoxicants: nicotine and chlorpyrifos." *Environ Health Perspect* **107 Suppl 1**: 71-80.

Slotkin, T. A. (2004a). "Cholinergic systems in brain development and disruption by neurotoxicants: nicotine, environmental tobacco smoke, organophosphates." *Toxicol Appl Pharmacol* **198**(2): 132-151.

Slotkin, T. A. (2004b). "Guidelines for Developmental Neurotoxicity and Their Impact on Organophosphate Pesticides: A Personal View from an Academic Perspective." *Neurotoxicology* **25**(4): 631-640.

Slotkin, T. A. et al. (2009). "Developmental neurotoxicity of parathion: progressive effects on serotonergic systems in adolescence and adulthood." *Neurotoxicol Teratol* **31**(1): 11-17.

Slotkin, T. A. et al. (2008). "Developmental Neurotoxicity of Low-Dose Diazinon Exposure of Neonatal Rats: Effects on Serotonin Systems in Adolescence and Adulthood." *Brain Res Bull* **75**(5): 640-647.

Slotkin, T. A. and F. J. Seidler (2011). "Developmental exposure to organophosphates triggers transcriptional changes in genes associated with Parkinson's disease in vitro and in vivo." *Brain Res Bull* **86**(5-6): 340-347.

Slotkin, T. A. et al. (2015a). "Prenatal nicotine changes the response to postnatal chlorpyrifos: Interactions targeting serotonergic synaptic function and cognition." *Brain Res Bull* **111**: 84-96.

Slotkin, T. A. et al. (2015b). "Prenatal drug exposures sensitize noradrenergic circuits to subsequent disruption by chlorpyrifos." *Toxicology* **338**: 8-16.

Slotkin, T. A. et al. (2017). "Diazinon and parathion diverge in their effects on development of noradrenergic systems." *Brain Res Bull* **130**: 268-273.

Slotkin, T. A. et al. (2002). "Functional alterations in CNS catecholamine systems in adolescence and adulhood after neonatal chlorpyrifos exposure." *Developmental Brain Research* **133**: 163-173.

Slotkin, T. A. et al. (2006). "Organophosphate insecticides target the serotonergic system in developing rat brain regions: disparate effects of diazinon and parathion at doses spanning the threshold for cholinesterase inhibition." *Environ Health Perspect* **114**(10): 1542-1546.

Speed, H. E. et al. (2012). "Delayed reduction of hippocampal synaptic transmission and spines following exposure to repeated subclinical doses of organophosphorus pesticide in adult mice." *Toxicol Sci* **125**(1): 196-208.

Spilker, C. and M. R. Kreutz (2010). "RapGAPs in brain: multipurpose players in neuronal Rap signalling." *Eur J Neurosci* **32**(1): 1-9.

Steenland, K. et al. (1994). "Chronic Neurological Sequelae to Organophosphate Pesticide Poisoning." *American Journal of Public Health* **84**(5): 731-736.

Stella, N. et al. (1997). "A second endogenous cannabinoid that modulates long-term potentiation." *Nature* **388**(6644): 773-778.

Stephens, R. et al. (1995). "Neuropsychological effects of long-term exposure to organophosphates in sheep dip." *Lancet* **345**(8958): 1135-1139.

Suarez, I. et al. (2004). "Down-regulation of the AMPA glutamate receptor subunits GluR1 and GluR2/3 in the rat cerebellum following pre- and perinatal delta9-tetrahydrocannabinol exposure." *Cerebellum* **3**(2): 66-74.

Sun, J. and B. C. Lynn (2009). "Development of a LC/MS/MS method to analyze butyrylcholinesterase inhibition resulting from multiple pesticide exposure." *J Chromatogr B Analyt Technol Biomed Life Sci* **877**(29): 3681-3685.

Suratman, S. et al. (2015). "Organophosphate pesticides exposure among farmworkers: pathways and risk of adverse health effects." *Rev Environ Health* **30**(1): 65-79.

Sutton, L. P. et al. (2016). "Regulator of G-Protein Signaling 7 Regulates Reward Behavior by Controlling Opioid Signaling in the Striatum." *Biol Psychiatry* **80**(3): 235-245.

Suvrathan, A. et al. (2014). "Stress enhances fear by forming new synapses with greater capacity for long-term potentiation in the amygdala." *Philos Trans R Soc Lond B Biol Sci* **369**(1633): 20130151.

Takahashi, L. K. (1986). "Postweaning environmental and social factors influencing the onset and expression of agonistic behavior in Norway rats." *Behav Processes* **12**(3): 237-260.

Tau, G. Z. and B. S. Peterson (2010). "Normal development of brain circuits." *Neuropsychopharmacology* **35**(1): 147-168.

Terry-Lorenzo, R. T. et al. (2005). "Neurabin/Protein Phosphatase-1 Complex Regulates Dendritic Spine Morphogenesis and Maturation." *Molecular Biology of the Cell* **16**: 2349-2362.

Terry, A. V., Jr. (2012). "Functional consequences of repeated organophosphate exposure: potential non-cholinergic mechanisms." *Pharmacol Ther* **134**(3): 355-365.

Terry, A. V., Jr. et al. (2012). "Chronic impairments in spatial learning and memory in rats previously exposed to chlorpyrfos or diisopropylfluorophosphate." *Neurotoxicol Teratol* **34**(1): 1-8.

Terry, A. V., Jr. et al. (2011). "Repeated, intermittent exposures to diisopropylfluorophosphate in rats: protracted effects on cholinergic markers, nerve growth factor-related proteins, and cognitive function." *Neuroscience* **176**: 237-253.

Terry, A. V., Jr. et al. (2007). "Chronic, intermittent exposure to chlorpyrifos in rats: protracted effects on axonal transport, neurotrophin receptors, cholinergic markers, and information processing." *J Pharmacol Exp Ther* **322**(3): 1117-1128.

Terry, A. V., Jr. et al. (2003). "Repeated exposures to subthreshold doses of chlorpyrifos in rats: hippocampal damage, impaired axonal transport, and deficits in spatial learning." *J Pharmacol Exp Ther* **305**(1): 375-384.

Tian, J. et al. (2015). "The effect of HMGB1 on sub-toxic chlorpyrifos exposure-induced neuroinflammation in amygdala of neonatal rats." *Toxicology* **338**: 95-103.

Torres-Altoro, M. I. et al. (2011). "Organophosphates dysregulate dopamine signaling, glutamatergic neurotransmission, and induce neuronal injury markers in striatum." *J Neurochem* **119**(2): 303-313.

Trapnell, C. et al. (2013). "Differential analysis of gene regulation at transcript resolution with RNA-seq." *Nat Biotechnol* **31**(1): 46-53.

Trezza, V. et al. (2010). "The pleasures of play: pharmacological insights into social reward mechanisms." *Trends Pharmacol Sci* **31**(10): 463-469.

Trezza, V. et al. (2011a). "Evaluating the rewarding nature of social interactions in laboratory animals." *Dev Cogn Neurosci* **1**(4): 444-458.

Trezza, V. et al. (2011b). "Nucleus accumbens mu-opioid receptors mediate social reward." *J Neurosci* **31**(17): 6362-6370.

Trezza, V. et al. (2012). "Endocannabinoids in amygdala and nucleus accumbens mediate social play reward in adolescent rats." *J Neurosci* **32**(43): 14899-14908.

Trezza, V. and L. J. Vanderschuren (2008a). "Bidirectional cannabinoid modulation of social behavior in adolescent rats." *Psychopharmacology (Berl)* **197**(2): 217-227.

Trezza, V. and L. J. Vanderschuren (2008b). "Cannabinoid and opioid modulation of social play behavior in adolescent rats: differential behavioral mechanisms." *Eur Neuropsychopharmacol* **18**(7): 519-530.

Trezza, V. and L. J. Vanderschuren (2009). "Divergent effects of anandamide transporter inhibitors with different target selectivity on social play behavior in adolescent rats." *J Pharmacol Exp Ther* **328**(1): 343-350.

Tucker, J. B. (2006). War of Nerves: Chemical Warfare from World War I to Al-qaeda, Pantheon Books.

Udvari, E. B. et al. (2017). "Synaptic proteome changes in the hypothalamus of mother rats." *J Proteomics* **159**: 54-66.

Vanderschuren, L. J. et al. (2016). "The neurobiology of social play and its rewarding value in rats." *Neurosci Biobehav Rev* **70**: 86-105.

Vanderschuren, L. J. et al. (1995a). "Mu- and kappa-opioid receptor-mediated opioid effects on social play in juvenile rats." *Eur J Pharmacol* **276**(3): 257-266.

Vanderschuren, L. J. et al. (1997a). "The neurobiology of social play behavior in rats." *Neurosci Biobehav Rev* **21**(3): 309-326.

Vanderschuren, L. J. M. J. et al. (1995b). "Influence of environmental factor on social play behavior of juvenile rats." *Physiol. Behav.* **58**: 119-123.

Vanderschuren, L. J. M. J. et al. (1997b). "The Neurobiology of Social Play Behavior in Rats." *Neurosci Biobehav Rev* **21**(3): 309-326.

Vanderschuren, L. J. M. J. and V. Trezza (2014). "What the Laboratory Rat has Taught us About Social Play Behaviour: Role in Behavioral Development and Neural Mechanisms." *The Neurobiology of Childhood* **16**: 189-212.

Veenema, A. H. et al. (2012). "Vasopressin regulates social recognition in juvenile and adult rats of both sexes, but in sex- and age-specific ways." *Horm Behav* **61**(1): 50-56.

Venerosi, A. et al. (2006). "A social recognition test for female mice reveals behavioral effects of developmental chlorpyrifos exposure." *Neurotoxicol Teratol* **28**(4): 466-471.

Venerosi, A. et al. (2008). "Neonatal exposure to chlorpyrifos affects maternal responses and maternal aggression of female mice in adulthood." *Neurotoxicol Teratol* **30**(6): 468-474.

Venerosi, A. et al. (2010). "Gestational exposure to the organophosphate chlorpyrifos alters social-emotional behaviour and impairs responsiveness to the serotonin transporter inhibitor fluvoxamine in mice." *Psychopharmacology (Berl)* **208**(1): 99-107.

Wang, A. et al. (2014). "The association between ambient exposure to organophosphates and Parkinson's disease risk." *Occup Environ Med* **71**(4): 275-281.

Wang, L. et al. (2016). "Chlorpyrifos exposure in farmers and urban adults: Metabolic characteristic, exposure estimation, and potential effect of oxidative damage." *Environ Res* **149**: 164-170.

Wang, Y. et al. (2010). "Regulation of AMPA receptors in spinal nociception." *Mol Pain* **6**: 5.

Wetmore, B. A. and B. A. Merrick (2004). "Toxicoproteomics: Proteomics Applied to Toxicology and Pathology." *Toxicologic Pathology* **32**: 619-642.

Wettschureck, N. and S. Offermanns (2005). "Mammalian G proteins and their cell type specific functions." *Physiol Rev* **85**(4): 1159-1204.

Whitney, K. D. et al. (1995a). "Developmental Neurotoxicity of Chlorpyrifos: Cellular Mechanisms." *Toxicol Appl Pharmacol* **134**(1): 53-62.

Whitney, K. D. et al. (1995b). "Developmental neurotoxicity of chlorpyrifos: cellular mechanisms." *Toxicol Appl Pharmacol* **134**(1): 53-62.

Whyatt, R. M. et al. (2005). "Biomarkers in assessing residential insecticide exposures during pregnancy and effects on fetal growth." *Toxicol Appl Pharmacol* **206**(2): 246-254.

Whyatt, R. M. et al. (2004). "Prenatal insecticide exposures and birth weight and length among an urban minority cohort." *Environ Health Perspect* **112**(10): 1125-1132.

Wolf-Yadlin, A. et al. (2007). "Multiple reaction monitoring for robust quantitative proteomic analysis of cellular signaling networks." *Proceedings of the National Academy of Sciences* **104**(14): 5860.

Young, J. G. et al. (2005). "Association between in utero organophosphate pesticide exposure and abnormal reflexes in neonates." *Neurotoxicology* **26**(2): 199-209.

Zahm, D. S. et al. (2013). "On lateral septum-like characteristics of outputs from the accumbal hedonic "hotspot" of Pecina and Berridge with commentary on the transitional nature of basal forebrain "boundaries"." *J Comp Neurol* **521**(1): 50-68.

Zanettini, C. et al. (2011). "Effects of endocannabinoid system modulation on cognitive and emotional behavior." *Front Behav Neurosci* **5**: 57.

Zare, Z. et al. (2017). "Differential expression of glutamate transporters in cerebral cortex of paraoxon-treated rats." *Neurotoxicol Teratol* **62**: 20-26.

Zelek-Molik, A. et al. (2012). "Morphine-induced place preference affects mRNA expression of G protein a subunits in rat brain." *Pharmacological Reports* **64**: 546-557.

Zhang, J. et al. (2015). "Neonatal chlorpyrifos exposure induces loss of dopaminergic neurons in young adult rats." *Toxicology* **336**: 17-25.

Zheng, Q. et al. (2000). "Comparative cholinergic neurotoxicity of oral chlorpyrifos exposures in preweanling and adult rats." *Toxicol Sci* **55**(1): 124-132.

Zhou, Y. and N. C. Danbolt (2013). "GABA and Glutamate Transporters in Brain." *Front Endocrinol (Lausanne)* **4**: 165.

Zhou, Y. and N. C. Danbolt (2014). "Glutamate as a neurotransmitter in the healthy brain." *J Neural Transm (Vienna)* **121**(8): 799-817.

APPENDIX A

SUPPLEMENTARY TABLES

Table A.1 List of differentially expressed proteins with p-value ≤ 0.05 in C NB vs C B comparison in Chapter II

ID	Entrez Gene Name	Symbol	Fold Change	p-value	Type
ACTC_RAT	actin, alpha, cardiac muscle 1	ACTC1	1.6	0.0001	enzyme
Q6T487_RAT	actinin alpha 1	ACTN1	-1.667	0.0017	transcription regulator
G3V9G1_RAT	adenylate cyclase 5	ADCY5	-10	0.037	enzyme
AGAP2_RAT	ArfGAP with GTPase domain, ankyrin repeat and PH domain 2	AGAP2	10	0.018	enzyme
D3Z9L0_RAT	acylglycerol kinase	AGK	-10	0.016	kinase
Q4G079_RAT	aminoacyl tRNA synthetase complex interacting multifunctional protein 1	AIMP1	9.1	0.031	cytokine
AL7A1_RAT	aldehyde dehydrogenase 7 family member A1	ALDH7A1	10	0.018	enzyme
Q5XI77_RAT	annexin A11	ANXA11	-10	0.037	other
ANXA3_RAT	annexin A3	ANXA3	-2	0.041	enzyme
Q6IMZ3_RAT	annexin A6	ANXA6	-5	0.00025	ion channel
D3ZWA8_RAT	adaptor protein, phosphotyrosine interacting with PH domain and leucine zipper 1	APPL1	13	0.0055	other
A0A0G2K336_RAT	aquaporin 4	AQP4	-10	0.016	transporter

Table A.1 (continued)

ATPA_RAT	ATP synthase, H+ transporting, mitochondrial F1 complex, alpha subunit 1, cardiac muscle	ATP5A1	1.5	0.0001	transporter
Q5M7T6_RAT	ATPase H+ transporting V0 subunit d1	ATP6V0D1	-1.667	0.041	transporter
VATE1_RAT	ATPase H+ transporting V1 subunit E1	ATP6V1E1	-1.429	0.026	transporter
D3ZUP5_RAT	BRICK1, SCAR/WAVE actin nucleating complex subunit	BRK1	-11.111	0.0071	other
BRSK1_RAT	BR serine/threonine kinase 1	BRSK1	-10	0.016	kinase
Q5U2P5_RAT	C2CD2 like	C2CD2L	4	0.05	transporter
A0A0G2K7E5_RAT	calcium voltage-gated channel auxiliary subunit alpha2delta 1	CACNA2D1	-2	0.041	ion channel
CALB1_RAT	calbindin 1	CALB1	-3.333	0.014	other
Q5RJK5_RAT	chromobox 3	CBX3	-2.5	0.04	transcription regulator
A0A0G2K0B0_RAT	CDV3 homolog	CDV3	9.3	0.031	other
M0RC17_RAT	cell adhesion molecule L1 like	CHL1	9.3	0.031	other
KCRB_RAT	creatine kinase B	CKB	2	0.0001	kinase

Table A.1 (continued)

M0RAD5_RAT	caseinolytic mitochondrial matrix peptidase proteolytic subunit	CLPP	11	0.018	Peptidase
A0A0G2JYW3_RAT	clathrin light chain A	CLTA	-16.667	0.0014	other
F1M779_RAT	clathrin heavy chain	CLTC	-1.25	0.0045	other
CNTN1_RAT	contactin 1	CNTN1	-1.667	0.0027	enzyme
CSRP1_RAT	cysteine and glycine rich protein 1	CSRP1	12	0.0099	other
A0A0G2JZ13_RAT	cortactin	CTTN	-5	0.023	other
A0A0G2JT00_RAT	cutA divalent cation tolerance homolog	CUTA	12	0.0099	other
D3ZFQ8_RAT	cytochrome c1	CYC1	-2.5	0.0046	enzyme
D4A8U7_RAT	dynactin subunit 1	DCTN1	1.9	0.0024	other
DDAH2_RAT	dimethylarginine dimethylaminohydrolase 2	DDAH2	4.3	0.027	enzyme
A0A096MIX2_RAT	DEAD-box helicase 17	Ddx17	2.3	0.049	transcription regulator
F1LP01_RAT	diacylglycerol kinase beta	DGKB	-3.333	0.014	kinase
D4A559_RAT	dematin actin binding protein	DMTN	-11.111	0.0071	other
Q5M9H7_RAT	DnaJ heat shock protein family (Hsp40) member A2	DNAJA2	2.6	0.05	enzyme
DPYL2_RAT	dihydropyrimidinase like 2	DPYSL2	2.5	0.0001	enzyme
IF5_RAT	eukaryotic translation initiation factor 5	EIF5	-5	0.023	translation regulator
ENOPH_RAT	enolase-phosphatase 1	ENOPH1	-11.111	0.0071	enzyme

Table A.1 (continued)

ERR1_RAT	estrogen related receptor, alpha	Esrra	8.7	0.031	transcription regulator
FHIT_RAT	fragile histidine triad	FHIT	-10	0.037	enzyme
FLOT1_RAT	flotillin 1	FLOT1	-3.333	0.043	other
LYAG_RAT	glucosidase alpha, acid	GAA	15	0.0031	enzyme
GBRA1_RAT	gamma-aminobutyric acid type A receptor alpha1 subunit	GABRA1	-10	0.016	ion channel
GFAP_RAT	glial fibrillary acidic protein	GFAP	-1.667	0.041	other
CXA1_RAT	gap junction protein alpha 1	GJA1	-3.333	0.024	transporter
GUAA_RAT	guanine monophosphate synthase	GMPS	11	0.018	enzyme
GNAO_RAT	G protein subunit alpha o1	GNAO1	-1.25	0.043	enzyme
A0A0G2K7W7_RAT	glycogen synthase kinase 3 alpha	GSK3A	3.1	0.035	kinase
A0A0G2KB98_RAT	glycogen synthase kinase 3 beta	GSK3B	13	0.0055	kinase
HPLN1_RAT	hyaluronan and proteoglycan link protein 1	HAPLN1	-20	0.00026	other
A0A0G2JSV6_RAT	hemoglobin, alpha 1	Hba1/Hba2	-1.429	0.0071	other
HBB1_RAT	hemoglobin subunit beta	HBB	-1.429	0.013	transporter
A0A0G2K7W8_RAT	histidine triad nucleotide binding protein 3	HINT3	8.9	0.031	other

Table A.1 (continued)

HMOX2_RAT	heme oxygenase 2	HMOX2	-10	0.037	Enzyme
F1LNF1_RAT	heterogeneous nuclear ribonucleoprotein A2/B1	HNRNPA2B1	-1.667	0.03	other
HPCL4_RAT	hippocalcin like 4	HPCAL4	-2	0.015	transporter
M0R8M9_RAT	heat shock protein family A (Hsp70) member 8	HSPA8	1.2	0.03	enzyme
A0A0G2K261_RAT	isoleucyl-tRNA synthetase 2, mitochondrial	IARS2	-16.667	0.0006	enzyme
D3ZV52_RAT	intersectin 1	ITSN1	9.4	0.031	other
KCAB2_RAT	potassium voltage-gated channel subfamily A regulatory beta subunit 2	KCNAB2	-10	0.037	ion channel
G3V6L4_RAT	kinesin family member 5C	KIF5C	2.4	0.024	enzyme
LASP1_RAT	LIM and SH3 protein 1	LASP1	16	0.0017	transporter
G3V7U4_RAT	lamin B1	LMNB1	-14.286	0.0014	other
F1LM33_RAT	leucine rich pentatricopeptide repeat containing	LRPPRC	-10	0.037	other
AOFA_RAT	monoamine oxidase A	MAOA	-5	0.00019	enzyme
F1LNK0_RAT	microtubule associated protein 2	MAP2	1.2	0.015	other
MK01_RAT	mitogen-activated protein kinase 1	MAPK1	-1.429	0.046	kinase
MBP_RAT	myelin basic protein	Mbp	-1.25	0.023	other
A0A0G2K459_RAT	mitochondrial carrier 2	MTCH2	-10	0.037	other

Table A.1 (continued)

MYADM_RAT	myeloid associated differentiation marker	MYADM	-12.5	0.0071	Other
G3V9Y1_RAT	myosin heavy chain 10	MYH10	-3.333	0.0001	enzyme
NNRE_RAT	NAD(P)HX epimerase	NAXE	-12.5	0.0031	enzyme
NDUAA_RAT	NADH:ubiquinone oxidoreductase subunit A10	NDUFA10	-3.333	0.0025	transporter
NDUAB_RAT	NADH:ubiquinone oxidoreductase subunit A11	NDUFA11	-5	0.023	enzyme
D3ZE15_RAT	NADH:ubiquinone oxidoreductase subunit A13	NDUFA13	-10	0.037	enzyme
NDUA9_RAT	NADH:ubiquinone oxidoreductase subunit A9	NDUFA9	-3.333	0.017	enzyme
D4A0T0_RAT	NADH:ubiquinone oxidoreductase subunit B10	NDUFB10	-2.5	0.027	enzyme
D4A565_RAT	NADH:ubiquinone oxidoreductase subunit B5	NDUFB5	-10	0.037	enzyme
B2RYS8_RAT	NADH:ubiquinone oxidoreductase subunit B8	NDUFB8	-10	0.016	enzyme
NDUS1_RAT	NADH:ubiquinone oxidoreductase core subunit S1	NDUFS1	-1.667	0.0095	enzyme
NDUS2_RAT	NADH:ubiquinone oxidoreductase core subunit S2	NDUFS2	-20	0.00026	enzyme
Q5RJN0_RAT	NADH:ubiquinone oxidoreductase core subunit S7	NDUFS7	-3.333	0.03	enzyme
Q5XIH3_RAT	NADH:ubiquinone oxidoreductase core subunit V1	NDUFV1	-2	0.022	enzyme
F1LNP8_RAT	nectin cell adhesion molecule 1	NECTIN1	9.3	0.031	other
D3ZDC0_RAT	neuroligin 3	NLGN3	3.3	0.05	enzyme

Table A.1 (continued)

NRX3A_RAT	neurexin III	Nrxn3	-11.111	0.0071	other
A0A0G2K6U1_RAT	N-ethylmaleimide sensitive factor, vesicle fusing ATPase	NSF	-1.25	0.048	transporter
NTRK2_RAT	neurotrophic receptor tyrosine kinase 2	NTRK2	-10	0.037	kinase
ODO1_RAT	oxoglutarate dehydrogenase	OGDH	-1.429	0.019	enzyme
A0A0G2K3V4_RAT	O-linked N-acetylglucosamine (GlcNAc) transferase	OGT	-11.111	0.0071	enzyme
F7EYB9_RAT	oligodendrocyte myelin glycoprotein	OMG	-2.5	0.03	G-protein coupled receptor
PACS1_RAT	phosphofurin acidic cluster sorting protein 1	PACS1	4.4	0.013	other
PCYOX_RAT	prenylcysteine oxidase 1	PCYOX1	4.1	0.0042	enzyme
F1LX13_RAT	phosphodiesterase 10A	PDE10A	-14.286	0.0031	enzyme
PDE1B_RAT	phosphodiesterase 1B	PDE1B	-3.333	0.043	enzyme
A0A0G2JSZ5_RAT	protein disulfide isomerase family A member 6	PDIA6	2.1	0.027	enzyme
B5DFN4_RAT	prefoldin subunit 5	PFDN5	12	0.0099	transcription regulator
D3Z955_RAT	phosphoglucomutase 2 like 1	PGM2L1	12	0.0099	enzyme
PHB_RAT	prohibitin	PHB	-2.5	0.0036	transcription regulator
A0A0G2KB63_RAT	prohibitin 2	PHB2	-5		transcription regulator
D3Z981_RAT	plexin A1	PLXNA1	9	0.031	transmembrane receptor

Table A.1 (continued)

PPM1E_RAT	protein phosphatase, Mg2+/Mn2+ dependent 1E	PPM1E	3	0.016	Phosphatase
PPR1B_RAT	protein phosphatase 1 regulatory inhibitor subunit 1B	PPP1R1B	-3.333	0.014	phosphatase
PP1R7_RAT	protein phosphatase 1 regulatory subunit 7	PPP1R7	-2	0.0071	phosphatase
NEB1_RAT	protein phosphatase 1 regulatory subunit 9A	PPP1R9A	-10	0.037	other
A0A0G2JSH9_RAT	peroxiredoxin 2	PRDX2	-1.429	0.035	enzyme
G3V7I0_RAT	peroxiredoxin 3	PRDX3	-1.667	0.017	enzyme
PPCEL_RAT	prolyl endopeptidase-like	PREPL	2.3	0.022	peptidase
PRRT2_RAT	proline rich transmembrane protein 2	PRRT2	9.1	0.031	other
PSB1_RAT	proteasome subunit beta 1	PSMB1	3.4	0.05	peptidase
PRS7_RAT	proteasome 26S subunit, ATPase 2	PSMC2	3.6	0.032	peptidase
PRS6B_RAT	proteasome 26S subunit, ATPase 4	PSMC4	11	0.018	peptidase
PSMD1_RAT	proteasome 26S subunit, non-ATPase 1	PSMD1	3.3	0.05	other
O88321_RAT	proteasome 26S subunit, non-ATPase 4	PSMD4	12	0.0099	other
G3V8V3_RAT	glycogen phosphorylase, muscle associated	PYGM	-1.429	0.031	enzyme
RAB21_RAT	RAB21, member RAS oncogene family	RAB21	10	0.018	enzyme
PGTA_RAT	Rab geranylgeranyltransferase alpha subunit	RABGGTA	9.2	0.031	enzyme
RACK1_RAT	receptor for activated C kinase 1	RACK1	-2.5	0.0063	enzyme
F1LV89_RAT	RAP1 GTPase activating protein	RAP1GAP	-2.5	0.034	other

Table A.1 (continued)

D3ZHY9_RAT	RAS protein activator like 1	RASAL1	2.6	0.0059	other
RCN2_RAT	reticulocalbin 2	RCN2	3.6	0.032	other
D3ZWG2_RAT	regulator of G protein signaling 7	RGS7	-3.333	0.017	enzyme
A0A0G2K5N6_RAT	Rho associated coiled-coil containing protein kinase 2	ROCK2	16	0.0017	kinase
RL12_RAT	ribosomal protein L12	RPL12	-5	0.043	other
A0A0H2UHS7_RAT	ribosomal protein L18	RPL18	-10	0.037	other
RLA0_RAT	ribosomal protein lateral stalk subunit P0	RPLP0	-14.286	0.0031	other
Q6PDW1_RAT	ribosomal protein S12	RPS12	10	0.018	other
RTCB_RAT	RNA 2',3'-cyclic phosphate and 5'-OH ligase	RTCB	12	0.0099	enzyme
RTN1_RAT	reticulon 1	RTN1	-1.429	0.041	other
RUFY3_RAT	RUN and FYVE domain containing 3	RUFY3	1.9	0.032	other
SEP11_RAT	septin 11	SEPT11	1.7	0.037	other
SFXN5_RAT	sideroflexin 5	SFXN5	-16.667	0.0006	transporter
F1M1Y0_RAT	SH3 domain GRB2 like endophilin interacting protein 1	SGIP1	11	0.018	other
D3ZAS2_RAT	small G protein signaling modulator 1	SGSM1	-10	0.037	other
EAA2_RAT	solute carrier family 1 member 2	SLC1A2	-2	0.0001	transporter

Table A.1 (continued)

TXTP_RAT	solute carrier family 25 (mitochondrial carrier, citrate transporter), member 1	Slc25a1	-14.286	0.0014	transporter
G3V6H5_RAT	solute carrier family 25 member 11	SLC25A11	-2	0.028	transporter
G3V741_RAT	solute carrier family 25 member 3	SLC25A3	-2	0.00045	transporter
ADT1_RAT	solute carrier family 25 member 4	SLC25A4	-1.429	0.0043	transporter
A0A0G2K2S2_RAT	solute carrier family 2 member 1	SLC2A1	-11.111	0.0071	transporter
A0A0G2JZ69_RAT	spectrin alpha, non-erythrocytic 1	SPTAN1	-1.25	0.0025	other
Q6XDA0_RAT	spectrin beta, erythrocytic	SPTB	-1.111	0.045	other
F1MA36_RAT	spectrin beta, non-erythrocytic 2	SPTBN2	-1.25	0.013	other
SGT1_RAT	SGT1 homolog, MIS12 kinetochore complex assembly cochaperone	SUGT1	9.3	0.031	other
SV2A_RAT	synaptic vesicle glycoprotein 2A	SV2A	1.5	0.042	transporter
D4ABN3_RAT	synaptojanin 1	SYNJ1	1.4	0.049	phosphatase
Q6QI09_RAT	TATA-box binding protein associated factor 3	TAF3	-1.667	0.029	transcription regulator

Table A.1 (continued)

I6L9G6_RAT	TAR DNA binding protein	Tardbp	4.3	0.013	transcription regulator
THY1_RAT	Thy-1 cell surface antigen	THY1	-2	0.019	other
TOM22_RAT	translocase of outer mitochondrial membrane 22	TOMM22	-10	0.037	transporter
TOM34_RAT	translocase of outer mitochondrial membrane 34	TOMM34	11	0.018	other
TBB3_RAT	tubulin beta 3 class III	TUBB3	1.4	0.0001	other
UFM1_RAT	ubiquitin fold modifier 1	UFM1	9.3	0.031	other
QCR1_RAT	ubiquinol-cytochrome c reductase core protein 1	UQCRC1	-2	0.0013	enzyme
QCR2_RAT	ubiquinol-cytochrome c reductase core protein 2	UQCRC2	-1.667	0.017	enzyme
UCRI_RAT	ubiquinol-cytochrome c reductase, Rieske iron-sulfur polypeptide 1	UQCRFS1	-2.5	0.024	enzyme
SYVC_RAT	valyl-tRNA synthetase	VARS	9.1	0.031	enzyme
VDAC1_RAT	voltage dependent anion channel 1	VDAC1	-1.667	0.012	ion channel
VDAC2_RAT	voltage dependent anion channel 2	VDAC2	-2.5	0.00093	ion channel

Table A.1 (continued)

A0A0G2JSR0_RAT	voltage dependent anion channel 3	VDAC3	-2.5	0.009	ion channel
VISL1_RAT	visinin like 1	VSNL1	-1.667	0.023	other

Table A.2 List of differentially expressed genes with p-value ≤ 0.05 in C NB vs C B comparison in Chapter II

ID	Entrez Gene Name	Symbol	Fold Change	P-value	Type
ENSRNOG00000017897	ADAM metallopeptidase domain 8	ADAM8	-2.589	0.00035	peptidase
ENSRNOG00000014776	adenylate cyclase 7	ADCY7	-2.257	0.00025	enzyme
ENSRNOG00000009522	adrenoceptor alpha 1A	ADRA1A	-2.67	0.00025	G-protein coupled receptor
ENSRNOG00000021256	adrenoceptor alpha 1D	ADRA1D	5.453	0.00005	G-protein coupled receptor
ENSRNOG00000034269	argonaute 3, RISC catalytic component	AGO3	-2.259	0.00015	translation regulator
ENSRNOG00000055714	adenylate kinase 7	AK7	29.943	0.00035	kinase
ENSRNOG00000055049	aldehyde dehydrogenase 1 family member A2	ALDH1A2	-3.053	0.00005	enzyme
ENSRNOG00000008683	ALK receptor tyrosine kinase	ALK	-2.018	0.00005	kinase
ENSRNOG00000008990	angiomotin like 1	AMOTL1	-2.521	0.00005	other
ENSRNOG00000018241	ankyrin 1	ANK1	-2.401	0.00005	other
ENSRNOG00000023532	ankyrin-repeat and fibronectin type III domain containing 1	Ankfn1	-4.444	0.00055	other
ENSRNOG00000013937	ankyrin repeat domain 34C	ANKRD34C	-2.6	0.0002	other
ENSRNOG00000018159	annexin A4	ANXA4	2.79	0.00005	other
ENSRNOG00000011648	aquaporin 1 (Colton blood group)	AQP1	7.727	0.00005	transporter

Table A.2 (continued)

ENSRNOG00000043465	activity regulated cytoskeleton associated protein	ARC	2.595	0.00005	other
ENSRNOG00000005667	astrotactin 1	ASTN1	-2.152	0.00005	other
ENSRNOG00000015383	additional sex combs like 3, transcriptional regulator	Asxl3	-2.497	0.00035	other
ENSRNOG00000003031	ATPase plasma membrane Ca2+ transporting 4	ATP2B4	-2.166	0.00005	transporter
ENSRNOG00000008053	ATPase phospholipid transporting 8A2	ATP8A2	-2.368	0.00005	transporter
ENSRNOG00000021229	arginine vasopressin	AVP	-16.543	0.0005	other
ENSRNOG00000017893	BAI1-associated protein 3	Baiap3	-2.505	0.00005	other
ENSRNOG00000021745	basic helix-loop-helix family member e22	BHLHE22	5.569	0.00005	transcription regulator
ENSRNOG00000002863	calcium voltage-gated channel subunit alpha1 E	CACNA1E	-2.286	0.00005	ion channel
ENSRNOG00000060528	calcium voltage-gated channel subunit alpha1 G	CACNA1G	-2.214	0.00005	ion channel
ENSRNOG00000015835	calcium voltage-gated channel auxiliary subunit alpha2delta 2	CACNA2D2	-2.107	0.00005	ion channel
ENSRNOG00000038202	calmodulin like 4	CALML4	20.357	0.00005	other
ENSRNOG00000025518	capping protein regulator and myosin 1 linker 3	CARMIL3	-2.029	0.00005	other
ENSRNOG00000039086	coiled-coil domain containing 153	CCDC153	5.023	0.00005	other
ENSRNOG00000027392	coiled-coil domain containing 187	CCDC187	-4.122	0.0001	other
ENSRNOG00000025005	coiled-coil domain containing 190	CCDC190	5.121	0.0001	other

Table A.2 (continued)

ENSRNOG00000000321	CD24a antigen	Cd24a	2.032	0.00005	other
ENSRNOG00000052405	cadherin 4	CDH4	-2.137	0.00005	other
ENSRNOG00000013330	cadherin related family member 1	CDHR1	-2.168	0.00005	other
ENSRNOG00000053889	cadherin EGF LAG seven-pass G-type receptor 3	CELSR3	-2.129	0.00005	G-protein coupled receptor
ENSRNOG00000034221	cilia and flagella associated protein 126	CFAP126	22.055	0.0001	other
ENSRNOG00000036585	cilia and flagella associated protein 43	CFAP43	7.481	0.00005	other
ENSRNOG00000011268	chromodomain helicase DNA binding protein 5	CHD5	-2.389	0.00005	enzyme
ENSRNOG00000046972	cholinergic receptor, muscarinic 2	Chrm2	-2.447	0.00015	G-protein coupled receptor
ENSRNOG00000015867	carbohydrate sulfotransferase 9	CHST9	3.46	0.0001	enzyme
ENSRNOG00000001143	citron rho-interacting serine/threonine kinase	CIT	-2.091	0.00005	kinase
ENSRNOG00000002862	chloride voltage-gated channel 5	CLCN5	-2.815	0.00005	ion channel
ENSRNOG00000001926	claudin 1	CLDN1	5.082	0.00005	other
ENSRNOG00000054495	claudin 2	CLDN2	62.326	0.00005	other
ENSRNOG00000026870	chloride intracellular channel 6	CLIC6	73.669	0.00005	ion channel
ENSRNOG00000032206	contactin associated protein-like 5B	Cntnap5b	-2.254	0.00025	other
ENSRNOG00000043185	contactin associated protein-like 5C	Cntnap5c	-2.086	0.0002	other
ENSRNOG00000058560	collagen type II alpha 1 chain	COL2A1	-2.98	0.00005	other
ENSRNOG00000019648	collagen type VI alpha 3 chain	COL6A3	-2.39	0.0001	other
ENSRNOG00000014496	coronin 6	CORO6	-2.064	0.00005	other

Table A.2 (continued)

ENSRNOG00000019851	cytochrome c oxidase subunit 6A2	COX6A2	4.148	0.00065	enzyme
ENSRNOG00000020689	cytoplasmic polyadenylation element binding protein 3	CPEB3	-2.079	0.00005	translation regulator
ENSRNOG00000061215	crystallin mu	CRYM	2.072	0.00005	enzyme
ENSRNOG00000007057	CUB and Sushi multiple domains 2	CSMD2	-2.248	0.00005	other
ENSRNOG00000001259	cut like homeobox 2	CUX2	-2.151	0.00005	transcription regulator
ENSRNOG00000015076	cytochrome P450 family 26 subfamily B member 1	CYP26B1	-2.984	0.00005	enzyme
ENSRNOG00000016343	dickkopf WNT signaling pathway inhibitor 3	DKK3	2.053	0.00005	cytokine
ENSRNOG00000019584	delta like non-canonical Notch ligand 1	DLK1	-2.368	0.00005	other
ENSRNOG00000059865	dynein axonemal heavy chain 12	DNAH12	2.567	0.00005	other
ENSRNOG00000027992	DS cell adhesion molecule	DSCAM	-2.014	0.00005	other
ENSRNOG00000016502	DS cell adhesion molecule like 1	DSCAML1	-2.003	0.00005	other
ENSRNOG00000003977	dual specificity phosphatase 1	DUSP1	2.147	0.00005	phosphatase
ENSRNOG00000012450	dynein light chain roadblock-type 2	DYNLRB2	5.768	0.00005	other
ENSRNOG00000007440	double zinc ribbon and ankyrin repeat domains 1	DZANK1	-2.069	0.00005	other
ENSRNOG00000007408	early B cell factor 4	EBF4	-2.398	0.00005	transcription regulator

Table A.2 (continued)

ENSRNOG00000000190	E1A binding protein p300	EP300	-2.222	0.00005	transcription regulator
ENSRNOG00000037340	EPH receptor A10	EPHA10	-2.769	0.00005	transmembrane receptor
ENSRNOG00000002873	family with sequence similarity 183, member B	Fam183b	10.637	0.00005	Other
ENSRNOG00000009206	FEZ family zinc finger 2	FEZF2	2.807	0.00005	transcription regulator
ENSRNOG00000004679	fidgetin, microtubule severing factor	FIGN	-2.614	0.00025	other
ENSRNOG00000009470	filamin B	FLNB	-2.159	0.00005	other
ENSRNOG00000008015	Fos proto-oncogene, AP-1 transcription factor subunit	FOS	2.466	0.00005	transcription regulator
ENSRNOG00000010803	gamma-aminobutyric acid type A receptor alpha5 subunit	GABRA5	2.125	0.00005	ion channel
ENSRNOG00000003680	gamma-aminobutyric acid type A receptor beta2 subunit	GABRB2	-2.538	0.00005	ion channel
ENSRNOG00000061182	gamma-aminobutyric acid type A receptor epsilon subunit	GABRE	-2.242	0.0003	ion channel
ENSRNOG00000013588	glycine receptor alpha 1	GLRA1	-4.35	0.00035	ion channel
ENSRNOG00000014840	G protein subunit alpha 14	GNA14	4.614	0.00015	enzyme
ENSRNOG00000012995	G protein-coupled receptor 165	Gpr165	-2.18	0.0001	G-protein coupled receptor

Table A.2 (continued)

ENSRNOG00000008992	glutamate ionotropic receptor kainate type subunit 3	GRIK3	-2.084	0.00005	ion channel
ENSRNOG00000021063	glutamate ionotropic receptor NMDA type subunit 2D	GRIN2D	-2.652	0.00005	ion channel
ENSRNOG00000005723	glutamate ionotropic receptor NMDA type subunit 3A	GRIN3A	-2.253	0.00005	ion channel
ENSRNOG00000009450	hyperpolarization activated cyclic nucleotide gated potassium channel 4	HCN4	-2.077	0.00005	ion channel
ENSRNOG00000009253	immunoglobulin superfamily member 9B	IGSF9B	-2.491	0.00005	other
ENSRNOG00000004516	integrin subunit beta like 1	ITGBL1	3.944	0.00005	other
ENSRNOG00000062002	potassium voltage-gated channel subfamily A member 3	KCNA3	-2.174	0.00015	ion channel
ENSRNOG00000029811	potassium voltage-gated channel subfamily E regulatory subunit 2	KCNE2	4.544	0.00005	ion channel
ENSRNOG00000008471	kinesin family member 21B	KIF21B	-2.507	0.00005	other
ENSRNOG00000001092	klotho	KL	7.97	0.00005	enzyme
ENSRNOG00000009145	Kruppel like factor 12	KLF12	-2.331	0.0005	transcription regulator
ENSRNOG00000031100	kelch like family member 1	KLHL1	-2.345	0.0003	other
ENSRNOG00000015133	lysine methyltransferase 2A	KMT2A	-2.51	0.00005	transcription regulator
ENSRNOG00000061080	lysine methyltransferase 2C	KMT2C	-2.197	0.00005	transcription regulator
ENSRNOG00000009779	keratin 8	KRT8	7.601	0.00005	other

Table A.2 (continued)

ENSRNOG00000028630	kinase suppressor of ras 2	KSR2	-2.362	0.00005	kinase
ENSRNOG00000007044	L3MBTL1, histone methyl-lysine binding protein	L3MBTL1	-3.104	0.00005	other
ENSRNOG00000048230	similar to hypothetical protein 4930509O22	LOC300308	-2.099	0.00055	other
ENSRNOG00000001774	leucine rich repeats and calponin homology domain containing 3	LRCH3	-2.029	0.00015	other
ENSRNOG00000027935	leucine rich repeat containing 34	LRRC34	4.286	0.0002	other
ENSRNOG00000010158	MAGE family member L2	MAGEL2	-2.426	0.00005	enzyme
ENSRNOG00000014089	mitogen-activated protein kinase kinase kinase 2	MAP3K2	-2.133	0.00045	kinase
ENSRNOG00000007271	mitogen-activated protein kinase kinase kinase 9	MAP3K9	-2.413	0.00005	kinase
ENSRNOG00000014971	MAS1 proto-oncogene, G protein-coupled receptor	MAS1	2.53	0.0003	G-protein coupled receptor
ENSRNOG00000000536	MAM domain containing glycosylphosphatidylinositol anchor 1	MDGA1	-2.693	0.00005	other
ENSRNOG00000007003	meiotic double-stranded break formation protein 1	MEI1	3.149	0.00005	other
ENSRNOG00000039107	membrane frizzled-related protein	MFRP	25.841	0.00005	transmembrane receptor
ENSRNOG00000012827	myeloid leukemia factor 1	MLF1	12.046	0.0001	other
ENSRNOG00000006876	msh homeobox 1	MSX1	12.183	0.00005	transcription regulator

Table A.2 (continued)

ENSRNOG00000001959	MX dynamin-like GTPase 1	Mx1/Mx2	9.863	0.00005	enzyme
ENSRNOG00000027152	NEDD4 binding protein 2	N4BP2	-2.099	0.00015	enzyme
ENSRNOG00000008425	neuron navigator 1	NAV1	-2.06	0.00005	enzyme
ENSRNOG00000007975	nuclear receptor coactivator 2	NCOA2	-2.035	0.00005	transcription regulator
ENSRNOG00000009577	N-deacetylase and N-sulfotransferase 4	NDST4	-2.796	0.00005	enzyme
ENSRNOG00000026055	neuronal differentiation 6	NEUROD6	5.033	0.00005	transcription regulator
ENSRNOG00000030759	NHS actin remodeling regulator	NHS	-2.441	0.00005	other
ENSRNOG00000049128	natural killer cell triggering receptor	NKTR	-2.043	0.00005	other
ENSRNOG00000011011	neuromedin B	NMB	-3.909	0.0002	other
ENSRNOG00000001130	nitric oxide synthase 1	NOS1	-2.001	0.0003	enzyme
ENSRNOG00000020009	neuronal PAS domain protein 4	NPAS4	2.728	0.00005	transcription regulator
ENSRNOG00000008176	natriuretic peptide A	NPPA	2.689	0.0002	other
ENSRNOG00000052129	NACHT and WD repeat domain containing 1	NWD1	-2.074	0.00005	other
ENSRNOG00000048431	NYN domain and retroviral integrase containing	NYNRIN	-2.101	0.0002	other
ENSRNOG00000021225	oxytocin/neurophysin I prepropeptide	OXT	-18.591	0.00065	other

Table A.2 (continued)

ENSRNOG00000000606	protocadherin related 15	PCDH15	-2.484	0.00005	Other
ENSRNOG00000009491	polyhomeotic homolog 3	PHC3	-2.155	0.00005	transcription regulator
ENSRNOG00000016108	PH domain and leucine rich repeat protein phosphatase 2	PHLPP2	-2.071	0.00005	enzyme
ENSRNOG00000001825	plakophilin 2	PKP2	3.046	0.0001	other
ENSRNOG00000016838	phospholipase A2 group V	PLA2G5	7.113	0.00005	enzyme
ENSRNOG00000014550	phosphatidylinositol specific phospholipase C X domain containing 3	PLCXD3	-2.402	0.00005	other
ENSRNOG00000013072	plexin A4	PLXNA4	-2.078	0.00005	transmembrane receptor
ENSRNOG00000008674	PR/SET domain 11	PRDM11	-2.107	0.00035	other
ENSRNOG00000010217	proline rich coiled-coil 2B	PRRC2B	-2.105	0.00005	other
ENSRNOG00000032656	protein tyrosine phosphatase, receptor type, T	Ptprt	-2.001	0.00005	phosphatase
ENSRNOG00000006718	RNA binding motif protein 33	Rbm33	-2.037	0.00005	other
ENSRNOG00000011171	regulating synaptic membrane exocytosis 3	RIMS3	-2.377	0.00005	other
ENSRNOG00000014859	ring finger protein 152	RNF152	-2.347	0.00005	enzyme
ENSRNOG00000032825	ribosomal protein L30	RPL30	2.008	0.0003	other
ENSRNOG00000005109	reprimo, TP53 dependent G2 arrest mediator homolog	RPRM	-2.02	0.0001	other
ENSRNOG00000037687	R-spondin 2	RSPO2	6.563	0.00005	other
ENSRNOG00000020557	ryanodine receptor 1	RYR1	-2.827	0.00005	ion channel

Table A.2 (continued)

ENSRNOG00000012847	secretoglobin, family 1C, member 1	Scgb1c1	16.184	0.00005	other
ENSRNOG00000053122	sodium voltage-gated channel alpha subunit 1	SCN1A	-2.027	0.00005	ion channel
ENSRNOG00000015049	sodium voltage-gated channel alpha subunit 5	SCN5A	-3.501	0.00005	ion channel
ENSRNOG00000010617	signal peptide, CUB domain and EGF like domain containing 1	SCUBE1	-2.393	0.00005	transmembrane receptor
ENSRNOG00000024711	sidekick cell adhesion molecule 2	SDK2	-2.019	0.0001	other
ENSRNOG00000023337	semaphorin 3A	SEMA3A	-2.56	0.00005	other
ENSRNOG00000012989	serine incorporator 2	SERINC2	3.843	0.00005	transporter
ENSRNOG00000010378	solute carrier family 4 member 5	SLC4A5	17.274	0.00005	transporter
ENSRNOG00000028879	solute carrier family 4 member 8	SLC4A8	-2.654	0.00005	transporter
ENSRNOG00000005697	solute carrier family 6 member 11	SLC6A11	-2.141	0.00005	transporter
ENSRNOG00000015306	solute carrier family 9-member A4	SLC9A4	3.38	0.00005	transporter
ENSRNOG00000036802	small nucleolar RNA host gene 11	Snhg11	-2.049	0.00005	other
ENSRNOG00000053240	suppressor of glucose, autophagy associated 1	SOGA1	-2.415	0.00005	other
ENSRNOG00000005770	sclerostin domain containing 1	SOSTDC1	36.909	0.00005	growth factor
ENSRNOG00000043451	secreted phosphoprotein 1	SPP1	-2.635	0.00005	cytokine
ENSRNOG00000054548	SRSF protein kinase 3	SRPK3	-2.707	0.0003	kinase
ENSRNOG00000058561	serine/arginine repetitive matrix 2	Srrm2	-2.112	0.00005	other
ENSRNOG00000001141	serine/arginine repetitive matrix 4	Srrm4	-2.582	0.00005	other
ENSRNOG00000009590	storkhead box 2	STOX2	-2.145	0.00005	other
ENSRNOG00000018094	synaptic vesicle glycoprotein 2C	SV2C	-2.019	0.00005	other

Table A.2 (continued)

ENSRNOG00000052840	tetratricopeptide repeat, ankyrin repeat and coiled-coil containing 2	TANC2	-2.223	0.00005	transcription regulator
ENSRNOG00000011151	teneurin transmembrane protein 4	TENM4	-2.055	0.00005	other
ENSRNOG00000045829	thrombospondin 1	THBS1	-2.988	0.00015	other
ENSRNOG00000021569	T cell lymphoma invasion and metastasis 1	TIAM1	-2	0.00005	other
ENSRNOG00000014182	tensin 1	TNS1	-2.015	0.0002	other
ENSRNOG00000015347	tripartite motif containing 45	TRIM45	2.4	0.0003	other
ENSRNOG00000014373	tripartite motif containing 66	TRIM66	-2.138	0.0002	transcription regulator
ENSRNOG00000027233	transient receptor potential cation channel subfamily C member 5	TRPC5	-2.201	0.0004	ion channel
ENSRNOG00000048433	teashirt zinc finger homeobox 2	TSHZ2	-2.43	0.00005	other
ENSRNOG00000011059	tau tubulin kinase 2	TTBK2	-2.139	0.00005	kinase
ENSRNOG00000016275	transthyretin	TTR	211.357	0.00005	transporter
ENSRNOG00000046566	tubby bipartite transcription factor	TUB	-2.17	0.00005	transcription regulator
ENSRNOG00000005564	ubinuclein 2	UBN2	-2.016	0.00005	other
ENSRNOG00000028362	unc-80 homolog, NALCN channel complex subunit	UNC80	-2.224	0.00035	enzyme
ENSRNOG00000061121	WD repeat and FYVE domain containing 3	WDFY3	-2.113	0.00005	enzyme
ENSRNOG00000002831	WAP, follistatin/kazal, immunoglobulin, kunitz and netrin domain containing 2	WFIKKN2	4.585	0.00005	other

Table A.2 (continued)

ENSRNOG00000002537	WNK lysine deficient protein kinase 3	WNK3	-2.259	0.00005	kinase
ENSRNOG00000022039	zinc finger and BTB domain containing 40	ZBTB40	-2.12	0.00005	other
ENSRNOG00000012470	zinc finger CCCH-type containing 12C	ZC3H12C	-2.11	0.0004	other
ENSRNOG00000011285	zinc finger DHHC-type containing 22	ZDHHC22	-2.216	0.00005	other
ENSRNOG00000014452	zinc finger homeobox 3	ZFHX3	-2.453	0.00005	transcription regulator
ENSRNOG00000015071	zinc finger, imprinted 1	Zim1	-3.252	0.0001	other
ENSRNOG00000011697	zinc finger protein 827	ZNF827	-2.159	0.00005	other

Table A.3 List of differentially expressed proteins with p-value ≤ 0.05 for C NB vs CPF NB comparison in Chapter III

ID	Entrez Gene Name	Symbol	Fold Change	Expr p-value	Type
A0A0G2K642_RAT	acetyl-CoA acyltransferase 2	ACAA2	-14.28	0.0022	enzyme
D3ZT36_RAT	ADAM metallopeptidase domain 23	ADAM23	10	0.015	peptidase
F1LM19_RAT	alpha 2-HS glycoprotein	AHSG	-20	0.00028	other
AL7A1_RAT	aldehyde dehydrogenase 7 family member A1	ALDH7A1	14	0.0036	enzyme
VATB2_RAT	ATPase H+ transporting V1 subunit B2	ATP6V1B2	1.2	0.049	transporter
KCC2A_RAT	calcium/calmodulin dependent protein kinase II alpha	CAMK2A	1.3	0.031	kinase
CN37_RAT	2',3'-cyclic nucleotide 3' phosphodiesterase	CNP	1.3	0.02	enzyme
CSRP1_RAT	cysteine and glycine rich protein 1	CSRP1	12	0.0072	other
A0A0G2KB92_RAT	doublecortin-like kinase 1	Dclk1	-1.667	0.022	kinase
D4A559_RAT	dematin actin binding protein	DMTN	-10	0.017	other
ENOPH_RAT	enolase-phosphatase 1	ENOPH1	-12.5	0.0043	enzyme
A0A0G2JZI2_RAT	glutamyl-prolyl-tRNA synthetase	EPRS	-10	0.033	enzyme
FXL16_RAT	F-box and leucine rich repeat protein 16	FBXL16	-10	0.017	enzyme
G3V914_RAT	glutamate ionotropic receptor AMPA type subunit 2	GRIA2	-16.667	0.0022	ion channel

Table A.3 (continued)

HPLN1_RAT	hyaluronan and proteoglycan link protein 1	HAPLN1	-5	0.0014	other
A0A0G2JSV6_RAT	hemoglobin, alpha 1	Hba1/Hba2	-1.25	0.038	other
B4F7C7_RAT	heme binding protein 1	HEBP1	-3.333	0.036	other
F1LV13_RAT	heterogeneous nuclear ribonucleoprotein M	HNRNPM	-10	0.017	other
D3ZBS2_RAT	inter-alpha-trypsin inhibitor heavy chain 3	ITIH3	8.8	0.029	other
D3ZU22_RAT	60S ribosomal protein L7a-like	LOC108349606	-10	0.033	other
MBP_RAT	myelin basic protein	Mbp	1.3	0.012	other
NFL_RAT	neurofilament light	NEFL	1.6	0.02	other
NONO_RAT	non-POU domain containing octamer binding	NONO	-3.333	0.02	other
NPTN_RAT	neuroplastin	NPTN	-1.429	0.036	other
D3Z955_RAT	phosphoglucomutase 2 like 1	PGM2L1	12	0.0072	enzyme
MYPR_RAT	proteolipid protein 1	PLP1	1.4	0.01	other
D3ZCA0_RAT	pyridoxal phosphate binding protein	PLPBP	3.7	0.03	enzyme
NEB1_RAT	protein phosphatase 1 regulatory subunit 9A	PPP1R9A	-10	0.033	other
PSA2_RAT	proteasome subunit alpha 2	PSMA2	-10	0.033	peptidase
G3V7Q6_RAT	proteasome subunit beta 5	PSMB5	12	0.0072	peptidase

Table A.3 (continued)

O88321_RAT	proteasome 26S subunit, non-ATPase 4	PSMD4	12	0.0072	Other
A0A0G2K5N6_RAT	Rho associated coiled-coil containing protein kinase 2	ROCK2	11	0.015	kinase
SAC1_RAT	SAC1 like phosphatidylinositide phosphatase	SACM1L	8.9	0.029	phosphatase
SFXN5_RAT	sideroflexin 5	SFXN5	-14.286	0.0022	transporter
B2RZ27_RAT	SH3 domain binding glutamate rich protein like 3	SH3BGRL3	-10	0.017	other
S6A11_RAT	solute carrier family 6 member 11	SLC6A11	2.1	0.013	transporter
G3V7I8_RAT	STE20 like kinase	SLK	8.8	0.029	kinase
F1MA36_RAT	spectrin beta, non-erythrocytic 2	SPTBN2	-1.25	0.021	other
TRAP1_RAT	TNF receptor associated protein 1	TRAP1	-5	0.0036	enzyme

Table A.4 List of differentially expressed proteins with p-value ≤ 0.05 for C NB vs PF NB comparison in Chapter III

ID	Entrez Gene Name	Symbol	Fold Change	p-value	Type
ACTC_RAT	actin, alpha, cardiac muscle 1	ACTC1	1.7	0.0001	enzyme
Q6T487_RAT	actinin alpha 1	ACTN1	-1.429	0.0025	transcription regulator
D3ZT36_RAT	ADAM metallopeptidase domain 23	ADAM23	12	0.0082	peptidase
ALDR_RAT	aldo-keto reductase family 1member B	AKR1B1	-1.667	0.046	enzyme
ALBU_RAT	albumin	ALB	-1.25	0.02	transporter
AL7A1_RAT	aldehyde dehydrogenase 7 family member A1	ALDH7A1	11	0.015	enzyme
Q5XI77_RAT	annexin A11	ANXA11	-10	0.041	other
ANXA5_RAT	annexin A5	ANXA5	-2.5	0.05	transporter
Q6IRJ7_RAT	annexin A7	ANXA7	11	0.015	ion channel
D3ZWA8_RAT	adaptor protein, phosphotyrosine interacting with PH domain and leucine zipper 1	APPL1	11	0.015	other
ATPA_RAT	ATP synthase F1 subunit alpha	ATP5F1A	1.2	0.026	transporter
VATF_RAT	ATPase H+ transporting V1 subunit F	ATP6V1F	9.1	0.027	enzyme
ATX10_RAT	ataxin 10	ATXN10	2.9	0.027	other
BRSK1_RAT	BR serine/threonine kinase 1	BRSK1	-10	0.019	kinase
A0A0G2K7E5_RAT	calcium voltage-gated channel auxiliary subunit alpha2delta 1	CACNA2D1	1.8	0.015	ion channel
CALB1_RAT	calbindin 1	CALB1	-3.333	0.0088	other

Table A.4 (continued)

CALR_RAT	calreticulin	CALR	-1.429	0.03	transcription regulator
TCPB_RAT	chaperonin containing TCP1 subunit 2	CCT2	-1.429	0.047	kinase
OX2G_RAT	CD200 molecule	CD200	-20	0.00035	other
CDK5_RAT	cyclin dependent kinase 5	CDK5	-10	0.041	kinase
CHRD1_RAT	cysteine and histidine rich domain containing 1	CHORDC1	9.1	0.027	other
KCRB_RAT	creatine kinase B	CKB	2	0.0001	kinase
CLIC4_RAT	chloride intracellular channel 4	CLIC4	7.7	0.05	ion channel
A0A0G2JYW3_RAT	clathrin light chain A	CLTA	-20	0.00016	other
CSN4_RAT	COP9 signalosome subunit 4	COPS4	8.2	0.05	peptidase
D3ZI16_RAT	COP9 signalosome subunit 6	COPS6	9.1	0.027	other
CSRP1_RAT	cysteine and glycine rich protein 1	CSRP1	21	0.00023	other
D4A6H8_RAT	catenin alpha 2	CTNNA2	-2.5	0.05	other
A0A0G2JZ13_RAT	cortactin	CTTN	-14.286	0.0017	other
D3ZFQ8_RAT	cytochrome c1	CYC1	-1.667	0.027	enzyme
OST48_RAT	dolichyl-diphosphooligosaccharide--protein glycosyltransferase non-catalytic subunit	DDOST	8.2	0.05	enzyme
A0A0G2KAT4_RAT	DExD-box helicase 39B	DDX39B	-3.333	0.05	enzyme
F1LP01_RAT	diacylglycerol kinase beta	DGKB	-5	0.0019	kinase
DPYL2_RAT	dihydropyrimidinase like 2	DPYSL2	2	0.0001	enzyme
DEST_RAT	destrin-like 1	Dstn/Dstnl1	-2	0.025	other

Table A.4 (continued)

EF1A1_RAT	eukaryotic translation elongation factor 1 alpha 1	EEF1A1	1.3	0.043	translation regulator
EF1A2_RAT	eukaryotic translation elongation factor 1 alpha 2	EEF1A2	1.5	0.0014	translation regulator
IF4A2_RAT	eukaryotic translation initiation factor 4A2	EIF4A2	-1.667	0.021	translation regulator
ENOPH_RAT	enolase-phosphatase 1	ENOPH 1	-14.286	0.0017	enzyme
Q9JMB3_RAT	erythrocyte membrane protein band 4.1 like 3	EPB41L 3	1.6	0.019	other
F1M471_RAT	EPM2A interacting protein 1	EPM2AI P1	12	0.0082	other
Q505I9_RAT	epsin 2	EPN2	-10	0.019	other
ERP29_RAT	endoplasmic reticulum protein 29	ERP29	2.3	0.033	transporte r
FHIT_RAT	fragile histidine triad	FHIT	-10	0.041	enzyme
B1H2A2_RAT	fibronectin type III and SPRY domain containing 1	Fsd1	-10	0.019	other
GBRL2_RAT	GABA type A receptor associated protein like 2	GABAR APL2	9.3	0.027	other
GBRA1_RAT	gamma-aminobutyric acid type A receptor alpha1 subunit	GABRA 1	-10	0.041	ion channel
GBRB1_RAT	gamma-aminobutyric acid type A receptor beta1 subunit	GABRB 1	8.2	0.05	ion channel
DCE2_RAT	glutamate decarboxylase 2	GAD2	1.7	0.039	enzyme
GIT1_RAT	GIT ArfGAP 1	GIT1	-11.111	0.0084	kinase
A0A0G2KB98 _RAT	glycogen synthase kinase 3 beta	GSK3B	14	0.0045	kinase
GELS_RAT	gelsolin	GSN	-2.5	0.05	other
HPLN1_RAT	hyaluronan and proteoglycan link protein 1	HAPLN 1	-3.333	0.0028	other
A0A0G2JSV6 _RAT	hemoglobin, alpha 1	Hba1/Hb a2	-1.429	0.021	other
B4F7C7_RAT	heme binding protein 1	HEBP1	-5	0.015	other
HMOX2_RAT	heme oxygenase 2	HMOX2	-10	0.041	enzyme

Table A.4 (continued)

ROA3_RAT	heterogeneous nuclear ribonucleoprotein A3	Hnrnpa3	-2	0.018	transporter
HNRPK_RAT	heterogeneous nuclear ribonucleoprotein K	HNRNPK	-1.667	0.03	transcription regulator
B0BMW2_RAT	hydroxysteroid 17-beta dehydrogenase 10	HSD17B10	-2.5	0.039	enzyme
HS90A_RAT	heat shock protein 90 alpha family class A member 1	HSP90AA1	-1.25	0.0059	enzyme
GRP78_RAT	heat shock protein family A (Hsp70) member 5	HSPA5	-1.429	0.024	enzyme
A0A0G2K261_RAT	isoleucyl-tRNA synthetase 2, mitochondrial	IARS2	-5	0.015	enzyme
ITPA_RAT	inosine triphosphatase	ITPA	-2	0.025	enzyme
LASP1_RAT	LIM and SH3 protein 1	LASP1	9.6	0.027	transporter
G3V7U4_RAT	lamin B1	LMNB1	-3.333	0.028	other
A0A0G2K0V8_RAT	nuclear migration protein nudC-like	LOC100911422	-10	0.041	other
F1LM33_RAT	leucine rich pentatricopeptide repeat containing	LRPPRC	-10	0.041	other
A0A0G2KA27_RAT	MAP kinase activating death domain	MADD	3.6	0.041	other
MP2K1_RAT	mitogen-activated protein kinase kinase 1	MAP2K1	-1.429	0.03	kinase
E9PSK7_RAT	mitogen-activated protein kinase 8 interacting protein 3	MAPK8IP3	-10	0.041	other
MPI_RAT	mannose phosphate isomerase	MPI	-10	0.019	enzyme
MYADM_RAT	myeloid associated differentiation marker	MYADM	-11.111	0.0084	other
A0A0G2K6S9_RAT	myosin heavy chain 11	MYH11	-1.667	0.016	other
NNRE_RAT	NAD(P)HX epimerase	NAXE	-3.333	0.05	enzyme
A0A0G2K0M8_RAT	neural cell adhesion molecule 1	NCAM1	-1.25	0.042	other

Table A.4 (continued)

D3ZS58_RAT	NADH:ubiquinone oxidoreductase subunit A2	NDUFA2	11	0.015	enzyme
D4A565_RAT	NADH:ubiquinone oxidoreductase subunit B5	NDUFB5	-10	0.041	enzyme
Q5RJN0_RAT	NADH:ubiquinone oxidoreductase core subunit S7	NDUFS7	-5	0.015	enzyme
NFL_RAT	neurofilament light	NEFL	1.7	0.011	other
NFM_RAT	neurofilament, medium polypeptide	Nefm	2.3	0.0046	other
NPTN_RAT	neuroplastin	NPTN	-1.667	0.0044	other
NTRK2_RAT	neurotrophic receptor tyrosine kinase 2	NTRK2	-10	0.019	kinase
PA2G4_RAT	proliferation-associated 2G4	PA2G4	-3.333	0.028	transcription regulator
PACS1_RAT	phosphofurin acidic cluster sorting protein 1	PACS1	4.6	0.01	other
PCYOX_RAT	prenylcysteine oxidase 1	PCYOX1	2.9	0.012	enzyme
D4AB17_RAT	phosphoribosylformylglycinamidine synthase	PFAS	3.2	0.028	enzyme
B5DFN4_RAT	prefoldin subunit 5	PFDN5	7.7	0.05	transcription regulator
PFKAP_RAT	phosphofructokinase, platelet	PFKP	-1.25	0.047	kinase
6PGD_RAT	phosphogluconate dehydrogenase	PGD	2.8	0.018	enzyme
D3Z955_RAT	phosphoglucomutase 2 like 1	PGM2L1	18	0.00075	enzyme
D3ZFX4_RAT	phosphoglucomutase 3	PGM3	13	0.0082	enzyme
PHYIP_RAT	phytanoyl-CoA 2-hydroxylase interacting protein	PHYHIP	-2	0.035	other
KPYM_RAT	pyruvate kinase M1/2	PKM	-1.25	0.016	kinase
PP1R7_RAT	protein phosphatase 1 regulatory subunit 7	PPP1R7	-2	0.024	phosphatase
NEB1_RAT	protein phosphatase 1 regulatory subunit 9A	PPP1R9A	-10	0.019	other

Table A.4 (continued)

D4A1A5_RAT	protein phosphatase 2, regulatory subunit B', gamma	Ppp2r5c	3.8	0.038	phosphatase
A0A0G2JTX2_RAT	PRA1 domain family member 2	PRAF2	7.9	0.05	other
PRPS1_RAT	phosphoribosyl pyrophosphate synthetase 1	PRPS1	-2.5	0.022	kinase
G3V8U9_RAT	proteasome subunit beta 4	PSMB4	-3.333	0.043	peptidase
G3V7Q6_RAT	proteasome subunit beta 5	PSMB5	9.6	0.027	peptidase
Q4V8E2_RAT	proteasome 26S subunit, non-ATPase 14	PSMD14	8.1	0.05	peptidase
O88321_RAT	proteasome 26S subunit, non-ATPase 4	PSMD4	12	0.0082	other
FAK2_RAT	protein tyrosine kinase 2 beta	PTK2B	-11.111	0.0084	kinase
RAB21_RAT	RAB21, member RAS oncogene family	RAB21	11	0.015	enzyme
A0A0G2K5N6_RAT	Rho-associated coiled-coil containing protein kinase 2	ROCK2	7.1	0.05	kinase
Q4V8I6_RAT	ribosomal protein L11	RPL11	-10	0.041	other
A0A0H2UHS7_RAT	ribosomal protein L18	RPL18	-10	0.041	other
RL19_RAT	ribosomal protein L19	RPL19	-10	0.041	other
Q6P3V9_RAT	ribosomal protein L4	RPL4	-16.667	0.00077	enzyme
RS11_RAT	ribosomal protein S11	RPS11	-10	0.041	other
RTCB_RAT	RNA 2',3'-cyclic phosphate and 5'-OH ligase	RTCB	9.7	0.027	enzyme
RUFY3_RAT	RUN and FYVE domain containing 3	RUFY3	2.1	0.023	other
Q5EBD0_RAT	SEC14 like lipid binding 2	SEC14L2	-2.5	0.05	transporter
SFXN5_RAT	sideroflexin 5	SFXN5	-5	0.015	transporter
F1M1Y0_RAT	SH3 domain GRB2 like endophilin interacting protein 1	SGIP1	5	0.0065	other

Table A.4 (continued)

D3ZAS2_RAT	small G protein signaling modulator 1	SGSM1	-11.111	0.0084	other
SIR5_RAT	sirtuin 5	SIRT5	8.1	0.05	enzyme
VGLU2_RAT	solute carrier family 17 member 6	SLC17A6	2.5	0.04	transporter
EAA2_RAT	solute carrier family 1 member 2	SLC1A2	-1.429	0.01	transporter
G3V741_RAT	solute carrier family 25 member 3	SLC25A3	-1.667	0.0086	transporter
A0A0H2UHB7_RAT	solute carrier family 4 member 4	SLC4A4	2	0.034	transporter
S6A11_RAT	solute carrier family 6 member 11	SLC6A11	3	0.0001	transporter
A0A0G2K1Y8_RAT	spectrin alpha, non-erythrocytic 1	SPTAN1	-1.111	0.023	other
Q6XDA0_RAT	spectrin beta, erythrocytic	SPTB	-1.111	0.037	other
F1MA36_RAT	spectrin beta, non-erythrocytic 2	SPTBN2	-1.429	0.001	other
ST4A1_RAT	sulfotransferase family 4A member 1	SULT4A1	12	0.0082	enzyme
LAP2_RAT	thymopoietin	TMPO	-5	0.028	other
TOM70_RAT	translocase of outer mitochondrial membrane 70	TOMM70	-1.429	0.047	transporter
TTYH1_RAT	tweety family member 1	TTYH1	-3.333	0.05	ion channel
TBA4A_RAT	tubulin alpha 4a	TUBA4A	2	0.0001	other
TBB5_RAT	tubulin beta class I	TUBB	1.3	0.0001	other
VDAC2_RAT	voltage dependent anion channel 2	VDAC2	-1.667	0.028	ion channel
F1LP80_RAT	VGF nerve growth factor inducible	VGF	-10	0.041	growth factor
XPO1_RAT	exportin 1	XPO1	-10	0.041	transporter
1433E_RAT	tyrosine 3-monooxygenase/tryptophan 5-monooxygenase activation protein epsilon	YWHAE	-1.111	0.029	other

Table A.5 List of differentially expressed proteins with p-value ≤ 0.05 for CB vs CPF B comparison in Chapter IV

ID	Entrez Gene Name	Symbol	Fold Change	P-value	Type
D3ZT36_RAT	ADAM metallopeptidase domain 23	ADAM23	3.8	0.032	peptidase
Q5XI77_RAT	annexin A11	ANXA11	8.5	0.031	other
AT1A3_RAT	ATPase Na+/K+ transporting subunit alpha 3	ATP1A3	1.1	0.0034	transporter
ATX10_RAT	ataxin 10	ATXN10	-3.333	0.033	other
F1LVR4_RAT	calcium/calmodulin dependent protein kinase ID	CAMK1D	-10	0.032	kinase
Q4KLZ3_RAT	DAZ associated protein 1	Dazap1	-10	0.032	other
DJB11_RAT	DnaJ heat shock protein family (Hsp40) member B11	DNAJB11	-10	0.032	other
A0A0G2K162_RAT	erythrocyte membrane protein band 4.1 like 2	EPB41L2	-2.5	0.039	other
Q505I9_RAT	epsin 2	EPN2	-10	0.016	other
A0A0G2JT50_RAT	growth arrest specific 7	GAS7	10	0.015	transcription regulator
A0A0G2JSH4_RAT	glycogen synthase kinase 3 beta	GSK3B	-20	0.0005	kinase
D4A5J1_RAT	kelch repeat and BTB domain containing 11	KBTBD11	8.6	0.031	other
LASP1_RAT	LIM and SH3 protein 1	LASP1	-3.333	0.029	transporter
F6T071_RAT	Golgi reassembly-stacking protein 2-like	LOC103690018	13	0.0038	other
LPPRC_RAT	leucine rich pentatricopeptide repeat containing	LRPPRC	3.8	0.032	other

Table A.5 (continued)

NDUS2_RAT	NADH:ubiquinone oxidoreductase core subunit S2	NDUFS2	13	0.0038	enzyme
Q5XIH3_RAT	NADH:ubiquinone oxidoreductase core subunit V1	NDUFV1	1.7	0.03	enzyme
A0A0G2K3V4_RAT	O-linked N-acetylglucosamine (GlcNAc) transferase	OGT	8.7	0.031	enzyme
PYC_RAT	pyruvate carboxylase	PC	1.6	0.05	enzyme
F1LX13_RAT	phosphodiesterase 10A	PDE10A	12	0.0076	enzyme
PDE1B_RAT	phosphodiesterase 1B	PDE1B	4	0.032	enzyme
B5DFI9_RAT	pyruvate dehydrogenase kinase 3	PDK3	-10	0.016	kinase
Q6MGC4_RAT	prefoldin subunit 6	PFDN6	8.7	0.031	other
NCPR_RAT	cytochrome p450 oxidoreductase	POR	-10	0.016	enzyme
PPM1H_RAT	protein phosphatase, Mg2+/Mn2+ dependent 1H	PPM1H	-16.667	0.002	phosphatase
A0A0G2JX67_RAT	prolyl endopeptidase like	PREPL	-2	0.025	peptidase
G3V7Q6_RAT	proteasome subunit beta 5	PSMB5	17	0.00095	peptidase
A0A0G2K9E0_RAT	ribonuclease/angiogenin inhibitor 1	RNH1	-10	0.016	other
SCN2A_RAT	sodium voltage-gated channel alpha subunit 2	SCN2A	11	0.015	ion channel
M0RD40_RAT	SIK family kinase 3	SIK3	10	0.015	kinase
G3V8D6_RAT	tripartite motif containing 3	TRIM3	-10	0.032	enzyme
A0A0G2K8V2_RAT		VCL	2.9	0.02	enzyme

Table A.6 List of differentially expressed proteins with p-value ≤ 0.05 for C B vs PF B comparison in Chapter IV

ID	Entrez gene name	Symbol	Fold Change	P-value	Type
ACTS_RAT	actin, alpha 1, skeletal muscle	ACTA1	-1.111	0.00045	other
ADHX_RAT	alcohol dehydrogenase 5 (class III), chi polypeptide	ADH5	-20	0.00019	enzyme
Q6IMZ3_RAT	annexin A6	ANXA6	4.2	0.0007	ion channel
B0BN83_RAT	armadillo repeat containing 1	ARMC1	-10	0.037	other
B2GV73_RAT	actin related protein 2/3 complex subunit 3	ARPC3	3.6	0.044	other
CALB1_RAT	calbindin 1	CALB1	2.9	0.035	other
CATA_RAT	catalase	CAT	11	0.013	enzyme
Q4KLZ3_RAT	DAZ associated protein 1	Dazap1	-10	0.037	other
DJB11_RAT	DnaJ heat shock protein family (Hsp40) member B11	DNAJB11	-10	0.037	other
DPP3_RAT	dipeptidyl peptidase 3	DPP3	3.3	0.0088	peptidase
DPYL2_RAT	dihydropyrimidinase like 2	DPYSL2	-1.25	0.0027	enzyme
DEST_RAT	destrin-like 1	Dstn/Dstnl1	1.8	0.045	other
ENOG_RAT	enolase 2	ENO2	1.2	0.038	enzyme
A0A0A0MY13_RAT	G protein-coupled receptor 158	GPR158	3	0.028	G-protein coupled receptor
F1LNE4_RAT	glutamate ionotropic receptor AMPA type subunit 2	GRIA2	-10	0.019	ion channel
A0A0G2JXE0_RAT	histone cluster 1 H2B family member b	HIST1H2BB	3.6	0.044	other
HMOX2_RAT	heme oxygenase 2	HMOX2	9.1	0.026	enzyme

Table A.6 (continued)

LONM_RAT	lon peptidase 1, mitochondrial	LONP1	-11.111	0.0099	peptidase
F1LM33_RAT	leucine rich pentatricopeptide repeat containing	LRPPRC	3.7	0.044	other
F1MAQ5_RAT	microtubule associated protein 2	MAP2	-1.111	0.039	other
A0A0U1RRS7_RAT	mitogen-activated protein kinase 10	MAPK10	3.1	0.044	kinase
MBP_RAT	myelin basic protein	Mbp	1.3	0.014	other
NDUS2_RAT	NADH:ubiquinone oxidoreductase core subunit S2	NDUFS2	10	0.013	enzyme
NFL_RAT	neurofilament light	NEFL	1.6	0.00032	other
A0A0G2K3V4_RAT	O-linked N-acetylglucosamine (GlcNAc) transferase	OGT	16	0.0014	enzyme
F1LX13_RAT	phosphodiesterase 10A	PDE10A	29	0.0001	enzyme
PDE1B_RAT	phosphodiesterase 1B	PDE1B	6.1	0.0025	enzyme
B5DFI9_RAT	pyruvate dehydrogenase kinase 3	PDK3	-10	0.019	kinase
D3Z955_RAT	phosphoglucomutase 2 like 1	PGM2L1	-12.5	0.0051	enzyme
PPM1H_RAT	protein phosphatase, Mg2+/Mn2+ dependent 1H	PPM1H	-3.333	0.042	phosphatase
PPR1B_RAT	protein phosphatase 1 regulatory inhibitor subunit 1B	PPP1R1B	3.2	0.0019	phosphatase
G3V7Q6_RAT	proteasome subunit beta 5	PSMB5	16	0.0014	peptidase
FAK2_RAT	protein tyrosine kinase 2 beta	PTK2B	-11.111	0.0099	kinase
PGTA_RAT	Rab geranylgeranyltransferase alpha subunit	RABGGTA	-10	0.019	enzyme

Table A.6 (continued)

RL12_RAT	ribosomal protein L12	RPL12	4	0.044	other
RLA1_RAT	ribosomal protein lateral stalk subunit P1	RPLP1	-11.111	0.0099	other
RS11_RAT	ribosomal protein S11	RPS11	-11.111	0.0099	other
M0RD40_RAT	SIK family kinase 3	SIK3	11	0.013	kinase
A0A0G2K1Y8_RAT	spectrin alpha, non-erythrocytic 1	SPTAN1	1.1	0.041	other
A0A0G2JWK7_RAT	transgelin	TAGLN	3.2	0.035	other
D3ZT58_RAT	talin 2	TLN2	-2	0.034	other
G3V8D6_RAT	tripartite motif containing 3	TRIM3	-10	0.037	enzyme
TBB3_RAT	tubulin beta 3 class III	TUBB3	-1.111	0.0001	other
UFM1_RAT	ubiquitin fold modifier 1	UFM1	-10	0.019	other
VDAC2_RAT	voltage dependent anion channel 2	VDAC2	1.9	0.027	ion channel
F8WFH8_RAT	tryptophanyl-tRNA synthetase	WARS	-11.111	0.0099	enzyme

Table A.7 List of differentially expressed proteins with p-value ≤ 0.05 for CPF NB vs CPF B comparison in Chapter IV

ID	Entrez Gene Name	Symbol	Fold Change	P-value	Type
A0A0G2K642_RAT	acetyl-CoA acyltransferase 2	ACAA2	10	0.018	enzyme
A0A0G2K3K2_RAT	actin beta	ACTB	1.5	0.0001	other
O88768_RAT	ArfGAP with dual PH domains 1	ADAP1	-2	0.049	other
FETUA_RAT	alpha 2-HS glycoprotein	AHSG	17	0.0018	other
Q6IMZ3_RAT	annexin A6	ANXA6	-3.333	0.0099	ion channel
M0R7G4_RAT	apolipoprotein O	APOO	-3.333	0.043	other
PUR9_RAT	5-aminoimidazole-4-carboxamide ribonucleotide formyltransferase/IMP cyclohydrolase	ATIC	2.7	0.017	enzyme
AT1A3_RAT	ATPase Na+/K+ transporting subunit alpha 3	ATP1A3	1.2	0.00013	transporter
ATPA_RAT	ATP synthase F1 subunit alpha	ATP5F1A	1.8	0.0001	transporter
VATB2_RAT	ATPase H+ transporting V1 subunit B2	ATP6V1B2	-1.25	0.019	transporter
VATE1_RAT	ATPase H+ transporting V1 subunit E1	ATP6V1E1	-1.667	0.0041	transporter
ATX10_RAT	ataxin 10	ATXN10	-5	0.023	other
BASP1_RAT	brain abundant, membrane attached signal protein 1	Basp1	1.4	0.0076	transcription regulator
A0A0G2K079_RAT	breast carcinoma amplified sequence 1	BCAS1	-2	0.029	other
D3ZUP5_RAT	BRICK1, SCAR/WAVE actin nucleating complex subunit	BRK1	-11.111	0.0071	other

Table A.7 (continued)

CYBP_RAT	calcyclin binding protein	CACYBP	-10	0.037	other
F1LLX6_RAT	calcium dependent secretion activator	CADPS	-1.429	0.035	other
CALB1_RAT	calbindin 1	CALB1	-3.333	0.0069	other
KCC2A_RAT	calcium/calmodulin dependent protein kinase II alpha	CAMK2A	-1.667	0.00035	kinase
CAN2_RAT	calpain 2	CAPN2	-10	0.037	peptidase
CBS_RAT	cystathionine-beta-synthase	CBS/CBSL	9.1	0.031	enzyme
OX2G_RAT	CD200 molecule	CD200	-3.333	0.016	other
M0RC17_RAT	cell adhesion molecule L1 like	CHL1	9.2	0.031	other
KCRB_RAT	creatine kinase B	CKB	1.9	0.0001	kinase
A0A0G2JYW3_RAT	clathrin light chain A	CLTA	-5	0.012	other
F1M779_RAT	clathrin heavy chain	CLTC	-1.429	0.00072	other
CN37_RAT	2',3'-cyclic nucleotide 3' phosphodiesterase	CNP	-1.429	0.0021	enzyme
CNTN1_RAT	contactin 1	CNTN1	-1.429	0.019	enzyme
SYDC_RAT	aspartyl-tRNA synthetase	DARS	-10	0.037	enzyme
ACBP_RAT	diazepam binding inhibitor, acyl-CoA binding protein	DBI	12	0.0099	other
A0A0G2KB92_RAT	doublecortin-like kinase 1	Dclk1	1.6	0.039	kinase
D4A8U7_RAT	dynactin subunit 1	DCTN1	1.6	0.025	other
F1LMR7_RAT	dipeptidyl peptidase like 6	DPP6	-1.667	0.04	other
DPYL2_RAT	dihydropyrimidinase like 2	DPYSL2	2.2	0.0001	enzyme
A0A0G2K3I9_RAT	dual specificity phosphatase 3	DUSP3	-2.5	0.047	phosphatase

Table A.7 (continued)

Q6AZ35_RAT	dynein cytoplasmic 1 intermediate chain 2	Dync1i2	9	0.031	other
IF5_RAT	eukaryotic translation initiation factor 5	EIF5	-3.333	0.043	translation regulator
A0A0G2K0F3_RAT	erythrocyte membrane protein band 4.1 like 1	EPB41L1	1.5	0.036	other
A0A0G2JZI2_RAT	glutamyl-prolyl-tRNA synthetase	EPRS	13	0.0056	enzyme
G3V6L9_RAT	FK506 binding protein 3	FKBP3	8.9	0.031	enzyme
FLOT1_RAT	flotillin 1	FLOT1	-14.286	0.0031	other
FUBP1_RAT	far upstream element binding protein 1	FUBP1	8.9	0.031	transcription regulator
FXYD7_RAT	FXYD domain containing ion transport regulator 7	FXYD7	8.9	0.031	ion channel
G3P_RAT	glyceraldehyde-3-phosphate dehydrogenase	GAPDH	1.9	0.0001	enzyme
A0A0G2JT50_RAT	growth arrest specific 7	GAS7	9.1	0.031	transcription regulator
GFAP_RAT	glial fibrillary acidic protein	GFAP	-2.5	0.0014	other
GNAO_RAT	G protein subunit alpha o1	GNAO1	-1.429	0.0028	enzyme
G3V914_RAT	glutamate ionotropic receptor AMPA type subunit 2	GRIA2	18	0.00099	ion channel
GRAP1_RAT	GRIP1 associated protein 1	GRIPAP1	-10	0.037	other
A0A0G2K7W7_RAT	glycogen synthase kinase 3 alpha	GSK3A	21	0.00031	kinase
Q4QQV4_RAT	histidyl-tRNA synthetase	HARS	3.3	0.05	enzyme
HBB1_RAT	hemoglobin subunit beta	HBB	-1.25	0.039	transporter
HDGR3_RAT	HDGF like 3	HDGFL3	-10	0.037	other
B4F7C7_RAT	heme binding protein 1	HEBP1	3.3	0.05	other
HXK1_RAT	hexokinase 1	HK1	-1.25	0.029	kinase

Table A.7 (continued)

HMOX2_RAT	heme oxygenase 2	HMOX2	-10	0.037	enzyme
HOME1_RAT	homer scaffolding protein 1	HOMER1	-10	0.016	other
M0R8M9_RAT	heat shock protein family A (Hsp70) member 8	HSPA8	1.3	0.0065	enzyme
A0A0G2K261_RAT	isoleucyl-tRNA synthetase 2, mitochondrial	IARS2	-5	0.023	enzyme
AINX_RAT	internexin neuronal intermediate filament protein alpha	INA	-1.429	0.035	other
M0RAK2_RAT	isochorismatase domain containing 2	ISOC2	13	0.0056	enzyme
D3ZBS2_RAT	inter-alpha-trypsin inhibitor heavy chain 3	ITIH3	-10	0.016	other
A0A0G2JSL0_RAT	proteasome subunit beta 6	LOC100360846/Psmb6	2.5	0.023	other
MAG_RAT	myelin associated glycoprotein	MAG	-2	0.036	other
AOFA_RAT	monoamine oxidase A	MAOA	-2.5	0.032	enzyme
MK01_RAT	mitogen-activated protein kinase 1	MAPK1	-1.429	0.028	kinase
E9PSK7_RAT	mitogen-activated protein kinase 8 interacting protein 3	MAPK8IP3	9.2	0.031	other
A0JN25_RAT	microtubule associated protein tau	MAPT	1.4	0.021	other
MBP_RAT	myelin basic protein	Mbp	-1.667	0.0001	other
MDHM_RAT	malate dehydrogenase 2	MDH2	-1.25	0.025	enzyme

Table A.7 (continued)

A0A0G2K1S6_RAT	malic enzyme 1	ME1	-11.111	0.0071	Enzyme
C1TC_RAT	methylenetetrahydrofolate dehydrogenase, cyclohydrolase and formyltetrahydrofolate synthetase 1	MTHFD1	10	0.018	enzyme
A0A0G2K926_RAT	murinoglobulin 1	Mug1 (includes others)	4	0.017	transporter
G3V9Y1_RAT	myosin heavy chain 10	MYH10	-1.667	0.013	enzyme
A0A0G2K9S4_RAT	myosin VA	MYO5A	-2	0.016	enzyme
NDUAA_RAT	NADH:ubiquinone oxidoreductase subunit A10	NDUFA10	-2.5	0.016	transporter
D3ZE15_RAT	NADH:ubiquinone oxidoreductase subunit A13	NDUFA13	-10	0.037	enzyme
A9UMV9_RAT	NADH:ubiquinone oxidoreductase subunit A7	NDUFA7	-10	0.037	enzyme
D4A0T0_RAT	NADH:ubiquinone oxidoreductase subunit B10	NDUFB10	-3.333	0.011	enzyme
D4A565_RAT	NADH:ubiquinone oxidoreductase subunit B5	NDUFB5	-11.111	0.0071	enzyme
B2RYS8_RAT	NADH:ubiquinone oxidoreductase subunit B8	NDUFB8	-10	0.037	enzyme
NDUS1_RAT	NADH:ubiquinone oxidoreductase core subunit S1	NDUFS1	-1.429	0.036	enzyme
Q5RJN0_RAT	NADH:ubiquinone oxidoreductase core subunit S7	NDUFS7	-10	0.016	enzyme
NDUV2_RAT	NADH:ubiquinone oxidoreductase core subunit V2	NDUFV2	-3.333	0.0099	enzyme

Table A.7 (continued)

NECP1_RAT	NECAP endocytosis associated 1	NECAP1	-3.333	0.03	other
F1LNP8_RAT	nectin cell adhesion molecule 1	NECTIN1	8.9	0.031	other
NFH_RAT	neurofilament heavy	NEFH	-5	0.0016	other
NONO_RAT	non-POU domain containing octamer binding	NONO	3.4	0.015	other
RASN_RAT	NRAS proto-oncogene, GTPase	NRAS	2.1	0.041	enzyme
F7EYB9_RAT	oligodendrocyte myelin glycoprotein	OMG	-2.5	0.024	G-protein coupled receptor
PACS1_RAT	phosphofurin acidic cluster sorting protein 1	PACS1	3.6	0.0074	other
PCLO_RAT	piccolo presynaptic cytomatrix protein	PCLO	3.3	0.008	transporter
PCYOX_RAT	prenylcysteine oxidase 1	PCYOX1	3.1	0.016	enzyme
F1LX13_RAT	phosphodiesterase 10A	PDE10A	-2	0.049	enzyme
PFKAP_RAT	phosphofructokinase, platelet	PFKP	-1.429	0.022	kinase
6PGL_RAT	6-phosphogluconolactonase	PGLS	16	0.0018	enzyme
D3ZP47_RAT	phosphohistidine phosphatase 1	PHPT1	-11.111	0.0071	phosphatase
MYPR_RAT	proteolipid protein 1	PLP1	-1.429	0.0056	other
PPM1E_RAT	protein phosphatase, Mg2+/Mn2+ dependent 1E	PPM1E	4.8	0.0085	phosphatase
NEB2_RAT	protein phosphatase 1 regulatory subunit 9B	PPP1R9B	-14.286	0.0014	enzyme
D4A1A5_RAT	protein phosphatase 2, regulatory subunit B', gamma	Ppp2r5c	13	0.0056	phosphatase
PSA2_RAT	proteasome subunit alpha 2	PSMA2	18	0.00099	peptidase
PSA5_RAT	proteasome subunit alpha 5	PSMA5	-3.333	0.024	peptidase

Table A.7 (continued)

PSB2_RAT	proteasome subunit beta 2	PSMB 2	-10	0.03 7	peptidase
PGTA_RAT	Rab geranylgeranyltransfera se alpha subunit	RABG GTA	9	0.03 1	enzyme
RACK1_RAT	receptor for activated C kinase 1	RACK 1	-3.333	0.00 17	enzyme
RD23B_RAT	RAD23 homolog B, nucleotide excision repair protein	RAD2 3B	-5	0.02 3	other
D3ZHY9_RAT	RAS protein activator like 1	RASA L1	1.9	0.04 8	other
D3ZWG2_RAT	regulator of G protein signaling 7	RGS7	-16.667	0.00 06	enzyme
RLA0_RAT	ribosomal protein lateral stalk subunit P0	RPLP0	-11.111	0.00 71	other
A0A0G2K757_ RAT	ribophorin II	RPN2	-10	0.03 7	enzyme
Q6PDW1_RAT	ribosomal protein S12	RPS12	10	0.01 8	other
RTCB_RAT	RNA 2',3'-cyclic phosphate and 5'-OH ligase	RTCB	13	0.00 56	enzyme
SCN2A_RAT	sodium voltage-gated channel alpha subunit 2	SCN2 A	9.5	0.03 1	ion channel
NLTP_RAT	sterol carrier protein 2	SCP2	-3.333	0.02 3	transporter
A0A0G2K8K0 _RAT	splicing factor proline and glutamine rich	SFPQ	2.3	0.04 4	other
B2RZ27_RAT	SH3 domain binding glutamate rich protein like 3	SH3B GRL3	8.9	0.03 1	other
EAA2_RAT	solute carrier family 1 member 2	SLC1A 2	-1.429	0.00 26	transporter
F1LX07_RAT	solute carrier family 25 member 12	Slc25a 12	-1.667	0.03	transporter
ADT1_RAT	solute carrier family 25 member 4	SLC25 A4	-1.25	0.03 2	transporter
A0A0G2K2S2_ RAT	solute carrier family 2 member 1	SLC2A 1	-11.111	0.00 71	transporter
G3V7I8_RAT	STE20 like kinase	SLK	-10	0.01 6	kinase
SODM_RAT	superoxide dismutase 2	SOD2	-1.667	0.04	enzyme

Table A.7 (continued)

A0A0G2JZ69_RAT	spectrin alpha, non-erythrocytic 1	SPTAN1	-1.25	0.00019	other
A0A0G2K8W9_RAT	spectrin beta, non-erythrocytic 1	SPTBN1	-1.25	0.019	other
STK39_RAT	serine/threonine kinase 39	STK39	12	0.0099	kinase
STX1A_RAT	syntaxin 1A	STX1A	1.5	0.037	transporter
STX7_RAT	syntaxin 7	STX7	-5	0.023	transporter
A0A096MIT7_RAT	synapsin III	SYN3	4.8	0.0085	other
Q6QI09_RAT	TATA-box binding protein associated factor 3	TAF3	-1.667	0.023	transcription regulator
TCPA_RAT	t-complex 1	TCP1	-1.667	0.039	other
TIM13_RAT	translocase of inner mitochondrial membrane 13	TIMM13	8.9	0.031	transporter
A0A096MJE6_RAT	tenascin R	TNR	-1.429	0.046	other
TRAP1_RAT	TNF receptor associated protein 1	TRAP1	4.4	0.028	enzyme
TBB3_RAT	tubulin beta 3 class III	TUBB3	1.5	0.0001	other
QCR1_RAT	ubiquinol-cytochrome c reductase core protein 1	UQCRC1	-1.429	0.047	enzyme
D3ZVQ0_RAT	ubiquitin specific peptidase 5	USP5	-1.429	0.043	peptidase
SYVC_RAT	valyl-tRNA synthetase	VARS	13	0.0056	enzyme
VDAC2_RAT	voltage dependent anion channel 2	VDAC2	-1.667	0.017	ion channel
A0A0G2JTS3_RAT	VPS29, retromer complex component	VPS29	-5	0.023	transporter
VISL1_RAT	visinin like 1	VSNL1	-1.667	0.017	other
WASF1_RAT	WAS protein family member 1	WASF1	2.2	0.044	other
SYYC_RAT	tyrosyl-tRNA synthetase	YARS	3	0.035	enzyme

Table A.7 (continued)

1433E_RAT	tyrosine 3-monooxygenase/tryptophan 5-monooxygenase activation protein epsilon	YWHAE	1.8	0.0001	other
1433T_RAT	tyrosine 3-monooxygenase/tryptophan 5-monooxygenase activation protein theta	YWHAQ	-1.429	0.025	other
ZWINT_RAT	ZW10 interacting kinetochore protein	ZWINT	-5	0.0063	other

Table A.8 List of differentially expressed proteins with p-value ≤ 0.05 for PF NB vs PF B comparison in Chapter IV

ID	Entrez Gene Name	Symbol	Fold Change	P-value	Type
BACH_RAT	acyl-CoA thioesterase 7	ACOT7	-1.429	0.05	enzyme
ACTS_RAT	actin, alpha 1, skeletal muscle	ACTA1	-1.25	0.0001	other
ADCY5_RAT	adenylate cyclase 5	ADCY5	-11.111	0.017	enzyme
D4AEH9_RAT	amylo-alpha-1, 6-glucosidase, 4-alpha-glucanotransferase	AGL	-3.333	0.037	enzyme
A0A0H2UHC0_RAT	Rho GTPase activating protein 44	ARHGAP44	10	0.014	other
AT1A3_RAT	ATPase Na+/K+ transporting subunit alpha 3	ATP1A3	1.1	0.017	transporter
AT1B1_RAT	ATPase Na+/K+ transporting subunit beta 1	ATP1B1	-1.429	0.021	transporter
ATPA_RAT	ATP synthase F1 subunit alpha	ATP5F1A	1.2	0.0092	transporter
ATPB_RAT	ATP synthase F1 subunit beta	ATP5F1B	-1.25	0.021	transporter
VATB2_RAT	ATPase H+ transporting V1 subunit B2	ATP6V1B2	-1.429	0.0088	transporter
VATF_RAT	ATPase H+ transporting V1 subunit F	ATP6V1F	-10	0.017	enzyme
A0A0G2K7E5_RAT	calcium voltage-gated channel auxiliary subunit alpha2delta 1	CACNA2D1	-2.5	0.00047	ion channel
CALB1_RAT	calbindin 1	CALB1	3.4	0.021	other
CALR_RAT	calreticulin	CALR	1.4	0.045	transcription regulator

Table A.8 (continued)

F1LM55_RAT	cell cycle and apoptosis regulator 2	CCAR2	12	0.007	Peptidase
OX2G_RAT	CD200 molecule	CD200	10	0.014	other
CD59_RAT	CD59 molecule (CD59 blood group)	CD59	-10	0.017	other
CDK5_RAT	cyclin dependent kinase 5	CDK5	10	0.014	kinase
CSN4_RAT	COP9 signalosome subunit 4	COPS4	-10	0.034	peptidase
CX6C2_RAT	cytochrome c oxidase subunit VIc	Cox6c	5.6	0.0031	enzyme
A0A0G2JSP3_RAT	cullin 3	CUL3	10	0.014	enzyme
CYC_RAT	cytochrome c, somatic	CYCS	-3.333	0.02	transporter
SYDC_RAT	aspartyl-tRNA synthetase	DARS	-11.111	0.0087	enzyme
ACBP_RAT	diazepam binding inhibitor, acyl-CoA binding protein	DBI	3.8	0.032	other
OST48_RAT	dolichyl-diphosphooligosaccharide--protein glycosyltransferase non-catalytic subunit	DDOST	-10	0.034	enzyme
F1M3W5_RAT	Dmx like 2	DMXL2	1.5	0.026	other
DPP3_RAT	dipeptidyl peptidase 3	DPP3	2.4	0.04	peptidase
DPYL5_RAT	dihydropyrimidinase like 5	DPYSL5	-1.25	0.041	enzyme
DEST_RAT	destrin-like 1	Dstn/Dstnl1	2.8	0.0013	other
EF1A1_RAT	eukaryotic translation elongation factor 1 alpha 1	EEF1A1	-1.429	0.011	translation regulator
EF1A2_RAT	eukaryotic translation elongation factor 1 alpha 2	EEF1A2	-1.25	0.018	translation regulator
EF2_RAT	eukaryotic translation elongation factor 2	EEF2	1.4	0.023	translation regulator

Table A.8 (continued)

ELOB_RAT	elongin B	Elob	2.9	0.034	transcription regulator
G3V774_RAT	F-box protein 2	FBXO2	-10	0.034	enzyme
FLOT1_RAT	flotillin 1	FLOT1	-14.286	0.0022	other
FUBP1_RAT	far upstream element binding protein 1	FUBP1	8.9	0.029	transcription regulator
GBRB1_RAT	gamma-aminobutyric acid type A receptor beta1 subunit	GABRB1	-10	0.034	ion channel
NEUM_RAT	growth associated protein 43	GAP43	1.5	0.015	other
GLSK_RAT	glutaminase	GLS	1.4	0.04	enzyme
GNAO_RAT	G protein subunit alpha o1	GNAO1	-1.429	0.017	enzyme
GPM6A_RAT	glycoprotein M6A	GPM6A	1.5	0.042	ion channel
A0A0G2JT06_RAT	G protein pathway suppressor 1	GPS1	4.1	0.017	other
F1LNE4_RAT	glutamate ionotropic receptor AMPA type subunit 2	GRIA2	-11.111	0.0087	ion channel
GELS_RAT	gelsolin	GSN	2.8	0.042	other
D4ABI7_RAT	3-hydroxyacyl-CoA dehydratase 3	HACD3	-10	0.017	enzyme
B4F7C7_RAT	heme binding protein 1	HEBP1	4.3	0.017	other
HINT3_RAT	histidine triad nucleotide binding protein 3	HINT3	12	0.007	other
HMOX2_RAT	heme oxygenase 2	HMOX2	8.9	0.029	enzyme
B0BMW2_RAT	hydroxysteroid 17-beta dehydrogenase 10	HSD17B10	2.8	0.012	enzyme
HS90A_RAT	heat shock protein 90 alpha family class A member 1	HSP90AA1	1.2	0.035	enzyme
HSP7C_RAT	heat shock protein family A (Hsp70) member 8	HSPA8	1.2	0.028	enzyme

Table A.8 (continued)

CH60_RAT	heat shock protein family D (Hsp60) member 1	HSPD1	1.2	0.041	enzyme
MIC60_RAT	inner membrane mitochondrial protein	IMMT	-2.5	0.013	other
D3ZBL5_RAT	inositol polyphosphate-4-phosphatase type I A	INPP4A	3.3	0.05	phosphatase
D4A781_RAT	importin 5	IPO5	8.7	0.029	transporter
KCAB2_RAT	potassium voltage-gated channel subfamily A regulatory beta subunit 2	KCNAB2	-10	0.034	ion channel
AMPL_RAT	leucine aminopeptidase 3	LAP3	1.9	0.041	peptidase
A0A0G2K0V8_RAT	nuclear migration protein nudC-like	LOC100911422	10	0.014	other
LONM_RAT	lon peptidase 1, mitochondrial	LONP1	-14.286	0.0022	peptidase
F1LM33_RAT	leucine rich pentatricopeptide repeat containing	LRPPRC	14	0.0035	other
G3V9Z3_RAT	monoamine oxidase A	MAOA	-5	0.022	enzyme
F1LST4_RAT	microtubule associated protein tau	MAPT	1.5	0.00088	other
MPI_RAT	mannose phosphate isomerase	MPI	17	0.00084	enzyme
C1TC_RAT	methylenetetrahydrofolate dehydrogenase, cyclohydrolase and formyltetrahydrofolate synthetase 1	MTHFD1	11	0.007	enzyme
NDUAB_RAT	NADH: ubiquinone oxidoreductase subunit A11	NDUFA11	-3.333	0.037	enzyme
NDUS2_RAT	NADH: ubiquinone oxidoreductase core subunit S2	NDUFS2	-2.5	0.031	enzyme

Table A.8 (continued)

NECP1_RAT	NECAP endocytosis associated 1	NECAP1	-10	0.034	Other
F1LRZ7_RAT	neurofilament heavy	NEFH	-2.5	0.016	other
NRX3A_RAT	neurexin III	Nrxn3	-14.286	0.0022	other
G3V964_RAT	neurotrimin	NTM	-2.5	0.024	other
A0A0G2K7Y2_RAT	oxidation resistance 1	OXR1	1.7	0.036	enzyme
PDIA1_RAT	prolyl 4-hydroxylase subunit beta	P4HB	1.7	0.041	enzyme
LIS1_RAT	platelet activating factor acetylhydrolase 1b regulatory subunit 1	PAFAH1B1	-1.667	0.03	enzyme
F1LX13_RAT	phosphodiesterase 10A	PDE10A	2.7	0.018	enzyme
A0A0G2JZH8_RAT	pyruvate dehydrogenase complex, component X	Pdhx	2.1	0.033	other
G3V6T7_RAT	protein disulfide isomerase family A member 4	PDIA4	10	0.014	enzyme
D3ZDU5_RAT	profilin 2	PFN2	1.8	0.022	enzyme
D3Z955_RAT	phosphoglucomutase 2 like 1	PGM2L1	-20	0.00029	enzyme
PHB_RAT	prohibitin	PHB	-1.667	0.038	transcription regulator
B0BNL2_RAT	peptidylprolyl cis/trans isomerase, NIMA-interacting 1	PIN1	2.4	0.05	enzyme
KPYM_RAT	pyruvate kinase M1/2	PKM	1.2	0.01	kinase
D4A1H2_RAT	phosphatidylinositol specific phospholipase C X domain containing 3	PLCXD3	-11.111	0.0087	other
PRRT2_RAT	proline rich transmembrane protein 2	PRRT2	14	0.0035	other
PRS7_RAT	proteasome 26S subunit, ATPase 2	PSMC2	3	0.034	peptidase

Table A.8 (continued)

Q4V8E2_RAT	proteasome 26S subunit, non-ATPase 14	PSMD14	-10	0.034	Peptidase
RCN2_RAT	reticulocalbin 2	RCN2	3.8	0.029	other
RGS7_RAT	regulator of G protein signaling 7	RGS7	-11.111	0.0087	enzyme
Q6P3V9_RAT	ribosomal protein L4	RPL4	20	0.0002	enzyme
RLA0_RAT	ribosomal protein lateral stalk subunit P0	RPLP0	-10	0.017	other
F7EMB2_RAT	RNA transcription, translation and transport factor	RTRAF	10	0.014	other
A0A096MJN4_RAT	septin 4	Sept4	8.5	0.029	enzyme
S12A5_RAT	solute carrier family 12 member 5	SLC12A5	-1.667	0.0092	transporter
VGLU2_RAT	solute carrier family 17 member 6	SLC17A6	-25	0.0001	transporter
EAA2_RAT	solute carrier family 1 member 2	SLC1A2	-1.429	0.01	transporter
F1LX07_RAT	solute carrier family 25 member 12	Slc25a12	-1.667	0.017	transporter
A0A0G2K2S2_RAT	solute carrier family 2 member 1	SLC2A1	-10	0.017	transporter
S4A4_RAT	solute carrier family 4 member 4	SLC4A4	-5	0.0001	transporter
S6A11_RAT	solute carrier family 6 member 11	SLC6A11	-2	0.0044	transporter
SYUA_RAT	synuclein alpha	SNCA	1.4	0.039	enzyme
B0BNJ1_RAT	sorcin	SRI	12	0.007	transporter
SYN1_RAT	synapsin I	SYN1	-1.25	0.032	transporter
M0R735_RAT	synaptotagmin binding, cytoplasmic RNA interacting protein	Syncrip	5.2	0.0017	other
D3ZSS1_RAT	TATA-box binding protein associated factor 15	Taf15	16	0.0017	other
TAGL2_RAT	transgelin 2	TAGLN2	9.4	0.014	other

Table A.8 (continued)

A0A0G2K6I5_RAT	transgelin 3	TAGLN3	1.8	0.0017	Other
M0RDJ7_RAT	transcription elongation factor A like 5	TCEAL5	3.6	0.05	other
A0A0G2JXG3_RAT	transmembrane protein 30A	TMEM30A	-10	0.034	transporter
LAP2_RAT	thymopoietin	TMPO	4	0.029	other
TRAP1_RAT	TNF receptor associated protein 1	TRAP1	-2.5	0.033	enzyme
TBB5_RAT	tubulin beta class I	TUBB	-1.111	0.048	other
VAMP1_RAT	vesicle-associated membrane protein 1	Vamp1	-12.5	0.0044	other
SYVC_RAT	valyl-tRNA synthetase	VARS	12	0.007	enzyme
1433E_RAT	tyrosine 3-monooxygenase/tryptophan 5-monooxygenase activating protein	YWHAE	1.1	0.02	other